Bays Eutrophication Model (BEM) Model Verification for the Period 2000-2001

Massachusetts Water Resources Authority

Environmental Quality Department
ENQUAD Report 2004-09

Citation: Jiang, M, and M Zhou. 2004. **Bays Eutrophication Model (BEM) Model Verification for the Period 2000-2001**. Boston: Massachusetts Water Resources Authority. Report ENQUAD 2004-09. 90 p.

Massachusetts Water Resources Authority
Boston, Massachusetts

Bays Eutrophication Model (BEM) Model Verification for the Period 2000-2001

Prepared by:
Mingshun Jiang & Meng Zhou
Department of Environmental, Earth and Ocean Sciences
University of Massachusetts Boston
100 Morrissey Blvd
Boston, MA 02125

December, 2004

TABLE OF CONTENTS

LIST OF FIGURES

LIST OF TABLES

1. INTRODUCTION

1.1 Project overview

The Boston Harbor, Massachusetts Bay and Cape Cod Bay system (MBS) is important to the regional economy by serving a busy commercial harbor, a productive fishing ground, a habitat of endangered North Atlantic Right whales and a prosperous tourism industry. A healthy marine environment is also important to the more than three million people living in the surrounding area. In the last decades, tremendous efforts have been made to clean up Boston Harbor, including the improvement of the sewage treatment system and the offshore relocation of sewage outfall. These represent one of the biggest human efforts to restore an urbanized harbor in the nation.

In order to evaluate the impacts of these changes on the MBS water quality and ecosystem and to monitor potential changes in the MBS, the Department of Environmental Protection (DEP) and Massachusetts Water Resource Authority (MWRA) have funded a number of projects to study the physical-biological-chemical processes and to monitor the marine environment in the MBS (Geyer et al., 1992; Werme and Hunt, 2002; Werme and Hunt, 2000; Werme and Hunt, 2003). Among these projects, numerical models have also been developed to simulate and predict the physical and biological environment. Simulations for periods of 1992-94 and 1998-99 have been carried out (HydroQual, 2000; HydroQual, 2003; HydroQual and Signell, 2001; Jiang and Zhou, 2004).

A long-term Cooperative Research Agreement was made in 2001 between the University of Massachusetts Boston (UMB) and MWRA, under which the UMB will maintain, enhance and apply the existing Massachusetts Bay Hydrodynamic and Water Quality Models (MB Model). The UMB will also provide model results to the MWRA for its obligations under the National Pollutant Discharge Elimination System (NDPES) permit. The hydrodynamic model of the MBS was constructed by the U.S. Geological Survey (USGS) in Woods Hole using the semi-implicit Estuarine, Coastal, Ocean Model (ECOM-si) developed by HydroQual Inc. (HydroQual) (Signell et al., 1996). The Water Quality Model was developed by HydroQual (HydroQual, 2000), which is also called

Bay Eutrophication Model (BEM). HydroQual had maintained and conducted model runs up to 1999. Under the agreement between the MWRA and HydroQual, the MB Model has been transferred to the UMB since 2001. To ensure the successful model transfer and consistency between model results produced by different computers and model code setups, comparison tasks between UMB and HydroQual model runs have been conducted at the UMB (Zhou, 2001; Jiang and Zhou, 2003).

1.2 Physical environment

The MBS is a semi-enclosed coastal embayment surrounded by the Boston metropolitan area in the north and west, Cape Cod in the south, and the Gulf of Maine (GOM) in the east (Figure 1.1). The MBS is about 100 km long, 50 km wide, and 35 m deep on average. Stellwagen Basin is the only deep basin with a depth up to 90 m, located to the west of Stellwagen Bank, of which the shallowest depth is appoximately 20 m. The water exchange between Stellwagen Basin and the GOM is largely blocked by the Stellwagen Bank, and occurs mainly only through the North Passage off Cape Ann and the South Passage off Race Point, respectively.

Previous studies have indicated that the hydrographical features and circulation in the MBS vary in response to short and long term local and remote forcing, including 1) wind stress and heat fluxes at the sea surface, 2) tides and mean surface slopes at the open boundary, and 3) fresh water runoff including the outfall effluent (Geyer et al., 1992; Signell et al., 1996). The annual mean circulation in the MBS is counterclockwise, which is primarily driven by both the intruding current through the North Passage associated with mean sea surface slopes, and the horizontal density gradients produced by intruding GOM water and freshwater runoff. Tides are dominated by the semidiurnal M_2 constituent. Tidal currents vary from 10 cm s^{-1} in the interior to 50 cm s^{-1} off Race Point. The water column stratification varies seasonally. The stratification is present in spring due to both freshwater runoff and surface heating, intensified in summer, and destratified in late fall due to surface cooling and increasing wind mixing.

The surface circulation in the MBS is strongly influenced by the Western Maine Coastal Current (WMCC), which flows southwestward along the northern Gulf of Maine.

Bigelow suggested that the WMCC breaks into two branches off Cape Ann: one intrudes deeply into Massachusetts Bay, and the other branch flows along the eastern edge of Stellwagen Bank (Bigelow, 1927; Lynch et al., 1996). During spring, the freshwater plume of the Merrimack River interacts with the WMCC, enhancing the WMCC intrusion into the MBS (Butman, 1976). The intruding current circulates counterclockwise along western Massachusetts Bay and frequently penetrates into Cape Cod Bay (CCB), especially in winter and spring seasons.

Our modeling study indicates pronounced short-term and seasonal variations in the circulation pattern in response to low frequency variability of local and remote forcing (Jiang and Zhou, 2004). In western Massachusetts Bay, the currents are primarily driven by surface wind. In winter and spring seasons, predominant northerly winds drive southward coastal currents creating a counter-clockwise circulation that is consistent with annual mean pattern (Geyer et al., 1992). In summer and early fall, predominant southwesterly wind drives offshore Ekman transports and coastal upwelling, which produces an overall northward coastal current along the western coast. This is confirmed by the moored ADCP (Acoustic Doppler Current Profiler) current measurements at the US Geological Survey buoy (Butman et al., 2002). The coastal upwelling and downwelling in this area have also been discussed in previous studies (e.g., Geyer et al., 1992; HydroQual and Signell, 2001). The short term and seasonal changes of circulation patterns may have significant implications to biological and chemical processes in the MBS to be discussed in section 5.

1.3 Biological environment

Phytoplankton growth in the MBS is primarily driven by nutrients, temperature and photosynthetic available radiation (PAR) (Libby et al., 1999; Libby et al., 2000). The spring bloom is triggered by the onset of stratification and strengthened with the increase in solar radiation. The timing of spring blooms varies, which is not well understood. The availability of both nitrogen and silica in the well mixed water column during winter leads to the dominance of diatoms. The stratification limits the upward nutrient fluxes, which in turn limits the primary production in the MBS during late spring and summer.

The abundance of phytoplankton cells reaches maximum at mid-summer, except in some exceptional years such as 2000, when the maximum abundance was reached during the spring bloom. The late summer assemblage is comprised of primarily dinoflagellates and mixed species of diatoms, mainly the genus *Chaetoceros*. In upwelling areas, the assemblage is dominated by the diatom *Leptocylindrus danicus*. The fall bloom typically occurs in late September when strong mixing produced by wind and surface cooling destratifies the water column and brings nutrients from deep water to the euphotic zone, and declines in November as solar radiation decreases. The fall bloom is characterized by increases of nutrient concentrations in the surface water and a 2-4 fold increase in diatom abundances. One of the prominent features of the MBS ecosystem is the occurrences of strong fall blooms in some years with the averaged chlorophyll in western Massachusetts Bay higher than 6 $\mu g\ l^{-1}$. The mechanisms that trigger strong fall blooms remain unclear.

Abundant phytoplankton in the MBS supports abundant zooplankton, ranging from 10 to 50×10^3 individuals m^{-3} (Turner, 1994; Libby et al., 1999; Libby et al., 2000). In winter, zooplankton assemblages are dominated by copepod nauplii, *Oithona similis* females and copepodites, gastropod veligers, and *Acartia hudsonica* females and copepodites. In late winter and early spring, in addition to these dominant species, subdominant species are bivalve veligers, copepodites of *Calanus finmarchicus, Pseudocalanus* and *Temora longicornis*, and *Oikopleura dioica*. In summer and early fall, marine cladoceran *Evadne nordmanni*, *Microsetella norvegica* and copepodites of the genus *Centropages* are added to the species spectrum. In winter, the copepod abundance decreases while the bivalve and gastropod abundances increase.

The sea floor in the MBS is complicated with a variety of bottom types. Soft-bottom occupies most areas in Boston Harbor, Cape Cod Bay and Stellwagen Basin, while hard-bottom dominates the shallow nearshore areas. The annelid worms are most abundant in soft-bottom communities, accounting for more than 80% of the fauna at most MWRA monitoring stations, and crustaceans are second most abundant fauna (Kropp et al., 2001; Kropp et al., 2002; Maciolek et al., 2003). The most dominant taxa in hard-bottom communities are algae, including *Lithothamnion spp*., dulse, and red filamentous species. The dominant animal taxa include *Asterias vulgaris*, and the horse mussel *Modiolus*

modiolus.

The benthic processes in Boston Harbor are dominated by biological processes, while in Massachusetts and Cape Cod Bays they are generally influenced by region-wide phenomena (Maciolek et al., 2003; Tucker et al., 2002). High sediment oxygen demand (SOD) and fluxes of dissolved inorganic nitrogen (DIN) have been observed in the harbor, both of which have been decreasing in the last decade due to the reduction in pollutant load to the harbor. Intensive denitrification also occurs in the harbor, which increases since the outfall relocation. Sediments in the MBS are well oxygenated; and the denitrification dominates DIN fluxes, accounting for about 60-80% of the total flux. No obvious seasonal pattern in DIN fluxes has been observed. On the contrary, the SOD fluxes exhibit strong seasonal patterns, which are well correlated with the bottom temperature.

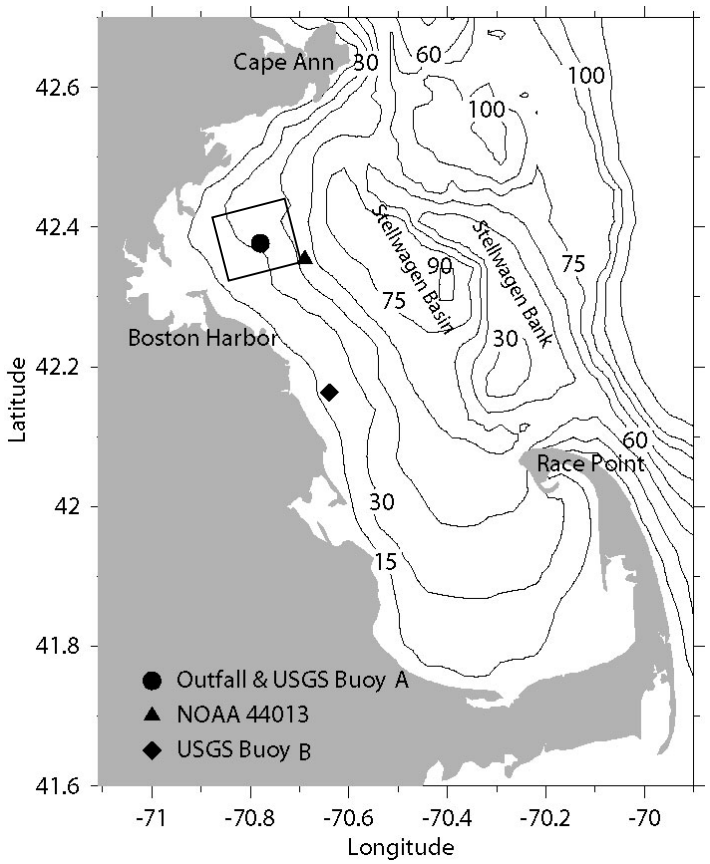

Figure 1.1 Bathymetry in the Boston Harbor, Massachusetts Bay and Cape Cod Bay system (MBS). The black box indicates the Massachusetts Water Resources Authority (MWRA) nearfield monitoring area.

2. MODEL DESCRIPTION

2.1 Model domain and grids

The BEM grids are essentially the same as the grids used for the hydrodynamic model with two modifications: 1) the model domain covers the entire MBS with the open boundary starting from Cape Ann to the outer edge of Cape Cod (Figure 2.1), that is, those grids east of this boundary in the hydrodynamic model are eliminated in the BEM; and 2) the top 3 sigma layers in the hydrodynamic model are integrated to 1 sigma layer in the BEM. The BEM has 54×68 horizontal grids and 10 vertical layers.

2.2 General structure: nutrient cycling

The water quality model describes the phytoplankton growth and nutrient cycling through a number of prognostic variables and a set of differential equations, which govern the temporal and spatial changes of these variables based on fluid motion, biochemical process rates and mass conservation. Most of the important biological and chemical processes are included in these equations based on theoretical and empirical relationships and parameters. The current BEM has 26 prognostic variables, which include salinity, 3 phytoplankton groups, 4 type of nutrients (C, N, P, Si) and related organic components, and dissolved oxygen (Table 2.1).

The biological and chemical processes in sediments and fluxes of related bio-chemical variables in the BEM are governed by a sediment sub-model. Particulate organic matter in water column settles down into the sediments. Fluxes of dissolved nutrients and sediment oxygen demand (SOD) through the water-sediment interface represent the interactions between bio-chemical processes in the water column and sediments. Nitrogen gas released by the denitrification process is removed from the system through outgassing to the atmosphere. Neither resuspension nor horizontal transport of sediments is simulated in the current BEM.

The model structures for nutrient cycling in water column are similar for all nutrients, including carbon and oxygen. Taking the nitrogen cycle as an example (Figure 2.2), the

central process is phytoplankton photosynthesis, which transforms dissolved inorganic nitrogen (DIN) to phytoplankton biomass. The DIN includes ammonium (NH_4), nitrate (NO_3) and nitrite (NO_2). The latter two are combined and denoted as NO_3. The NO_3 and NH_4 can be transformed into each other through nitrification and nitrate reduction. The living cells of phytoplankton can be transformed into non-living organic matter by respiration, mortality and zooplankton grazing. The zooplankton grazing is accounted for as instantaneous removal of 10% phytoplankton standing stocks. There are two non-living organic nitrogen types, dissolved organic nitrogen (DON) and particulate organic nitrogen (PON). They are further divided into refractory (RDON and RPON) and labile (LDON and LPON) forms. LDON and LPON are decomposed much faster than RDON and RPON. The regeneration process of organic matter by bacterial decomposition involves two steps: 1) particles break down to DON, and 2) DON is further remineralized to ammonia. Particles settled down into sediments will be decomposed and feed back to water column through fluxes of NO_3 and NH_4. In addition to internal cycling, the water column receives inputs of nitrogen from land sources as runoff and effluent containing inorganic and organic nutrients, from the atmosphere through gas exchange, and from the open boundary.

The cyclings of carbon and phosphorus have similar structures to that of nitrogen. However, there is only one dissolved inorganic form each for phosphorus and carbon. The oxygen cycle generally follows the cycling of carbon in the water column, while the exchange of oxygen with the air is driven by wind entrainment and solubility at the surface. Silicon has only one dissolved inorganic form (SiO_4) and one biogenic form (BSi). Detailed description can be found in earlier reports of this model (HydroQual, 2000; HydroQual, 2003; HydroQual and Normandeau, 1995).

2.3 Forcing

2.3.1 Surface forcing

The surface forcing in the BEM includes solar radiation, day length and wind (Figure 2.3). The winter experiences shortest day light and lowest solar radiation, while the summer has the longest day light and strongest radiation. The wind also exhibits a strong

seasonal pattern with the strongest winds in winter and weakest in summer (Jiang and Zhou, 2004b). The wind forcing primarily determines the air-sea gas exchanges, and affects the bio-chemical processes indirectly through vertical mixing and horizontal transport.

2.3.2 Nutrient loadings

As a shallow coastal embayment surrounded by a major metropolitan area, the MBS receives large anthropogenic inputs of nutrients and organic matter from sewage effluents, river discharges, and combined sewage overflows (CSO) (Figure 2.4). Other than the open boundary, the MWRA effluent is the dominant source for nitrogen and phosphorus. Among the other sources, non-MWRA wastewater treatment plant (WWTP) effluent is the largest for phosphorus, and the atmosphere provides most of the remaining nitrogen. Due to secondary wastewater treatment, carbon and phosphorus loads in the MWRA effluent have been significantly reduced in the last several years. The loads of carbon and phosphorus from non-MWRA WWTP have probably been reduced as well, but updated figures are not available. The total nitrogen loading in recent years is nearly unchanged compared to that of the baseline period from 1992 to 2000 (see Figure 2-1 in HydroQual, 2003). On September 6, 2000, the MWRA sewage effluent was diverted to new outfall site, which is 15 km offshore (Figure 1.1).

Because only total loading data of individual nutrients are available for MWRA effluents and other sources, they are converted to loadings of different components for each nutrient. For example, the total nitrogen flux is separated into fluxes of nitrate (including nitrite), ammonia, LPON, RPON, LDON and RDON. The partition coefficients for each nutrient in the previous simulations (1998 and 1999) are used in year 2000-2001 model runs (Table 2.2) (HydroQual, 2000; HydroQual, 2003; HydroQual and Normandeau, 1995).

2.3.3 Open boundary conditions

The open boundary conditions are constructed based on the same objective

interpolation procedure and software (OAX) used in the year 2000-2001 hydrodynamic model run, which was developed by Bedford Institute of Oceanography (http://www.mar.dfo-mpo.gc.ca/science /ocean/coastal_hydrodynamics/oax.html). The correlation function is specified because there are not enough data to compute the spatial and temporal decorrelation scales. All MWRA monitoring station data are used for the interpolation along the open boundary (Figure 2.5). A spatial correlation scale 20 km and a temporal correlation scale of 15 day are used to ensure that the results rely mainly on the observations near the open boundary. During months when there are no data collected at stations near the open boundary (F26, F27, F28 and F29), the boundary values are extrapolated from the observations inside the domain and should include significant errors. This leads us to use the nearfield values to predict the farfield boundary conditions and then to use the farfield boundary conditions to predict the nearfield values. Though the model prediction is determined by the combination of biogeochemical processes, local forcing, and open boundary conditions, a less accurate open boundary condition will lead to a less accurate prediction. The overall quality of data coverage is shown in Table 2.3. Our extrapolation seems to do a good job.

Our new procedure is significantly different from the procedure employed in previous simulations (HydroQual, 2000; HydroQual, 2003), which averages observed values at three stations F26, F27 and F29, closest to the boundary, and then applies the results uniformly to the boundary.

The objectively interpolated boundary conditions in April and August, 2000 are shown in Figures 2.6 and 2.7. The new procedure for constructing boundary conditions incorporates as many observed data as possible in a standardized objective way, and provides detailed boundary values and spatial structures, though in some months, interpolated results may not be very reliable due to the paucity of observations. Most variables show significant vertical and horizontal variability. In April, 2000, the high subsurface chlorophyll maximum is only present in the northern portion of the open boundary, the concentrations of nitrate and ammonia are minimal within the mixed layer, and a subsurface ammonia maximum exists below the thermocline. In August, 2000, the surface DIN is nearly depleted except in nearshore areas, and relatively high ammonia concentration is observed near the bottom in both the North Passage and the South

Passage. Overall, the spatial features of biological and chemical variables are well presented by the objective interpolation, which should improve the general quality of model results.

Interpolated organic matter is further separated into labile and refractory forms based on the partition coefficients used for anthropogenic loading (Table 2.2). Data for phytoplankton biomass are insufficient to construct the open boundary conditions directly because the measurements are only taken at several selected monitoring stations. Instead, chlorophyll data are used and converted to phytoplankton biomass. The conversion steps include: 1) the total chlorophyll is separated into three algal groups based on empirical percentages for individual groups (Table 2.4); and 2) the resulting chlorophyll values are converted to biomass using the base carbon to chlorophyll ratios (CChl) for the algal groups, which are parameters used to predict the actual carbon to chlorophyll ratios in the BEM (HydroQual, 2000; HydroQual, 2003). For the year 2000 simulation, the CChl used for the fall algal group is slightly modified based on a regression analysis between observed phytoplankton biomass and chlorophyll concentration (Figure 2.8). The regression uses all the available data for each spring, summer and fall. The regression yields a CChl of 40 (R^2=0.58) for spring 2000, which is exactly the value used for previous simulations (HydroQual, 2003). No significant correlation exists between measured biomass and chlorophyll for summer 2000. However, the regression yields a CChl of 30 (R^2=0.35) for fall 2000, which is two times the value used in the previous simulation (CChl=15). We adjusted the CChl for fall group to 25 in 2000 simulation.

This procedure is applied to construct the open boundary conditions for both years 2000 and 2001. Since the data are collected at the same monitoring stations, the stations used for the 2001 open boundary conditions are essentially the same as those for 2000 (Figure 2.5b). No adjustment is made for CChl values because the only significant correlation between measured biomass and chlorophyll is from the spring, which has a CChl of 33 (R^2=0.43), close to the CChl value (40) used for previous simulations. For example, the open boundary conditions for April and August 2001 are shown in Figures 2.9 and 2.10.

2.4 Numerical scheme

The BEM is offline-coupled with the hydrodynamic model, which is the estuarine, coastal, ocean model (ECOM-si) developed by HydroQual. The modeled hydrodynamic variables such as temperature, currents and turbulent mixing from ECOM-si are averaged in every hour and stored. These data are then input into the water quality model as the physical forcing. In the BEM, the top three layers in the ECOM-si are integrated into one top layer in the same way as used during previous runs. A collapse program is used to average hydrodynamic variables in the top three layers of the ECOM-si and assign the resulted values to the integrated top sigma layer in the BEM. The time dependent advection-diffusion-reaction equations in the BEM are integrated using the explicit upwind scheme and the Smolarkiewicz flux-correction algorithm (Smolarkiewicz, 1984). The variables at the open boundary are specified using the values derived from the objective interpolation and partitioning as discussed above.

2.5 Model parameters

All model parameters used in the 2000-2001 simulations are same as those of 1998-99 simulations (HydroQual, 2003) except the base light attenuation coefficient (k_0) in Boston Harbor. k_0 is defined by the water clarity during winter when chlorophyll concentration is generally low. In previous simulations, k_0 was estimated from field surveys conducted during late 1980s and early 1990s (HydroQual and Normandeau, 1995). The value of k_0 was 0.6 m^{-1} in Boston Harbor and less than 0.3m^{-1} in the rest of the MBS. Recent monitoring studies in Boston Harbor have revealed that the light attenuation coefficient is approximately 0.3m^{-1} during winter time in Boston Harbor (Taylor, 2001). Therefore the upper limit of k_0 is set to be 0.3 m^{-1} in the current model runs. This change will mainly affect the phytoplankton growth in Boston Harbor since k_0 is unchanged in the bays.

Table 2.1 Model variables

1 - SALINITY (SAL)	PPT
2 - PHYTOPLANKTON - WINTER DIATOMS (PHYT1)	MG C/L
3 - PHYTOPLANKTON - SUMMER ASSEMBLAGE (PHYT2)	MG C/L
4 - PARTICULATE ORGANIC PHOSPHOROUS - REFRACTORY (RPOP)	MG P/L
5 - PARTICULATE ORGANIC PHOSPHOROUS - LABILE (LPOP)	MG P/L
6 - DISSOLVED ORGANIC PHOSPHOROUS - REFRACTORY (RDOP)	MG P/L
7 - DISSOLVED ORGANIC PHOSPHOROUS - LABILE (LDOP)	MG P/L
8 - TOTAL DISSOLVED INORGANIC PHOSPHOROUS (PO4T)	MG P/L
9 - PARTICULATE ORGANIC NITROGEN - REFRACTORY (RPON)	MG N/L
10 - PARTICULATE ORGANIC NITROGEN - LABILE (LPON)	MG N/L
11 - DISSOLVED ORGANIC NITROGEN - REFRACTORY (RDON)	MG N/L
12 - DISSOLVED ORGANIC NITROGEN - LABILE (LDON)	MG N/L
13 - TOTAL AMMONIA (NH3T)	MG N/L
14 - NITRITE + NITRATE (NO23)	MG N/L
15 - BIOGENIC SILICA - UNAVAILABLE (BSI)	MG SI/L
16 - TOTAL SILICA - AVAILABLE (SIT)	MG SI/L
17 - PARTICULATE ORGANIC CARBON - REFRACTORY (RPOC)	MG C/L
18 - PARTICULATE ORGANIC CARBON - LABILE (LPOC)	MG C/L
19 - DISSOLVED ORGANIC CARBON - REFRACTORY (RDOC)	MG C/L
20 - DISSOLVED ORGANIC CARBON - LABILE (LDOC)	MG C/L
21 - DISSOLVED ORGANIC CARBON - REACTIVE (REDOC)	MG C/L
22 - DISSOLVED ORGANIC CARBON - ALGAL EXUDATE (EXDOC)	MG C/L
23 - O2* - AQUEOUS SOD (O2EQ)	MG O2/L
24 - DISSOLVED OXYGEN (DO)	MG O2/L
25 - TOTAL ACTIVE METAL (TAM)	MMOL/L
26 - PHYTOPLANKTON - FALL DIATOMS (PHYT3)	MG C/L

Table 2.2 Partition coefficients for organic matter

Nitrogen	**PON**	**DON**
Labile	0.5	0.5
Refractory	0.5	0.5
Phosphorus	***POP***	***DOP***
Labile	0.647	0.66
Refractory	0.353	0.33
Carbon	***POC***	***DOC***
Labile	0.1	0.15
Refractory	0.9	0.8
Reactive	-	0.025
Exudate	-	0.025

Table 2.3 Quality of data coverage for objective interpolation in 2000 and 2001

Year	Month	Rating*
2000	January 2000	-
	February	+
	March	-
	April	+
	May	-
	June	+
	July	-
	August	+
	September	-
	October	+
	November	-
	December	-
2001	January 2001	-
	February	+
	March	-
	April	+
	May	-
	June	+
	July	-
	August	+
	September	-
	October	+
	November	-
	December	-

* Definitions of symbols: + (good), 0 (fair), - (poor).

Table 2.4 Partition coefficients of chlorophyll at the open boundary

	Winter-spring diatoms	Summer assemblages	Fall diatoms
January-April	1.0	0	0
May	0.5	0.5	0
June-July	0	1.0	0
August	0	0.5	0.5
September-November	0	0	1.0
December	0.5	0	0.5

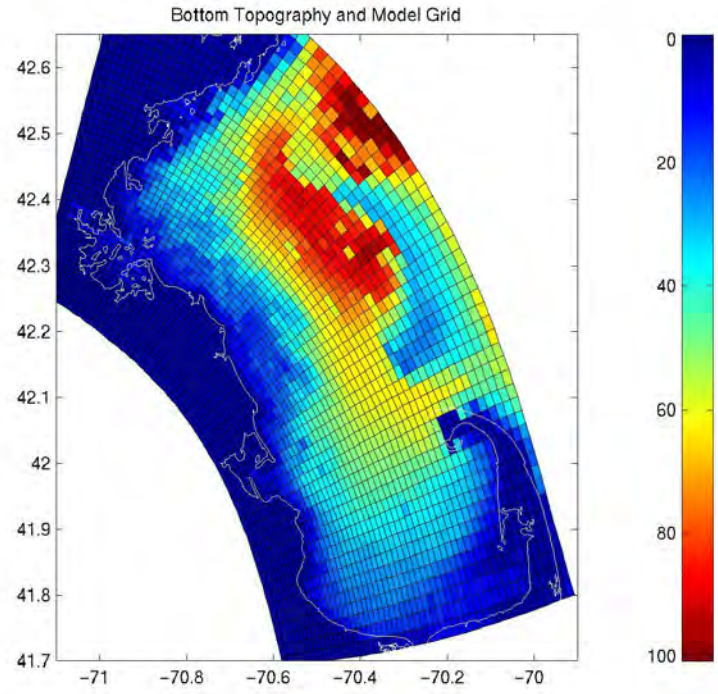

Figure 2.1. Model domain and grids in the MBS.

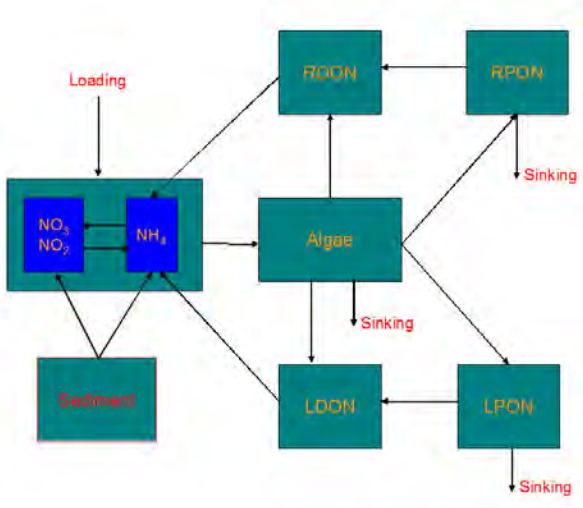

Figure 2.2. A schematic diagram of the nitrogen cycle in the BEM.

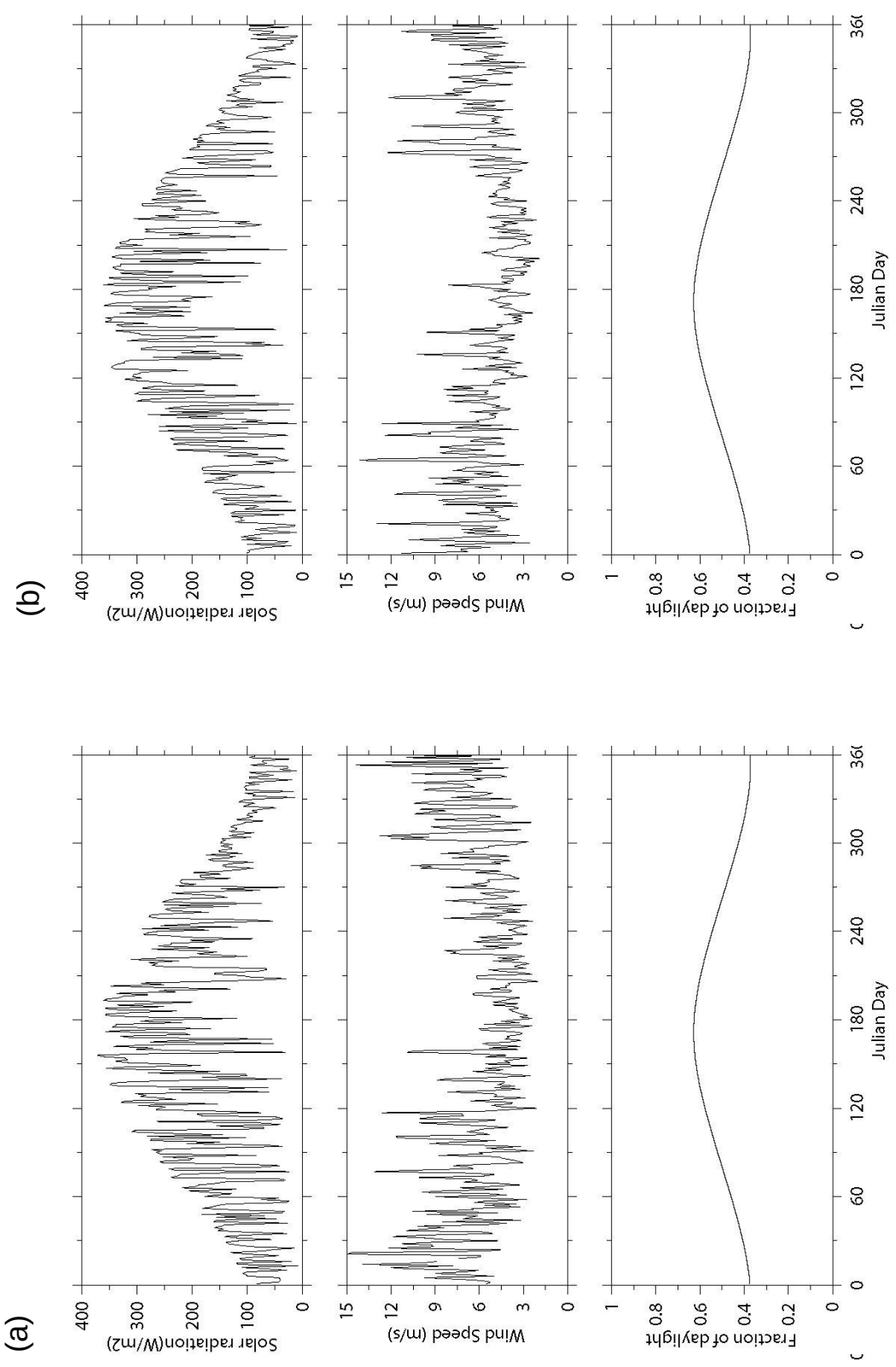

Figure 2.3. Solar radiation, wind speed, and fraction of daylight in (a) 2000 and (b) 2001.

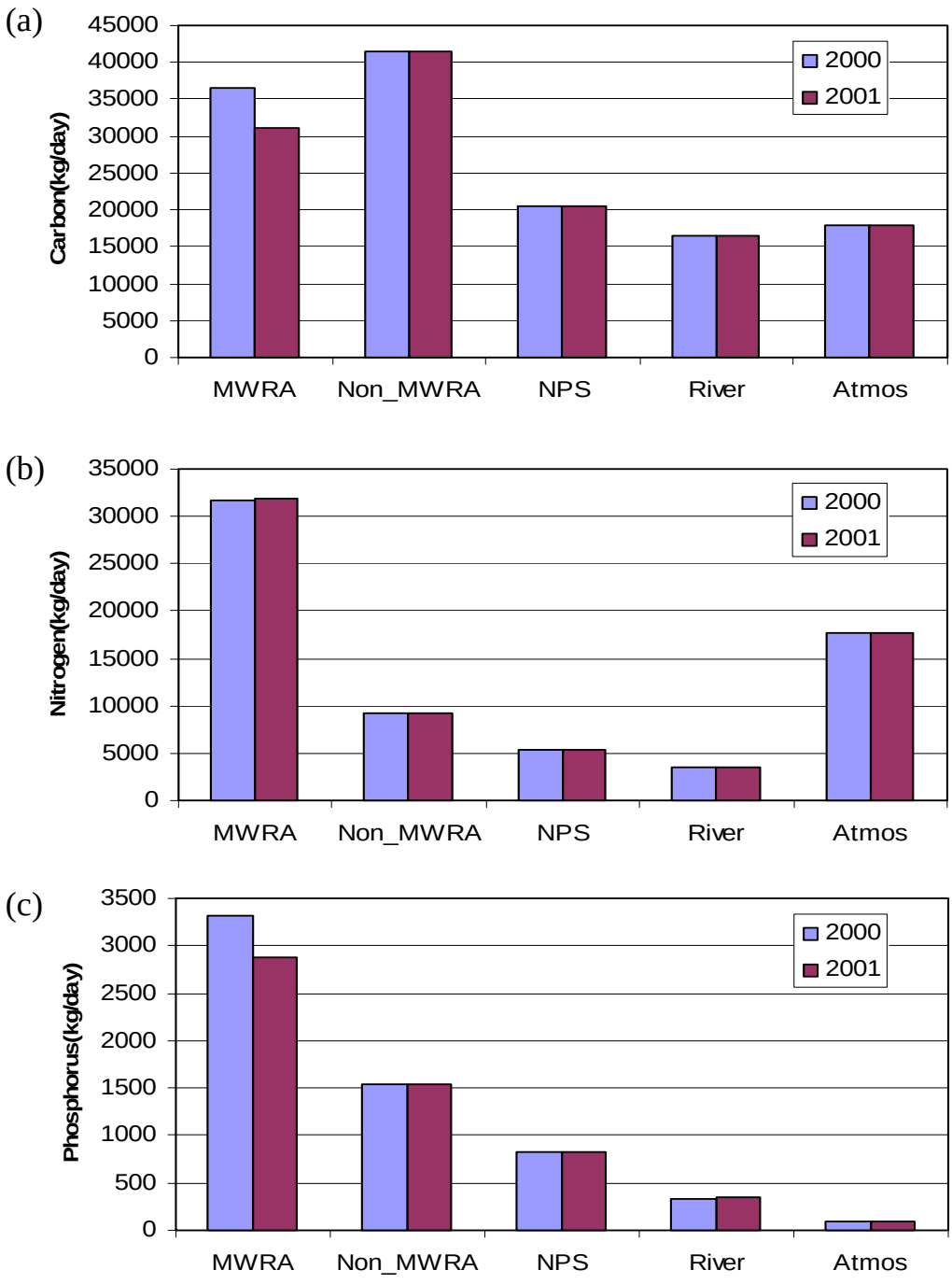

Figure 2.4. Nutrient loads: (a) carbon, (b) nitrogen and (c) phosphorus. The abbreviations are: MWRA = MWRA treatment plant effluent, non_MWRA = other treatment plant effluents, NPS = non-point sources including combined sewage overflows (CSO) and storm waters, River = river inputs, and Atmos = direct atmospheric deposition.

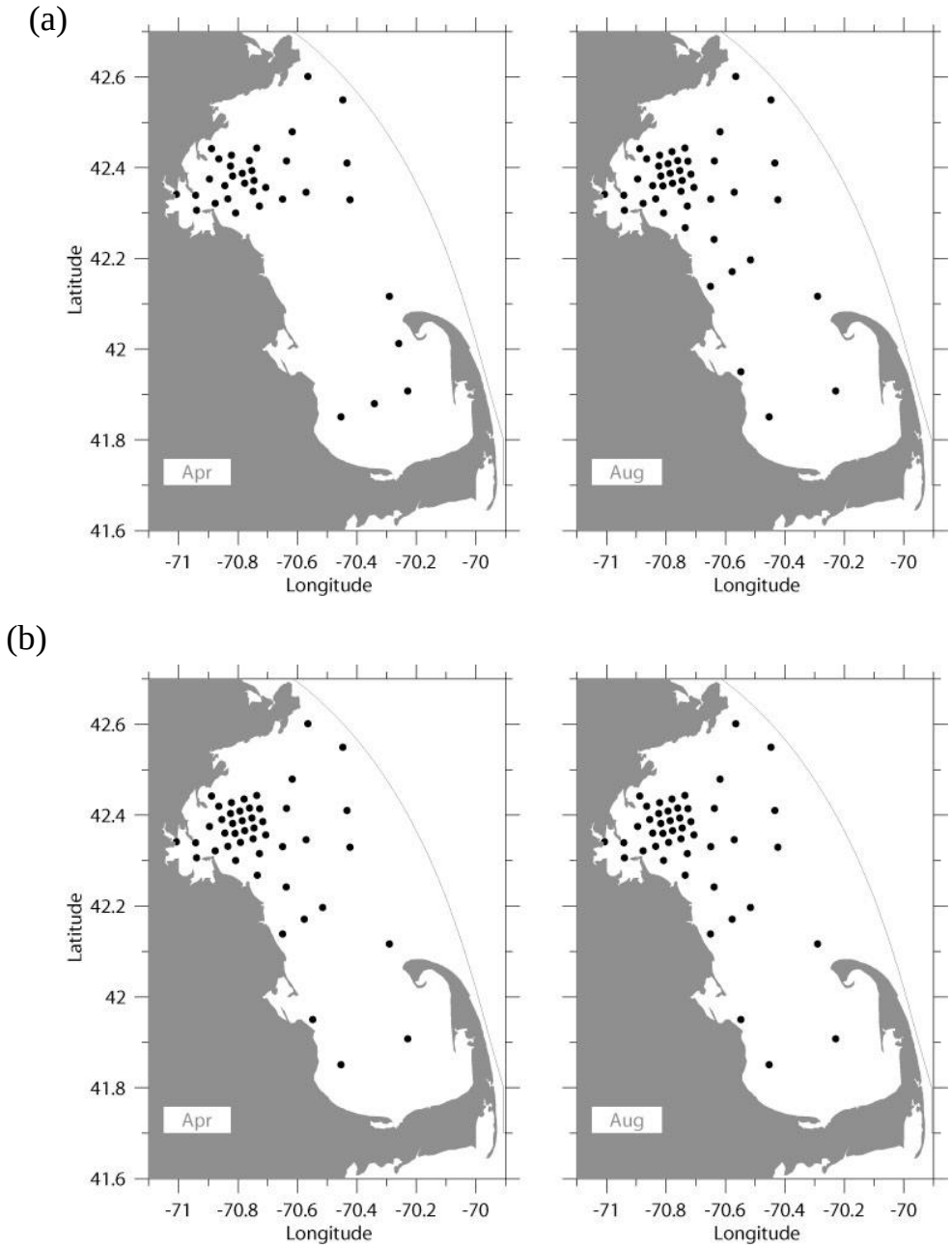

Figure 2.5. Station maps of available data in April and August, (a) 2000 and (b) 2001. Note that data collected at monitoring stations in Boston Harbor from Boston Harbor Water Quality Monitoring Project (not shown) are not included in the open boundary condition construction.

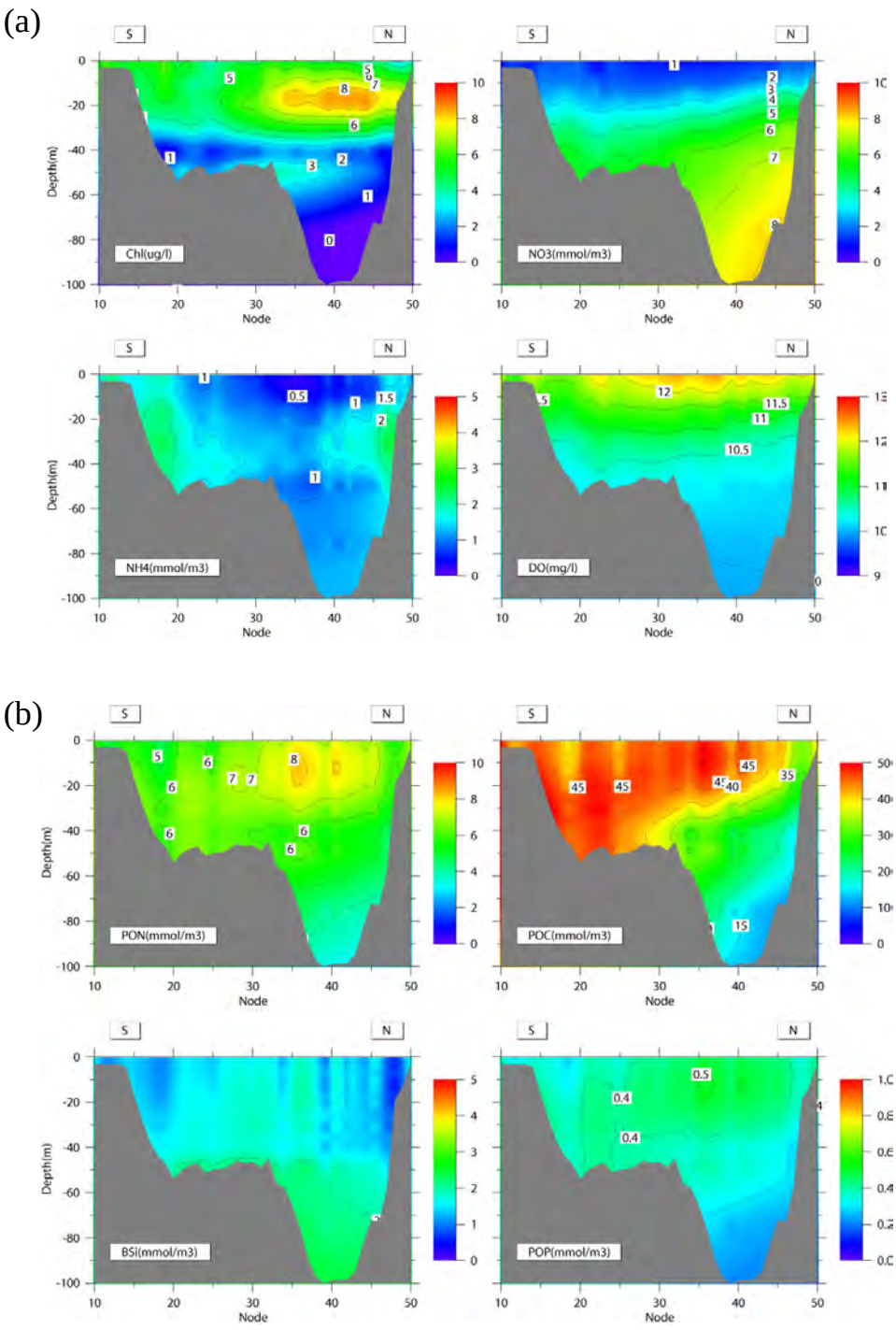

Figure 2.6. Open boundary conditions of (a) nutrients and (b) organic matter in April, 2000. Node 10 is near Race Point, and node 50 is close to Cape Ann.

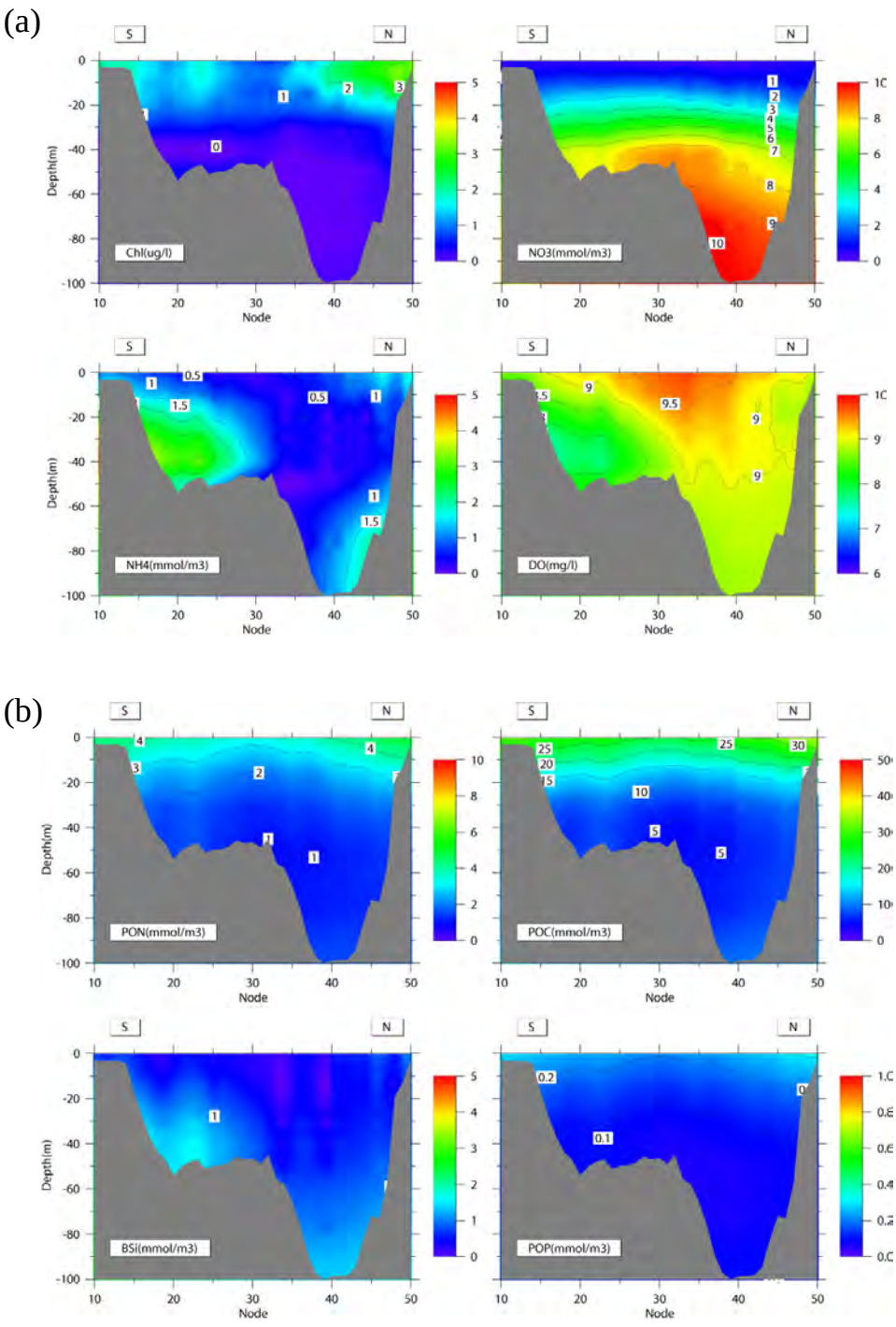

Figure 2.7. Open boundary conditions of (a) nutrients and (b) organic matter in August, 2000. Node 10 is near Race Point, and node 50 is close to Cape Ann.

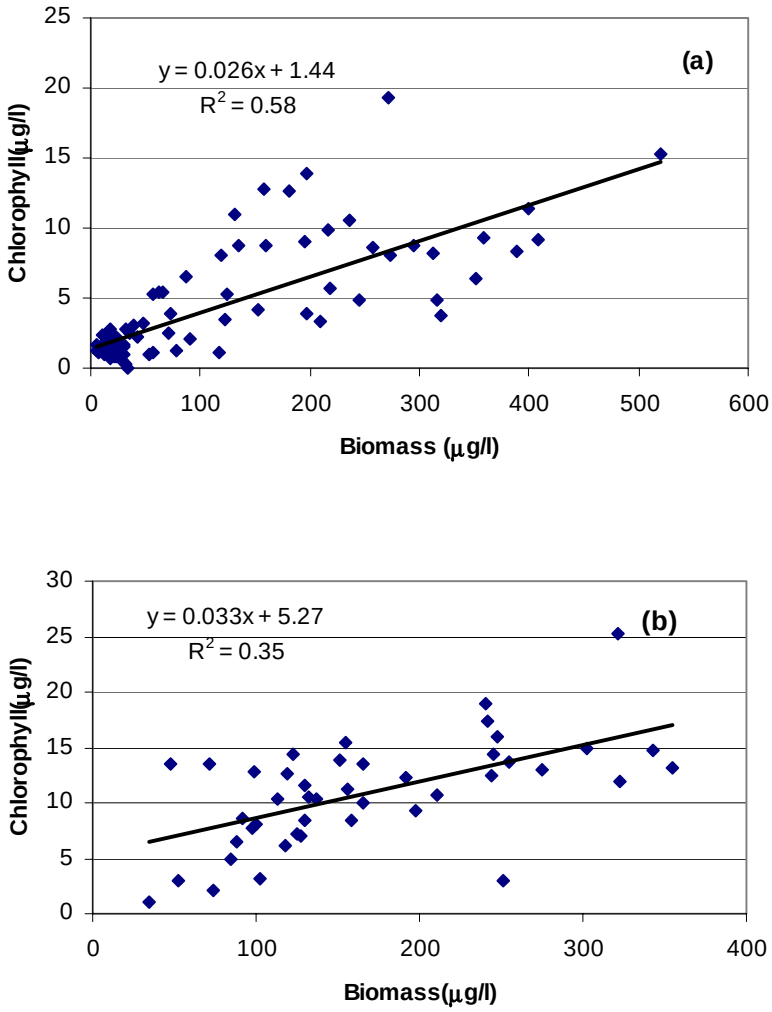

Figure 2.8. Regression between phytoplankton biomass and chlorophyll in (a) spring and (b) fall 2000.

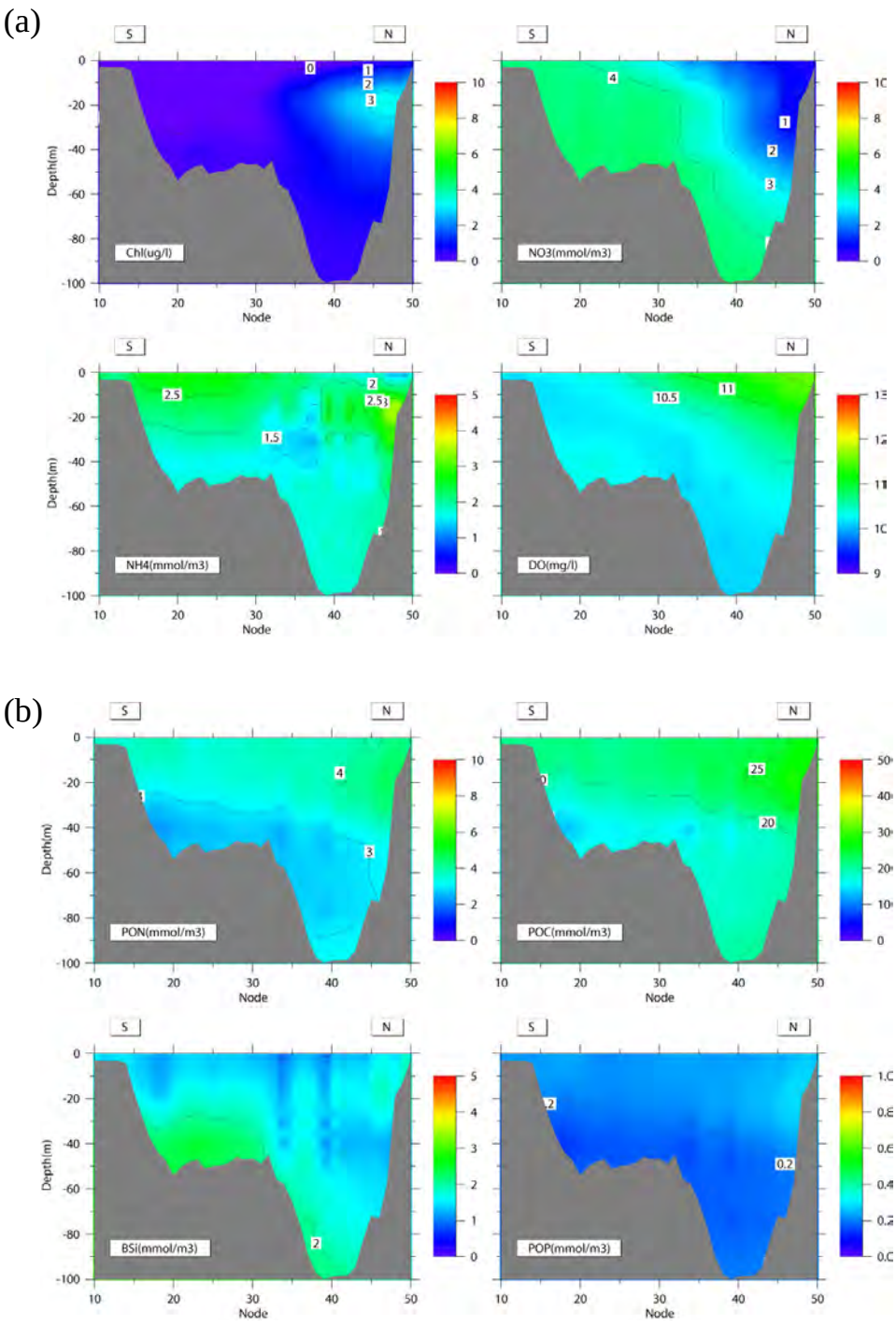

Figure 2.9. Open boundary conditions of (a) nutrients and (b) organic matter in April, 2001. Node 10 is near Race Point, and node 50 is close to Cape Ann.

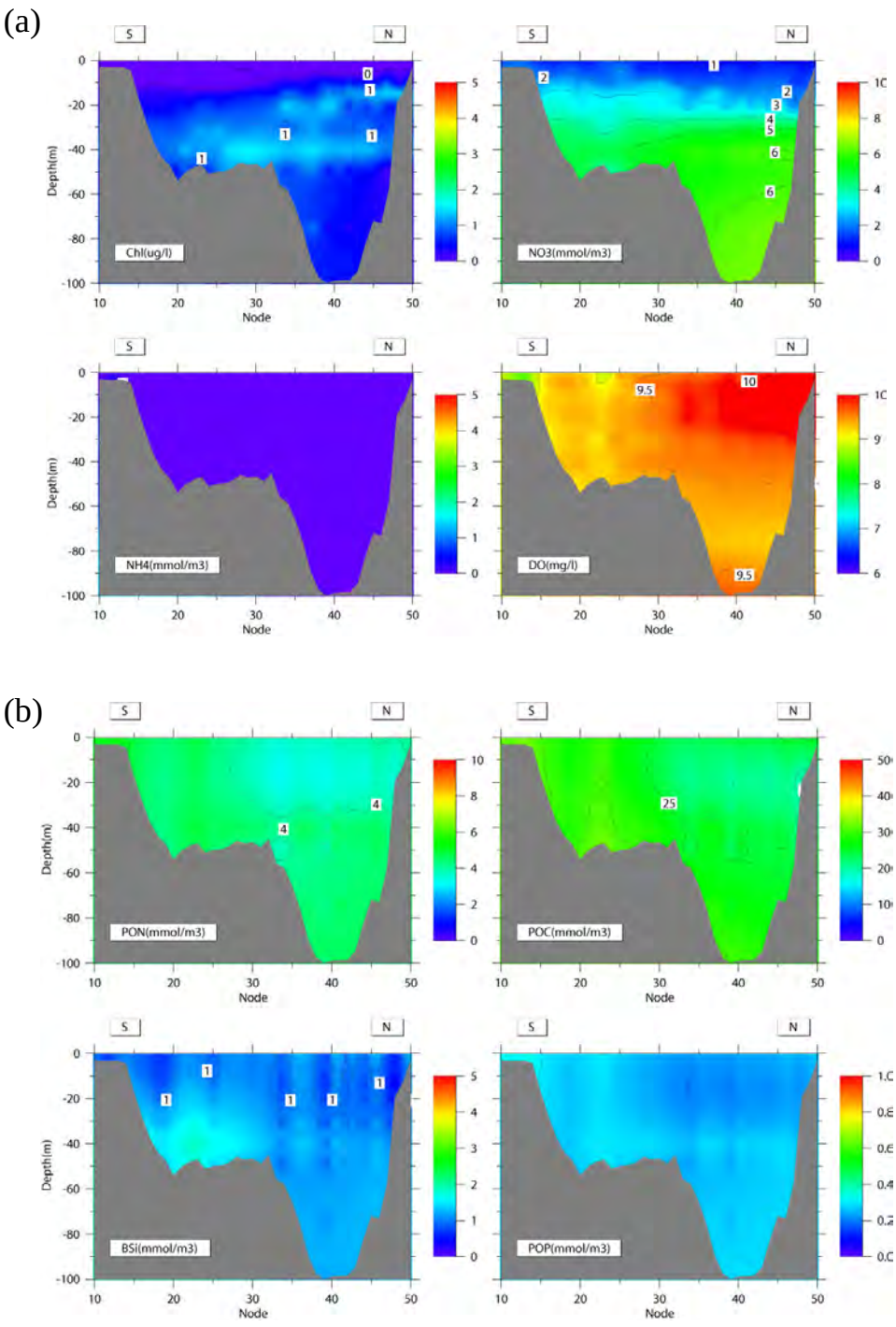

Figure 2.10. Open boundary conditions of (a) nutrients and (b) organic matter in August, 2001. Node 10 is near Race Point, and node 50 is close to Cape Ann.

3. CALIBRATION

3.1 Survey and data descriptions

Hydrography and water quality have been monitored in the MBS with 17 cruises per year at 21 nearfield and 20 farfield stations. Among them, only 6 cruises covered the entire bay. Each cruise lasted approximately 5-7 days. In addition to hydrographic measurements, water samples were collected at five standard depths to measure a number of biological and chemical variables including chlorophyll, nutrients, organic matter, dissolved oxygen and phytoplankton abundances. Primary productivity is also measured at three stations. One was close to Dear Island (F23) and the other two were offshore in the nearfield (N04 and N18). Not all biological and chemical variables were measured at every station. Different combinations of parameters are measured at different stations following a sampling protocol. Discrete net tows are conducted at some stations for zooplankton abundances and taxonomic information. Detailed information about samples and data can be found in the MWRA reports (e.g., Libby et al., 2000; Libby et al., 2001).

The water quality in Boston Harbor was extensively monitored through the Harbor Monitoring Project (HMP) (e.g., Taylor et al., 2001). The program started in 1993 as part of the bay-wide monitoring effort with water quality data collected at 6 stations in the North Harbor and 4 stations in the South Harbor. The water quality data collected, however, were not used for the construction of open boundary conditions in previous simulations (1998-1999) and this simulation (2000-2001) since they are far away from the boundary. Nevertheless, limited comparisons will be made between the model results and the HMP observations in the following sections.

The benthic metabolism and nutrient cycling were studied by taking sediment cores at 4 stations in Boston Harbor and 4 stations in Massachusetts Bay (Tucker et al., 2001; Tucker et al., 2002). The coupling of water column and sediment were measured through a number of nutrient fluxes, including nitrate, ammonia, denitrification, dissolved silica and SOD.

3.2 Concentrations in the water column

3.2.1 Time series

Key water quality state variables, such as chlorophyll, DIN, PON, DON, SiO_4 (silicic acid, silicate), and DO, are chosen for model verifications at six stations shown in Figure 3.1a as used by HydroQual in 1998-99 model calibration (HydroQual, 2003).

Both modeled and observed chlorophyll concentrations at the surface and bottom show pronounced seasonal cycles at all of these stations in 2000 (Figure 3.2a). From observations, in the spring a strong spring bloom occurred except at F23 in Boston Harbor, in the summer the observed chlorophyll concentrations were usually very low except for some high values found at some stations; and in the fall a strong fall bloom occurred at most monitoring stations. The water quality model overall reproduces this seasonal cycle.

The mismatches between the modeled and observed chlorophyll include: 1) the modeled spring bloom is weaker than the observed, 2) the modeled fall bloom peaks approximately two weeks behind the observed, and 3) at station F23, the high chlorophyll values in late summer contradict the observations from the two cruises during that period. However, the data collected through the HMP shows a wide range of concentration in July and August, indicating strong variability of chlorophyll.

The comparisons of modeled and observed DIN show a remarkable agreement at most stations except F01 and F23 (Figure 3.2b). This agreement indicates that the model correctly reproduces the seasonal patterns of the nitrogen cycling, including strong biological uptake during blooms and later regeneration processes, though modeled chlorophyll values show some differences from observations. At station F23 modeled DIN decreases rapidly in June along with a dramatic increase of chlorophyll, which occurred ahead of the observed decrease in DIN. Similarly, modeled SiO_4 agrees with data at most stations except F01 and F23 (Figure 3.2c)

The other two nitrogen pools, PON and DON, are compared in Figures 3.2d and 3.2e, respectively. The surface PON, surface DON and bottom DON agree well with observed data, but the model over-predicts the bottom PON by 2~3 fold most of the time. One

possible cause for this disagreement is the over-simplified zooplankton component used in the current model, that is, the zooplankton grazing in the model is imposed as 10% instantaneous removal of phytoplankton standing stock. Zooplankton removed phytoplankton biomass is directly added into total organic matter, which settles into bottom water causing the over-prediction of near bottom PON. This explanation is further supported by the over-prediction of POC concentration in bottom water (not shown).

The comparison between modeled and observed DO is shown in Figure 3.2f. Both modeled and observed DO show strong and consistent seasonal cycles at all stations. Both surface and bottom DO increase in winter and early spring due to deep mixing by surface cooling and wind stirring, and increasing primary production. They reach their peaks in February at shallow coastal stations (N10, F01 and F23) and in late March at offshore stations, and decline steadily throughout the late spring and summer, which is apparently associated with the decrease of saturation DO as the temperature increases in the water column. Surface DO reaches its minimum and remains so between August and October, and bottom DO reaches its minimum in late September and early October. Overall, the model reproduces this seasonal cycle quite well, though several differences can be identified. First, model under-predicts the peak DO concentration at the surface during the winter-spring transition. Second, modeled surface DO continues to decline from August to October, and modeled concentrations fall lower than the observed. Thirdly, the summer DO concentration at F23 is about 1-3 mg l^{-1} higher than the observed; this is consistent with the higher production and lower DIN simulated. During late summer, the lowest bottom DO in the MBS of about 5.5 mg l^{-1} is predicted at F01, which cannot be confirmed unfortunately from limited observations. The DO concentration observed during HMP is more variable and sometime the surface values agree with simulation results.

The comparison for year 2001 shows similar agreement between model runs and observations for most variables (Figure 3.3). The model run reproduces the spring and fall blooms of phytoplankton well, though it overestimates the summer chlorophyll, especially the bottom chlorophyll at shallow stations. The modeled spring bloom appears to be 2-3 weeks behind the observed. The modeled DIN again tracks the observed data

very well in most months except February, when modeled DIN is higher than the observed. This may be associated with the delay of the modeled spring bloom. Even in Boston Harbor, the modeled DIN during the spring and summer of year 2001 compares with observed data better than the year 2000 simulation. Similar to the simulation of year 2000, the surface PON compares reasonably well with data but the bottom PON is much higher than the observed in both the spring and summer. Modeled DON agrees remarkably with observed data except for a few extremely high values observed. SiO_4 also compares well with observed data except in Boston Harbor; modeled SiO_4 is nearly depleted in summer, while as high as 5 mmol m^{-3} of SiO_4 was observed. Modeled DO agrees with data well in most months except February, when the modeled DO is lower than observed probably due to the delay of the modeled spring bloom.

To examine the evolution of vertical profiles of nutrients and chlorophyll we chose three nearfield stations, N04, N10 and N14 (Figure 3.4-3.9). The model results at these three stations well represent the observed seasonal cycles, though the model variables appear to be more diffused vertically than observed. As indicated in the time series comparison at two fixed depths, both the modeled total DIN and chlorophyll at these stations agree well with observed data in showing strong seasonal variations especially associated with spring and fall blooms, though the timings of blooms are offset approximately 1-2 weeks. In 2001, the model over-predicts the sub-surface chlorophyll in late spring and summer at stations N10 and N14 (Figure 3.8-3.9). The model results also show several episodic events with the entrainment of high DIN into the mixed layer and phytoplankton blooms in summer for both 2000 and 2001. Each event lasts approximately one month and two weeks at stations N04 and N10, respectively. Comparisons of model results with observations for these short-term events prove to be difficult because monthly monitoring surveys missed most short term events except the chlorophyll bloom in July at station N04. At station N14, which is close to the MWRA new outfall site, both model and observations show very high concentrations of ammonia and nitrate since early September, 2000, which is likely contributed by the MWRA effluent (Figure 3.6). In 2001, model results at station N14 show continously high concentrations of ammonia and nitrate in the subsurface water since April, while the observed DIN concentration is lower and more variable most of the time.

While the modeled results for both years 2000 and 2001 agree with the observed reasonably well, the modeled results for 2001 are better in reproducing the magnitudes of spring and fall blooms than those of year 2000. One of possible reasons is the phytoplankton bloom patchiness in both space and time. For example, the surface chlorophyll on day 65 of 2000 at station N07 was about 4 times higher than that at a nearby station N04. Relatively, the chlorophyll patchiness in 2001 is reduced in our observations. It is possible that the stronger spring and fall blooms in 2000 could produce higher heterogeneity in chlorophyll distribution, which is more difficult to reproduce.

The modeled DO field in 2001 also compares better with observed than that of 2000, which is likely influenced by the boundary conditions and air-sea exchange algorithm. The open boundary of DO apparently affects the modeled DO in northwestern Massachusetts Bay (HydroQual, 2001). In 2000, the observed surface DO values at two boundary stations F26 and F27 on October 4 were less than 7.7 mg l^{-1}, the lowest in the year. On the contrary, the observed surface DO at F26 and F27 on October 21 2001 had already rebounded to higher than 9.3 mg l^{-1}. We suspect that there may be some uncertainties in the observations. Another cause for the mismatch between modeled and observed DO in late fall and early winter 2000 is likely due to an inadequate algorithm for surface air-sea exchange of DO. For example, the modeled DO concentration at F26 in late November 2000 is about 9.5 mg l^{-1}, while it is less than 8.5 mg l^{-1} at nearby N04, N07 and N10. A possible explanation is that the surface wind in late fall and early winter 2000 was stronger than that of 2001 (Figure 2.3). The surface DO concentration is more sensitive to the algorithm for air-sea DO exchange. A numerical experiment using a different algorithm yields a much better comparison (not shown).

3.2.2 Spatial structure

The spatial comparisons are made for biochemical variables along sections 1 and 2 (Figure 3.1). Since each monitoring cruise usually lasts 5-7 days, there are time gaps of several days between observations in the nearfield and farfield. The area map of an observed variable from a cruise is neither a snapshot of the observed variable at a given

time nor the mean distribution over the survey period. For convenience of comparison, we simply average the model results over a 3 day period centered at the median of each cruise period.

The modeled and observed nutrients and chlorophyll along section 1 in summer 2000 are shown in Figure 3.10. The modeled nitrate and DO well agree with observed data, whereas both modeled chlorophyll and ammonia are higher than the observed.

Along section 2, we compare three cases: the spring cruise in early April, the summer cruise in August and the fall cruise in early October (Figure 3.11). In the period between March 31 and April 3, the model results show similar patterns with the observed for all variables except ammonia (Figures 3.11 a and b). Both modeled and observed nitrate concentrations show a clear intrusion of high nitrate water from the Gulf of Maine. The model well reproduces the subsurface chlorophyll maximum extending from the mouth of Boston Harbor to the North Passage though it is more diffused vertically than the observed. The vertical gradient of DO around the thermocline is less pronounced than the observed.

During the period between August 16 and 20, modeled nitrate and ammonia show good agreements with observed data (Figures 3.11 c and d). Ammonia shows near bottom accumulation over the slope, corresponding to the low DO concentration in both the model results and observations. However, the observed high ammonia and low DO are restricted near the mouth of Boston Harbor while the model results extend further onto the shelf slope. The modeled DO shows coherent high values in subsurface and, deep basin waters. The modeled chlorophyll concentrates in the nearshore area, while the observations show relatively high values in offshore surface waters.

The effects of the new outfall site, which was online since September 6, 2000, can be clearly identified in the modeled high ammonia fields over the slope during the cruise in October 3-5, 2000 (Figures 3.11 e and f). The modeled ammonia is relatively diffused and stretched over the slope area. The modeled nitrate agrees well with observations both in spatial distribution and magnitude. The modeled chlorophyll and DO agree with the observed except near the North Passage where the modeled chlorophyll is lower than the observed and the model DO is much higher than the observed.

3.3 Primary productivity

The comparisons of vertically integrated primary production (PP) and net primary production (NPP) between modeled and observed in 2000 are shown in Figure 3.12, where the NPP is defined as PP minus respiration. The modeled PP and NPP at station N04 agree fairly with observed data. The modeled PP and NPP at N18 also agree with the observed except that the model under-predicts the production during three major blooms. At station F23, the observed PP and NPP were lower than 1 gC m^{-2} day^{-1} except in early April when both PP and NPP were higher than 5 gC m^{-2} day^{-1}. This observed seasonal pattern of production is very different from the modeled production, which increases continuously from winter to late summer and declines sharply in fall. This difference between modeled and observed production has been encountered during earlier simulations (HydroQual, 2000; HydroQual, 2003). For example, the observed PP and NPP peaked in early April and mid-June 1999 while the modeled PP and NPP peak in late August 1999.

The modeled PP and NPP in 2001 show similar seasonal variations to the observed at all these three stations (Figure 3.13). High PP and NPP during fall indicate a strong fall bloom as well, though the chlorophyll concentration was lower than that of fall 2000 (Figures 3.2a and 3.3a). In December, high productivity was observed at the two nearfield stations, which might be due to the presence of stratified conditions or increased nutrient availability (Libby et al., 2002). At station F23, the model clearly reproduces the seasonal pattern observed, though it still over-predicts the production in fall.

3.4 Sediment fluxes

The coupling between water column and sediment processes are verified through fluxes of nitrate (JNO_3), ammonia (JNH_4), silicate (JSi), phosphate (JPO_4), denitrification (JN_2) and SOD. The comparisons of modeled and observed in 2001 are shown in Figure 3.14. In Boston Harbor, the model reproduces the overall seasonal trends but fails to capture the magnitudes of most fluxes. The exceptions are the modeled phosphate and SOD fluxes, both of which are well compared with observed data in seasonal patterns and magnitudes. Modeled ammonia fluxes are much higher at these stations than the

observed except in Quincy Bay (BH08A). Both modeled nitrate and silicate fluxes well agree with observed data at stations BH02 and BH03, but are obviously lower than the observed data at station BH08A.

In Massachusetts Bay, model results agree well with the observed data in magnitudes at all stations. The model results show clear seasonal patterns in all fluxes which are not clear in observed data. The model under-estimates the silicate fluxes at station MB03 in July and at station MB05 in both the spring and summer.

The comparisons of modeled and observed nutrient fluxes in 2001 yield similar results to those of 2000 (Figure 3.15). One difference is that the observed SOD in Quincy Bay peaks much earlier than the modeled.

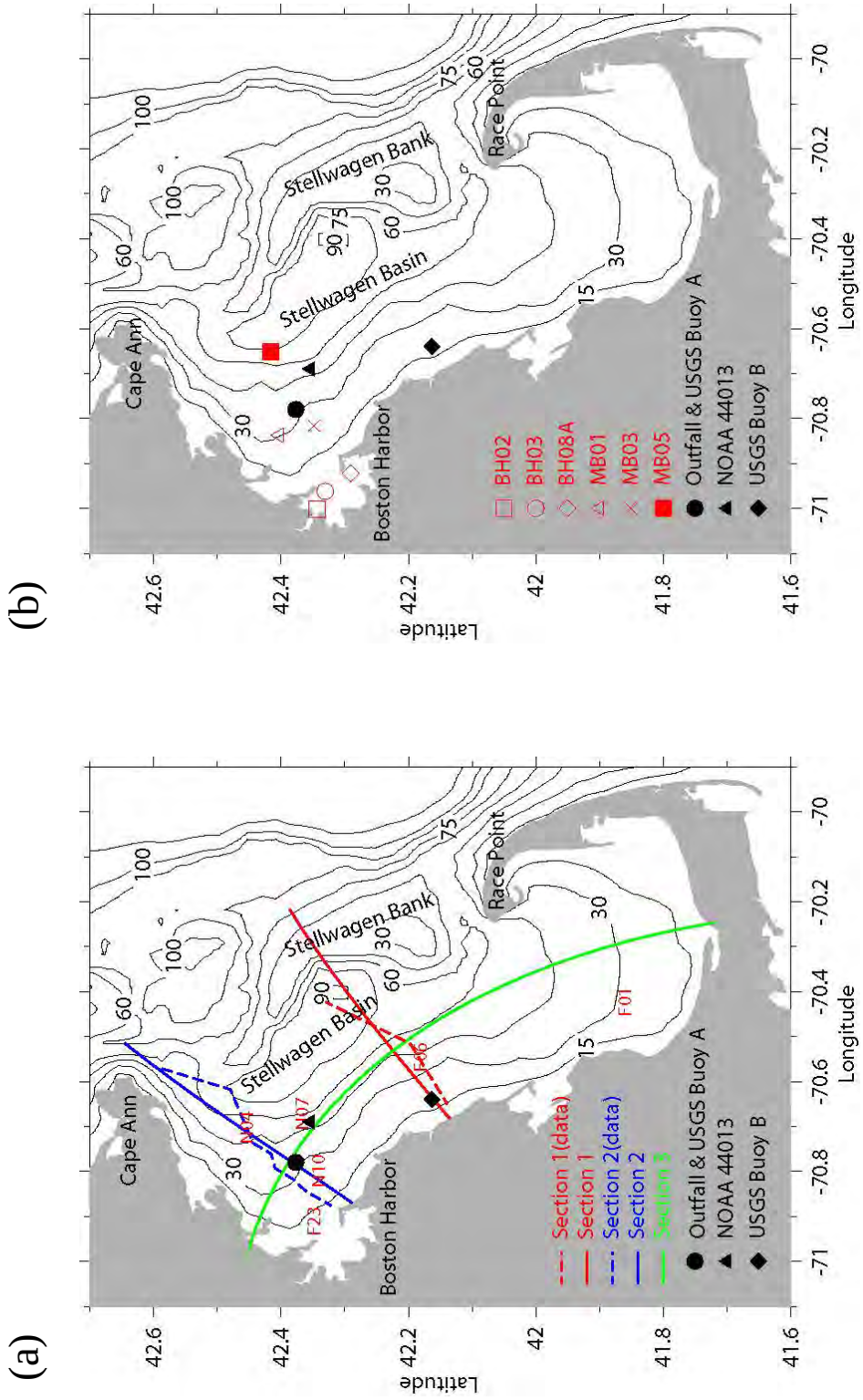

Figure 3.1. Station maps for the model calibration: (a) stations and sections for water column comparisons, and (b) stations for sediment flux comparisons.

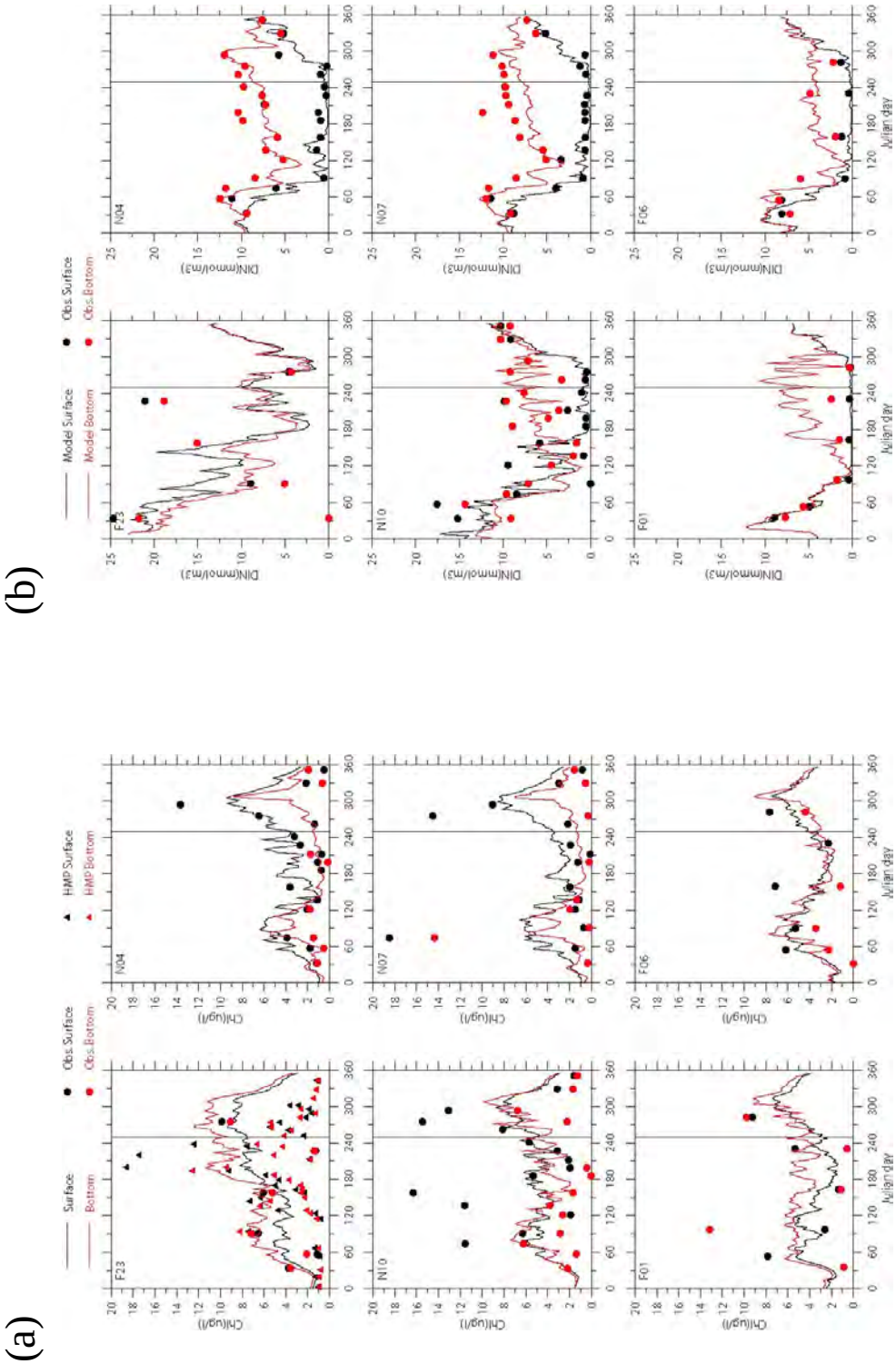

Figure 3.2. Time series of modeled and observed variables in 2000: (a) chlorophyll, (b) DIN, (c) SiO_4, (d) PON, (e) DON and (f) DO. HMP indicates harbor monitoring project. The solid vertical line marks the startup of new outfall discharge (day 249). (to be continued on the next page)

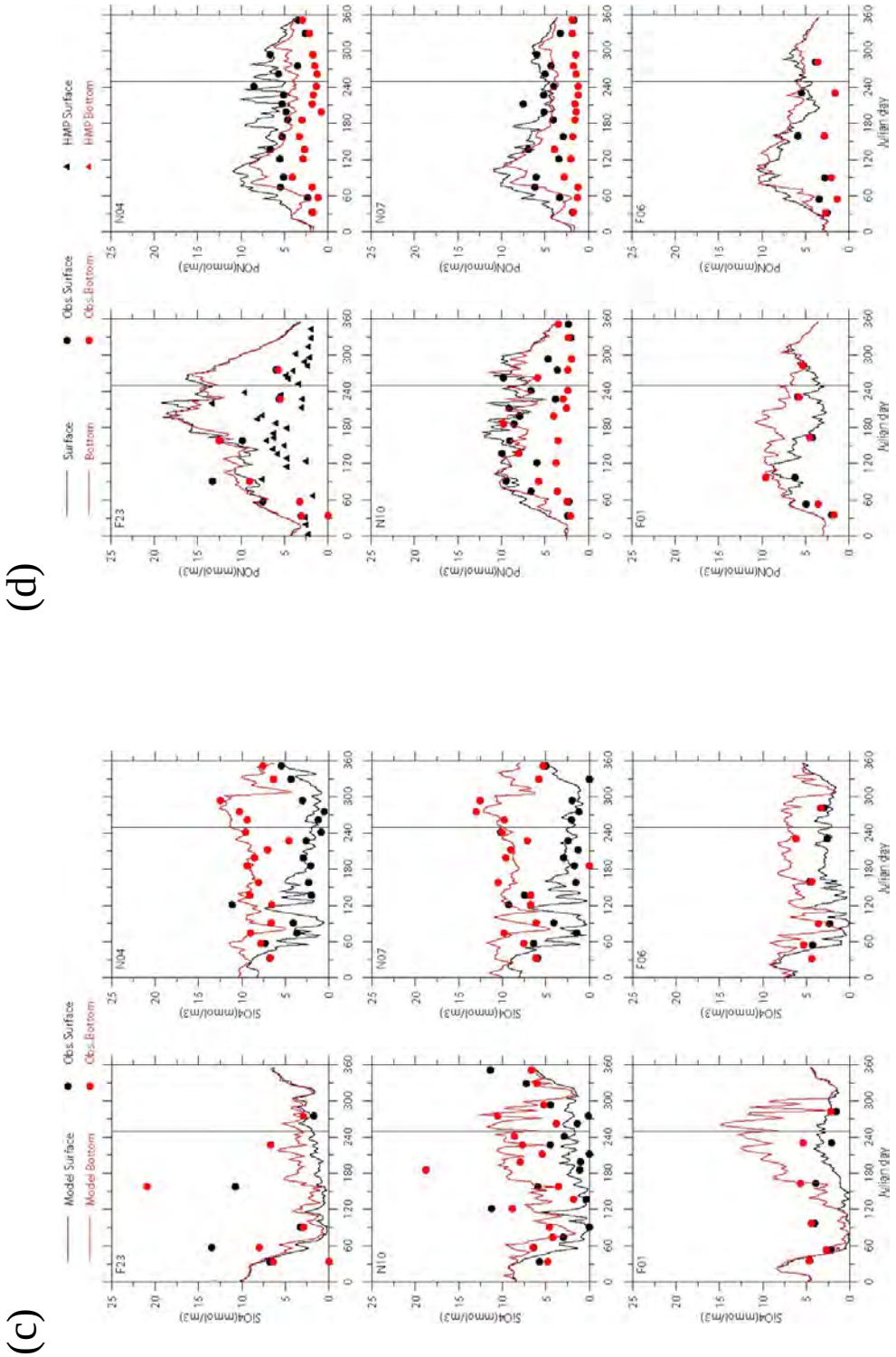

Figure 3.2. Continued.

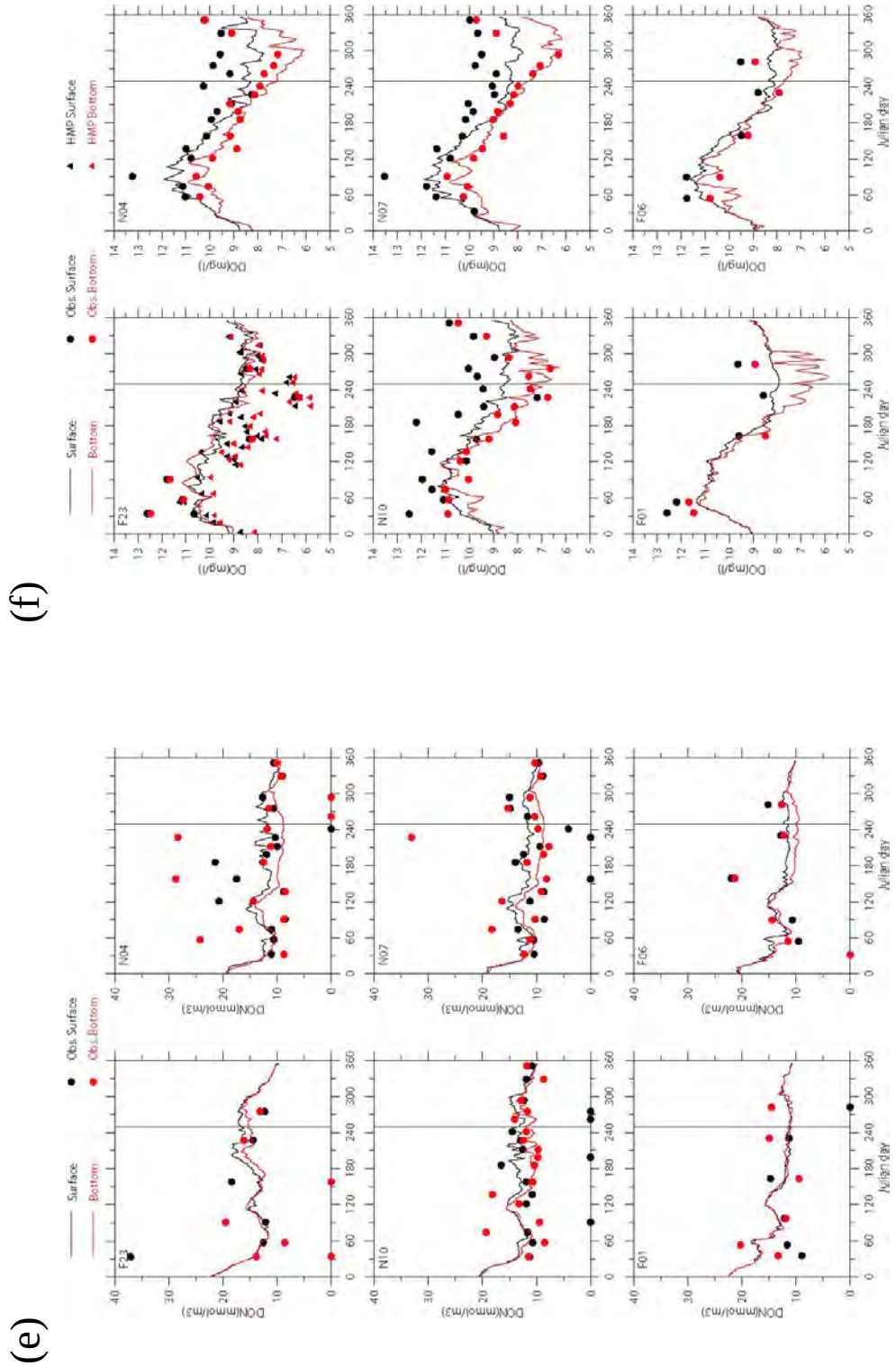

Figure 3.2. Continued

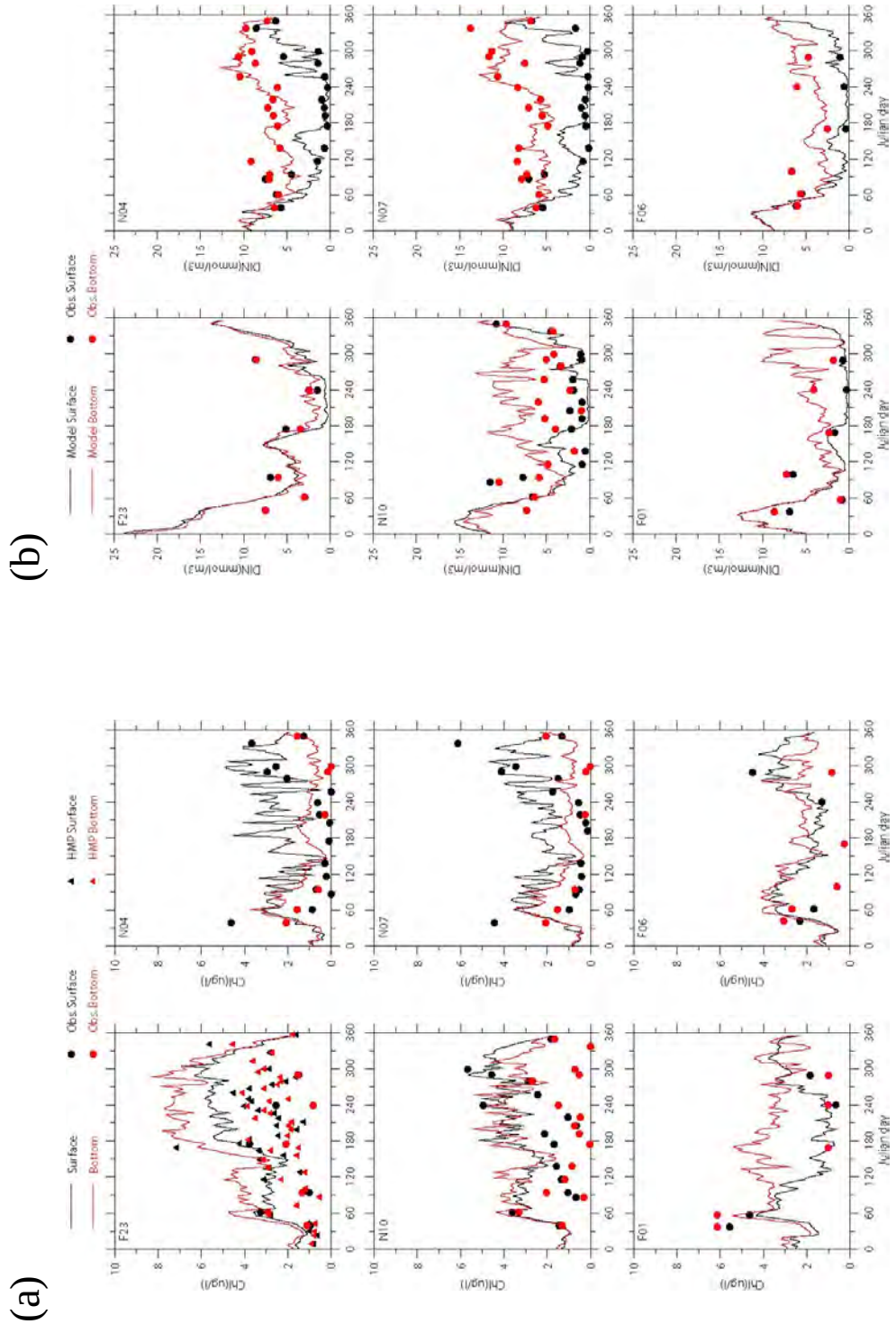

Figure 3.3. Time series of modeled and observed variables in 2001: (a) chlorophyll, (b) DIN, (c) SiO_4, (d) PON, (e) DON, and (f) DO. HMP indicates harbor monitoring project. (to be continued on the next page)

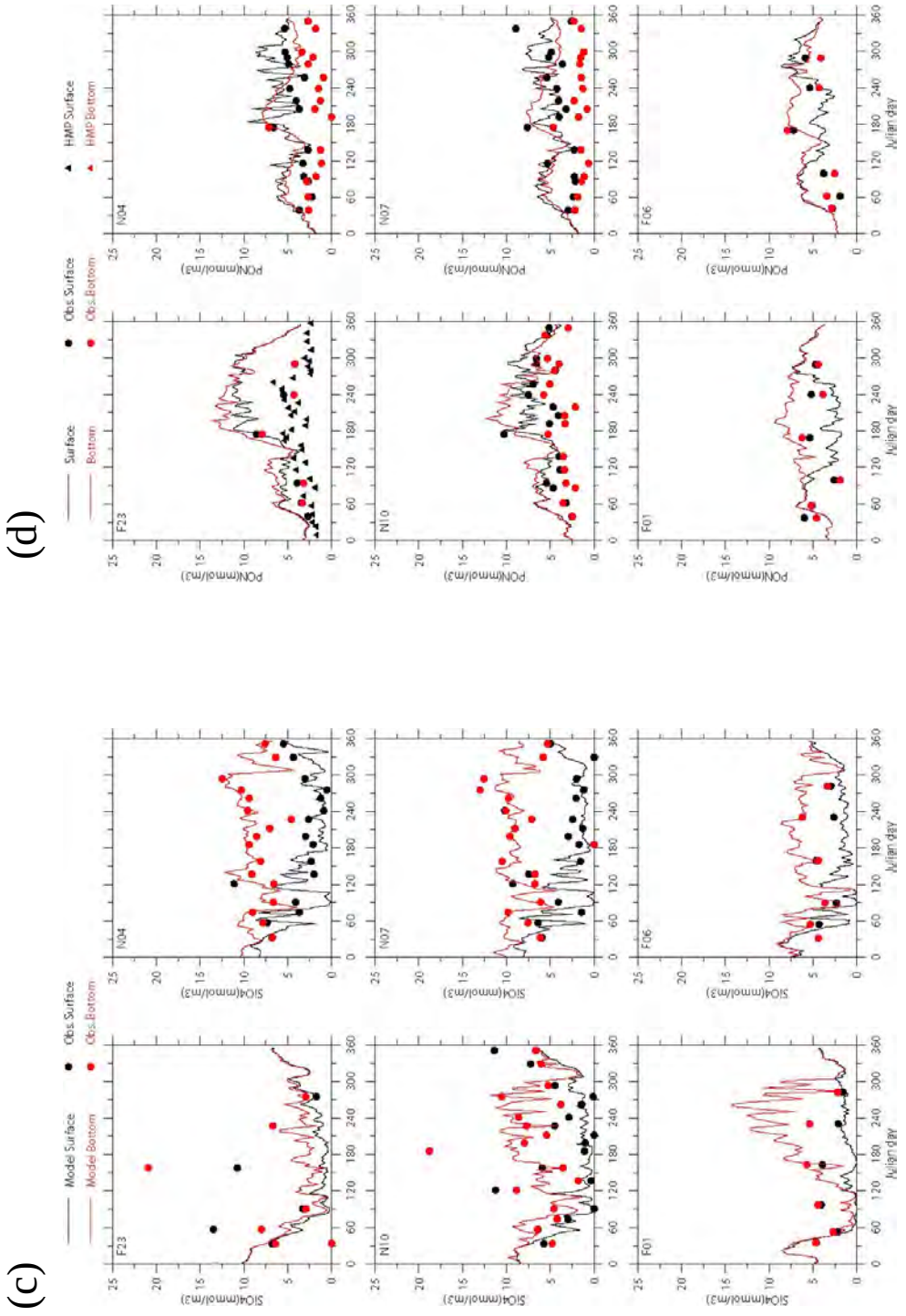

Figure 3.3. Continued.

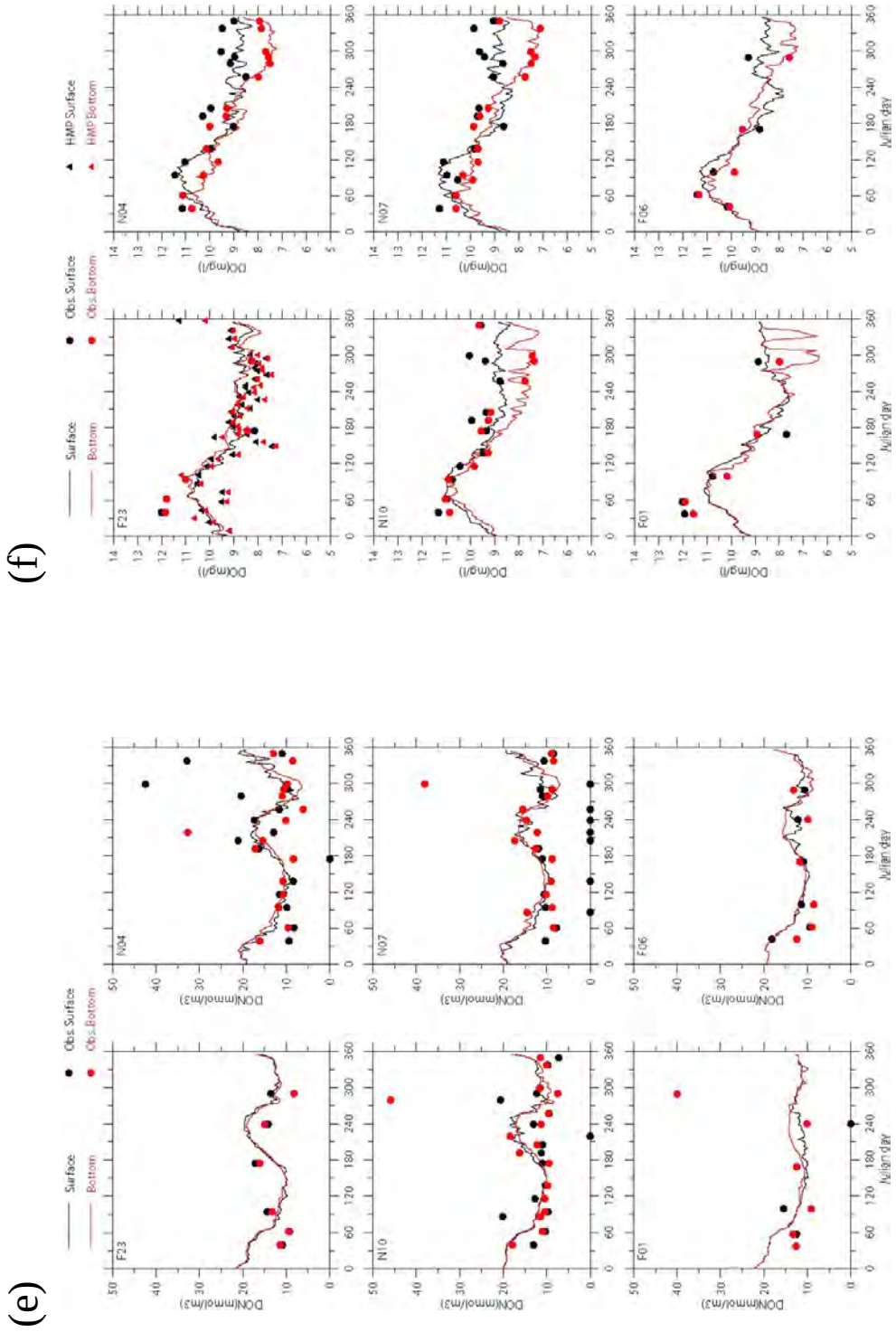

Figure 3.3. Continued.

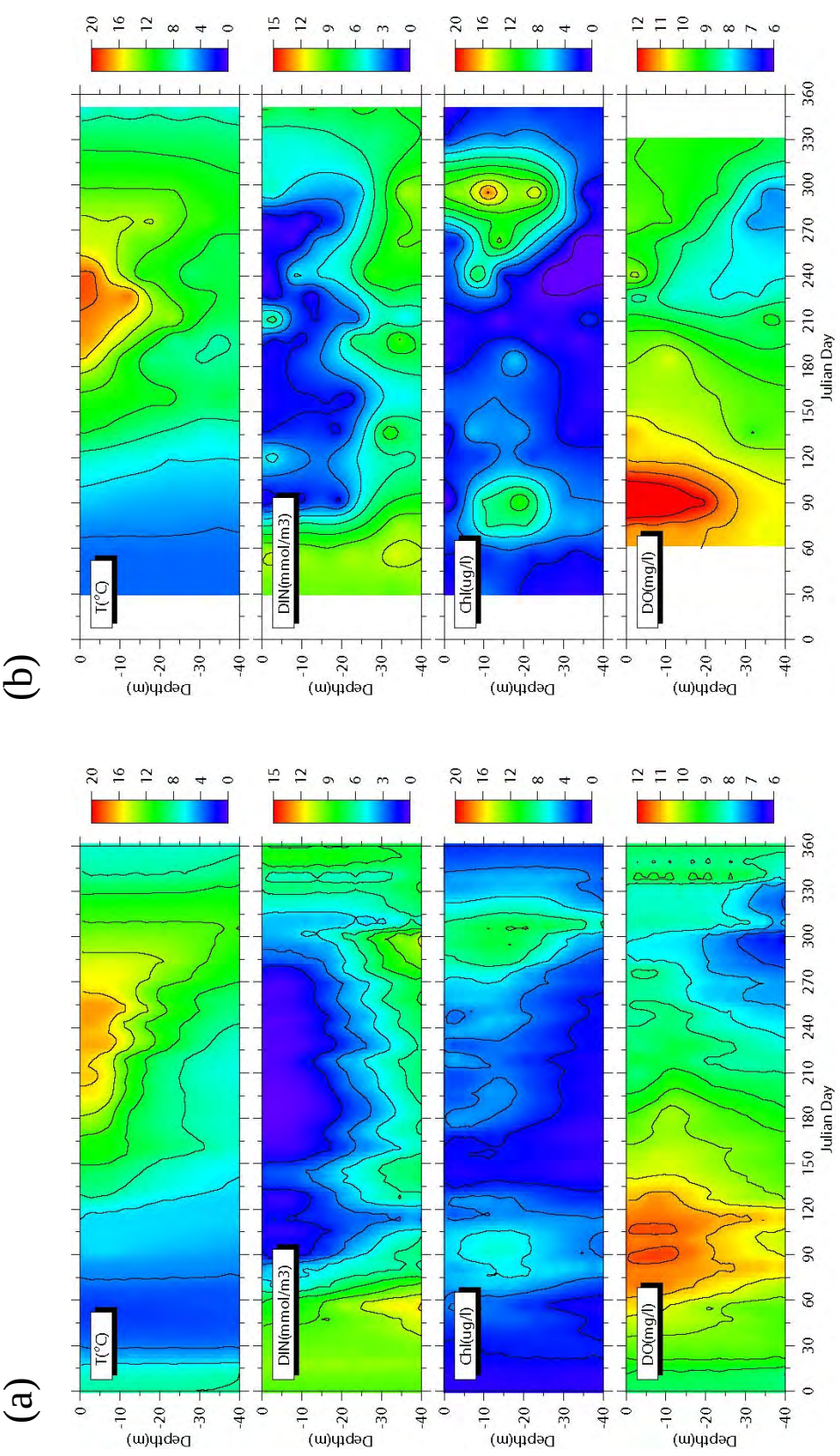

Figure 3.4. Time series of (a) modeled and (b) observed vertical distributions of temperature, DIN, Chl and DO at station N04 in 2000.

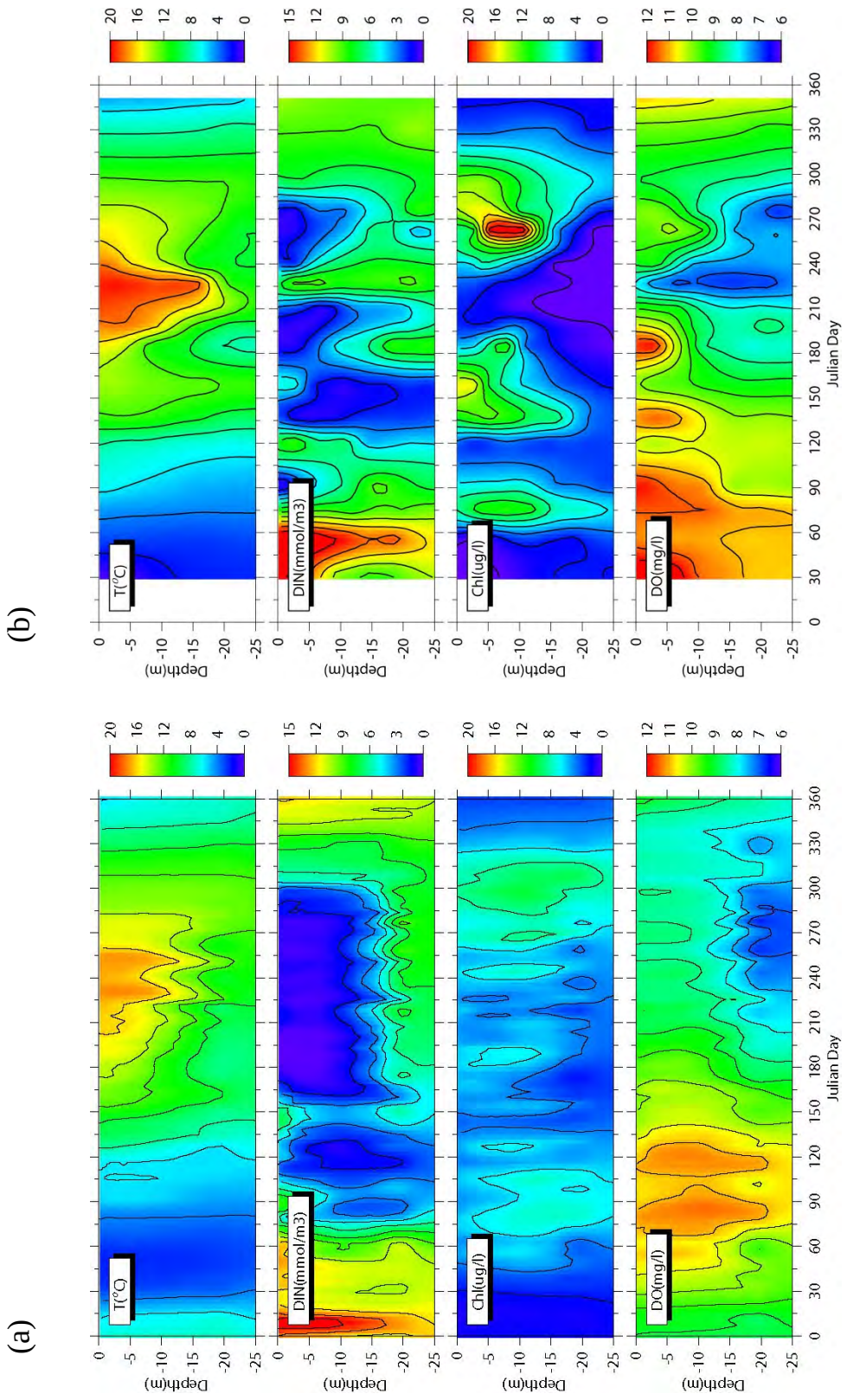

Figure 3.5. Time series of (a) modeled and (b) observed vertical distributions of temperature, DIN, Chl and DO at station N10 in 2000.

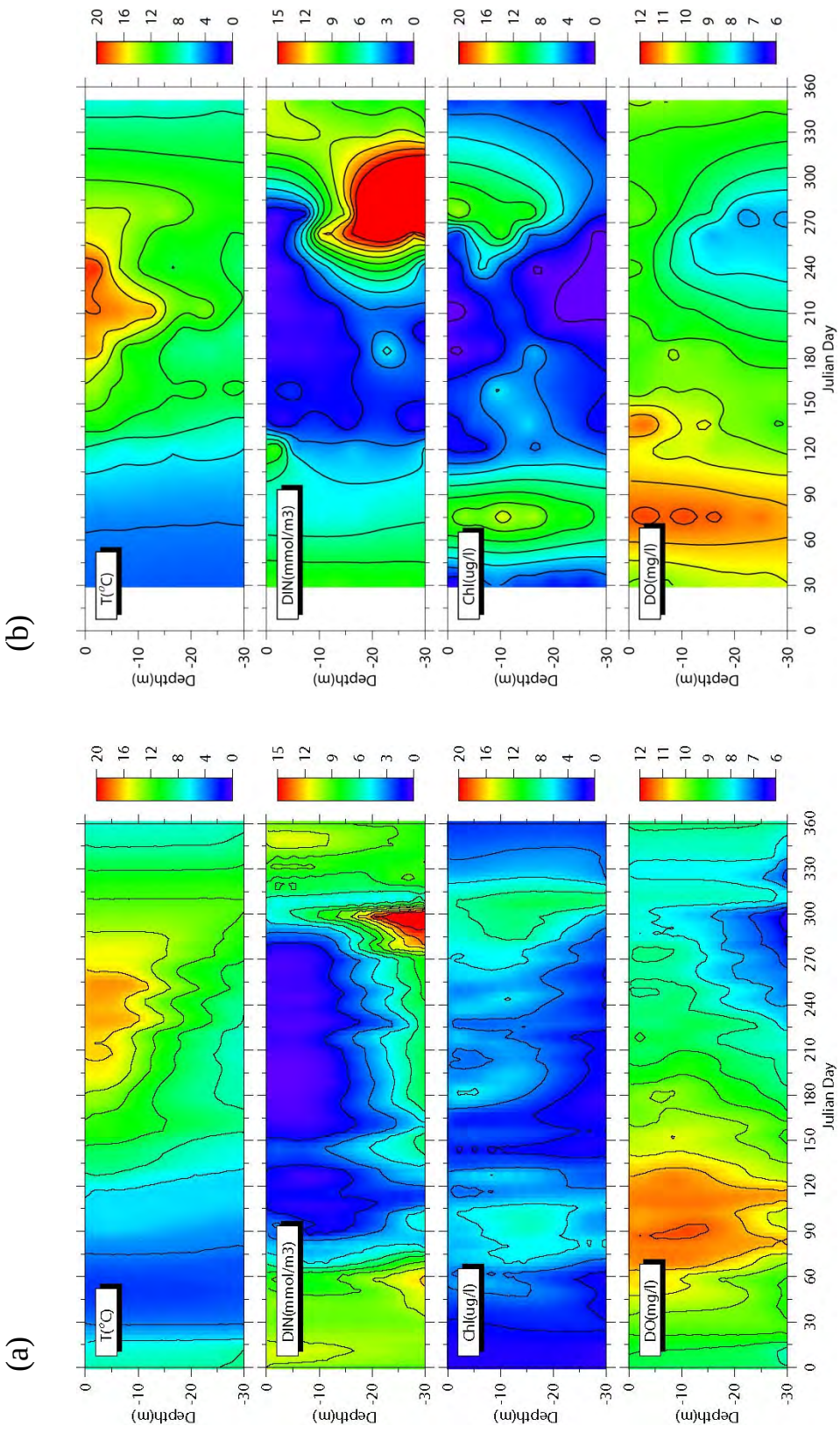

Figure 3.6. Time series of (a) modeled and (b) observed vertical distributions of temperature, DIN, Chl and DO at station N14 in 2000.

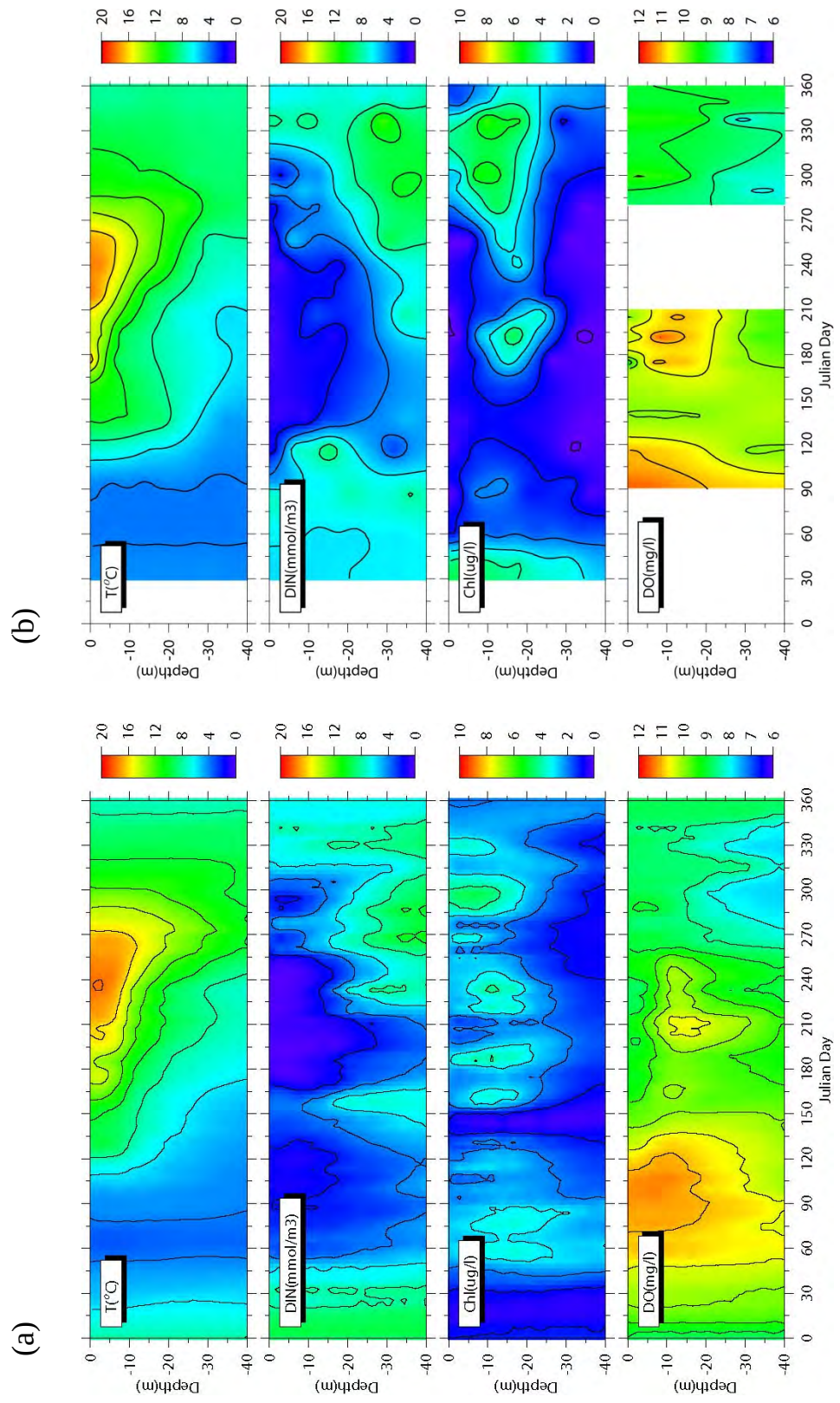

Figure 3.7. Time series of (a) modeled and (b) observed vertical distributions of temperature, DIN, Chl and DO at station N04 in 2001.

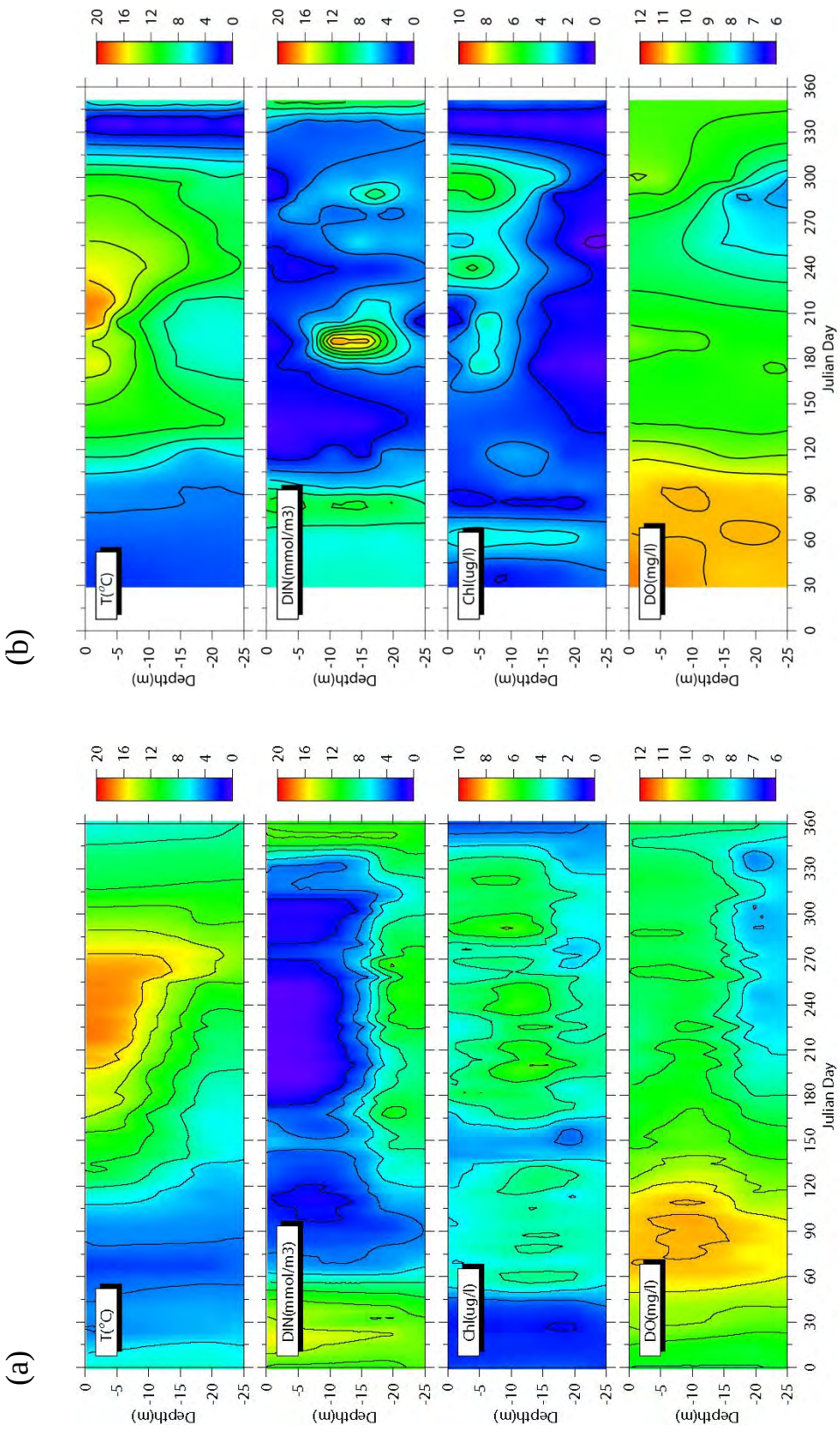

Figure 3.8. Time series of (a) modeled and (b) observed vertical distributions of temperature, DIN, Chl and DO at station N10 in 2001.

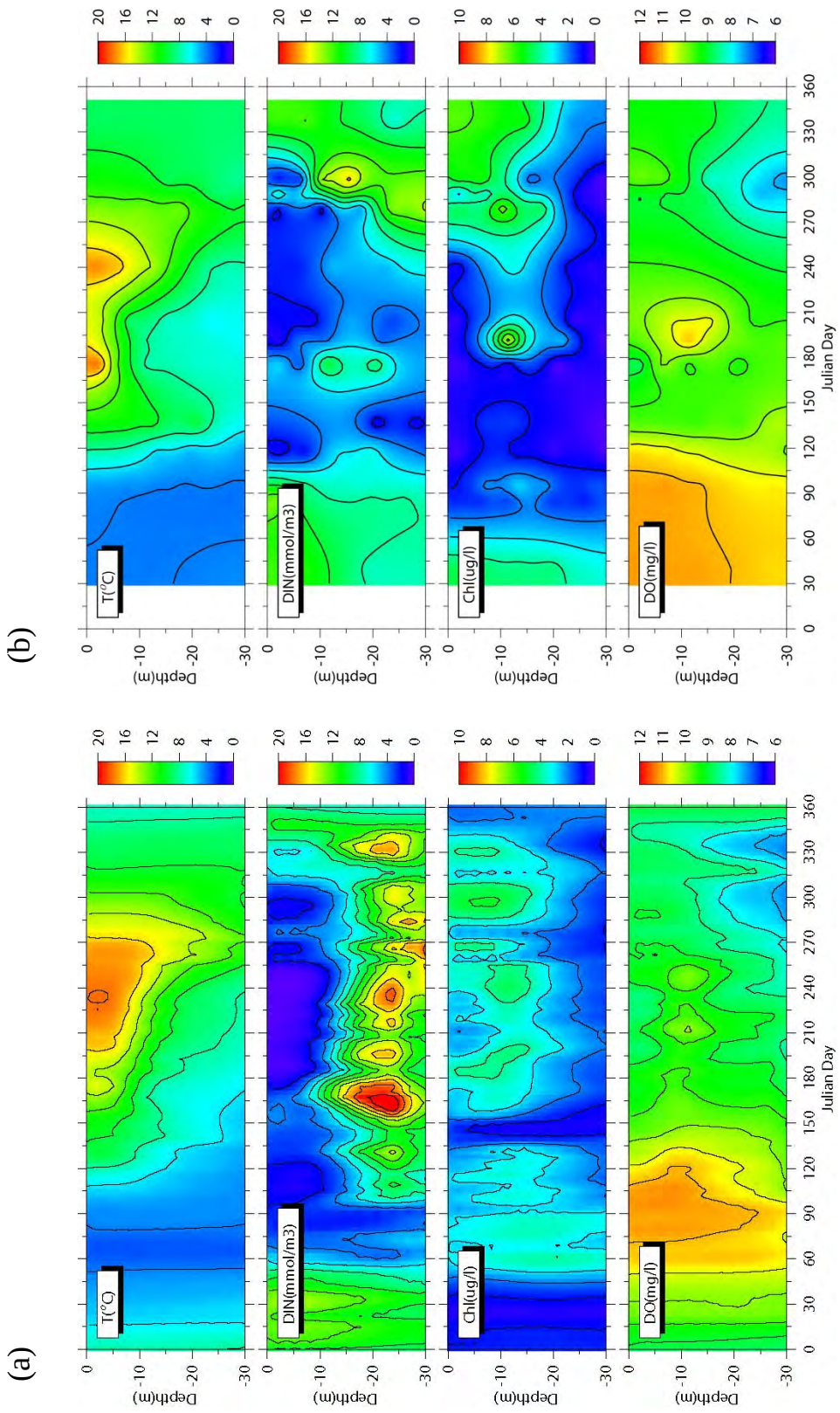

Figure 3.9. Time series of (a) modeled and (b) observed vertical distributions of temperature, DIN, Chl and DO at station N14 in 2001.

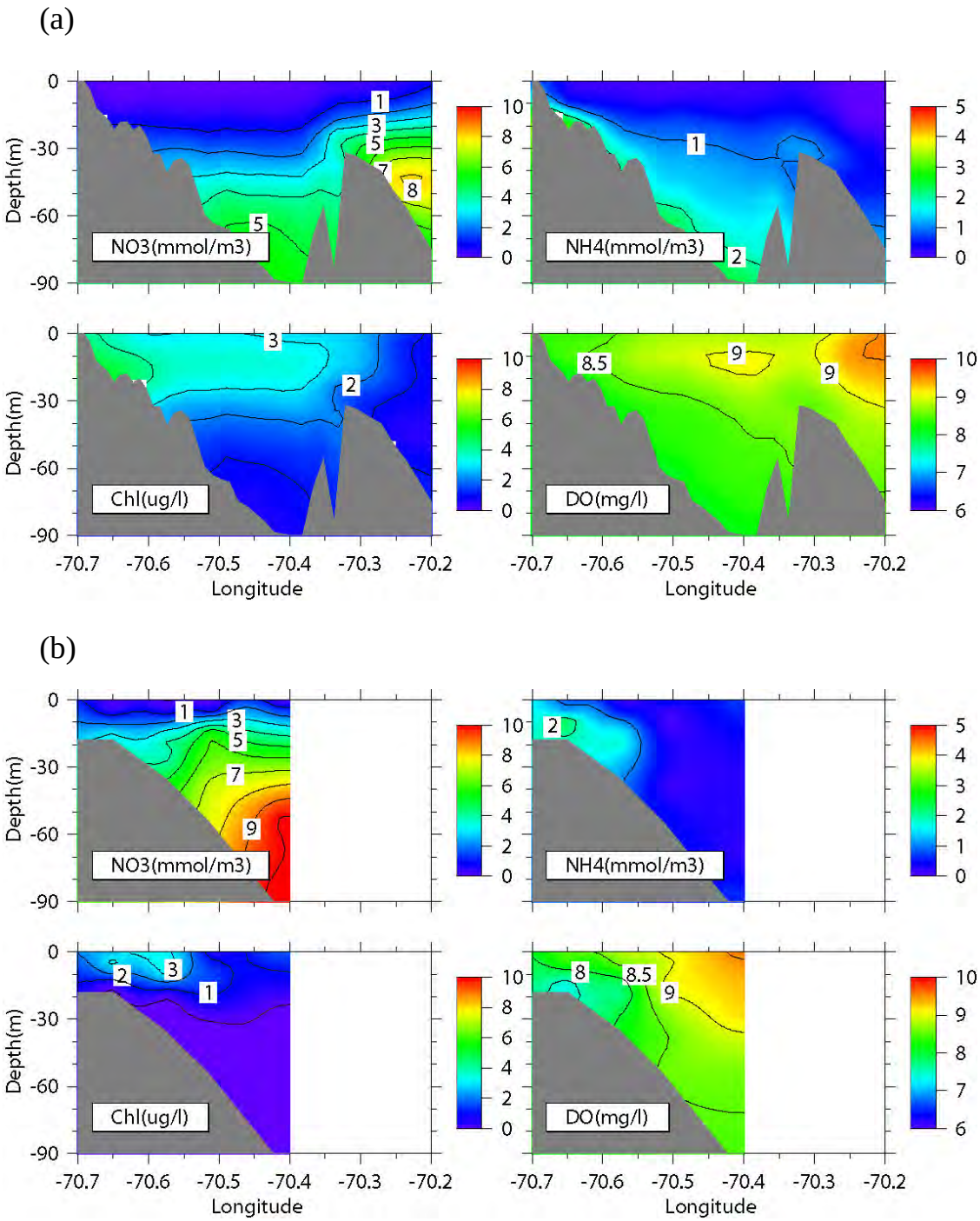

Figure 3.10. Vertical transects of NO_3, NH_4, chlorophyll, and DO along section 1 (Scituate to Stellwagen) on August 17, 2000: (a) model, and (b) observation.

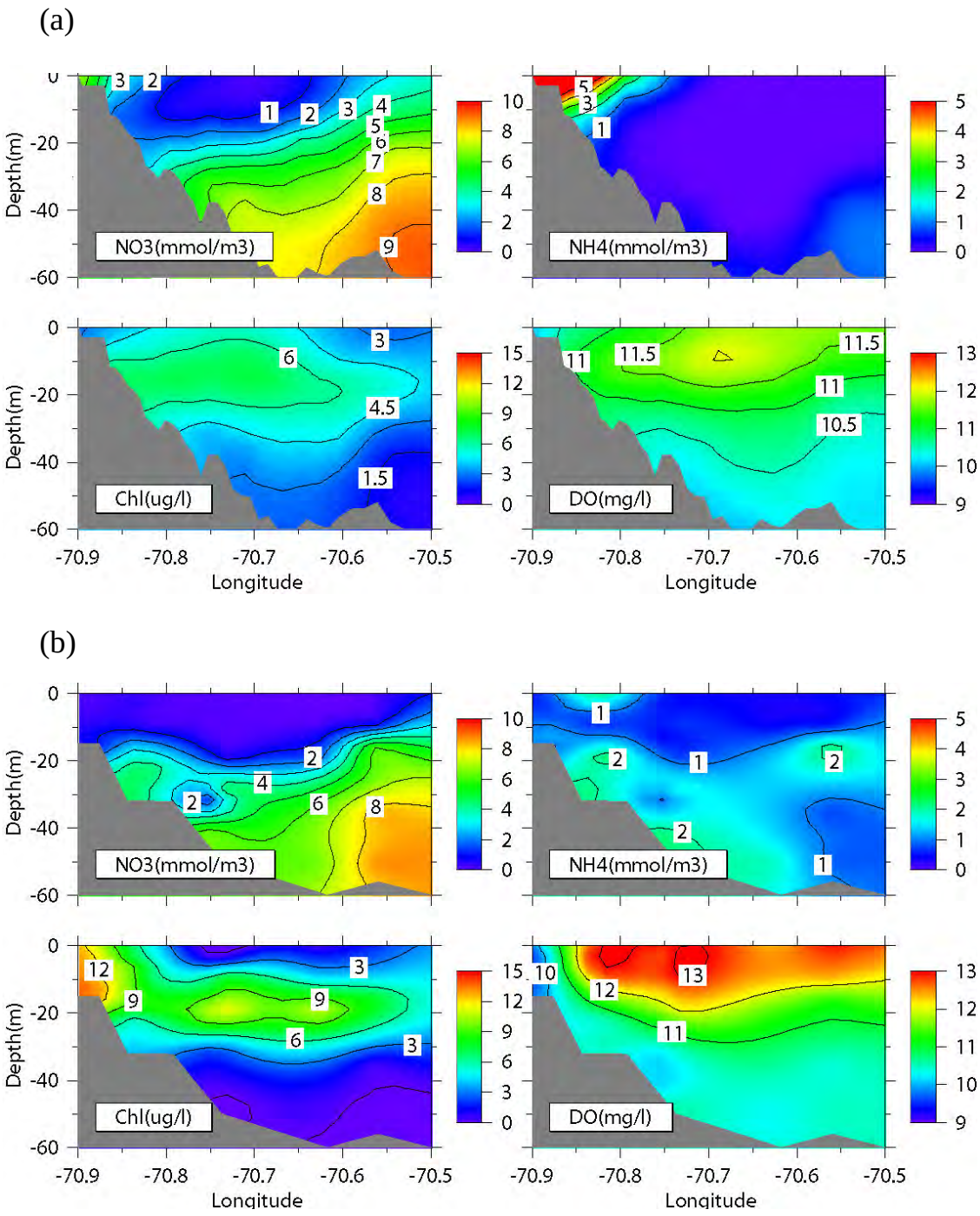

Figure 3.11. Vertical transects of NO_3, NH_4, chlorophyll, and DO along section 2 (Hull to North Passage) for selected cruises in 2000: (a) model on April 2, (b) observation in March 31-April 3, (c) model on August 17, (d) observation in August 16-20, (e) model on Oct.5, and (f) observation in Oct.3-5. (to be continued on the next page)

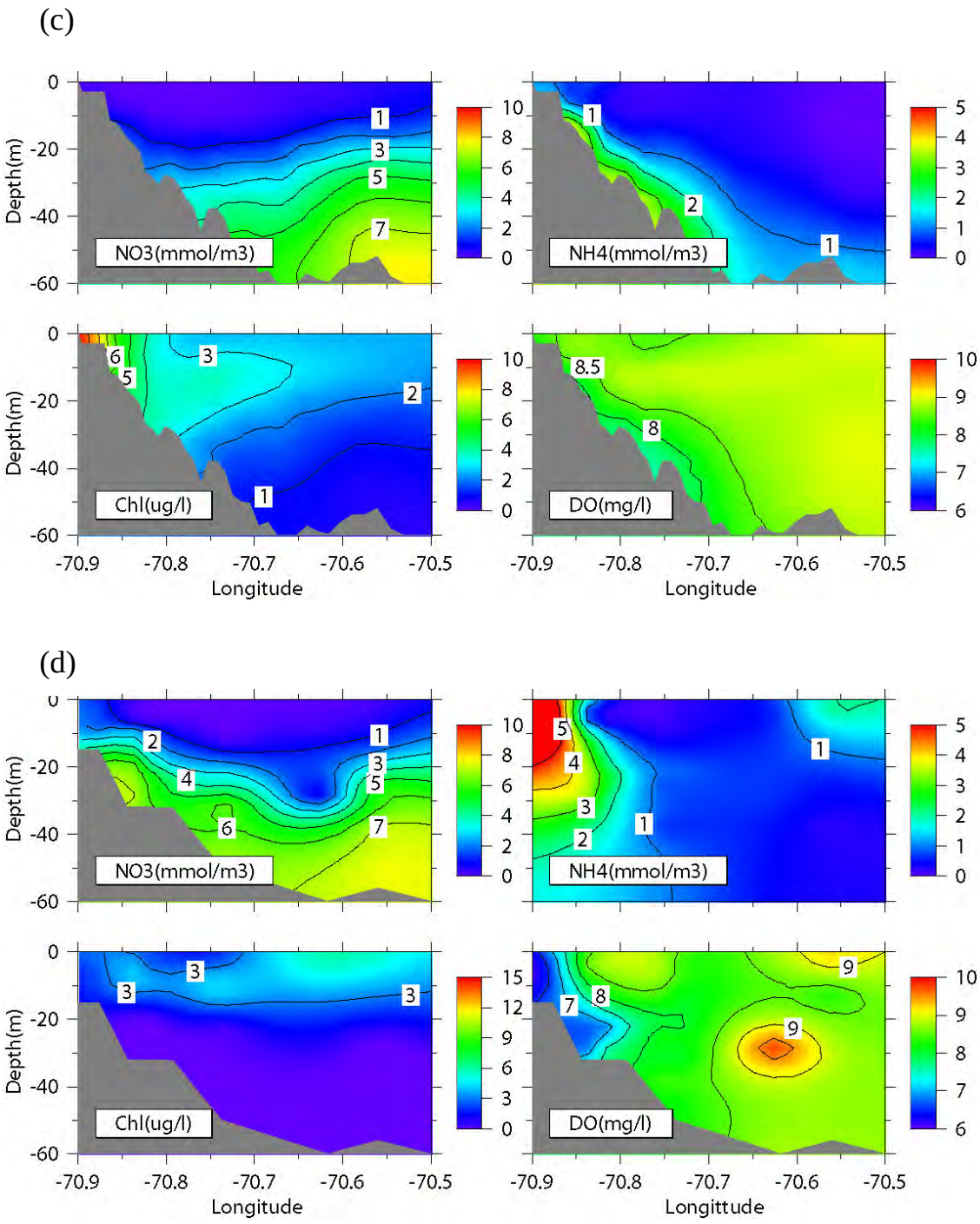

Figure 3.11. Continued.

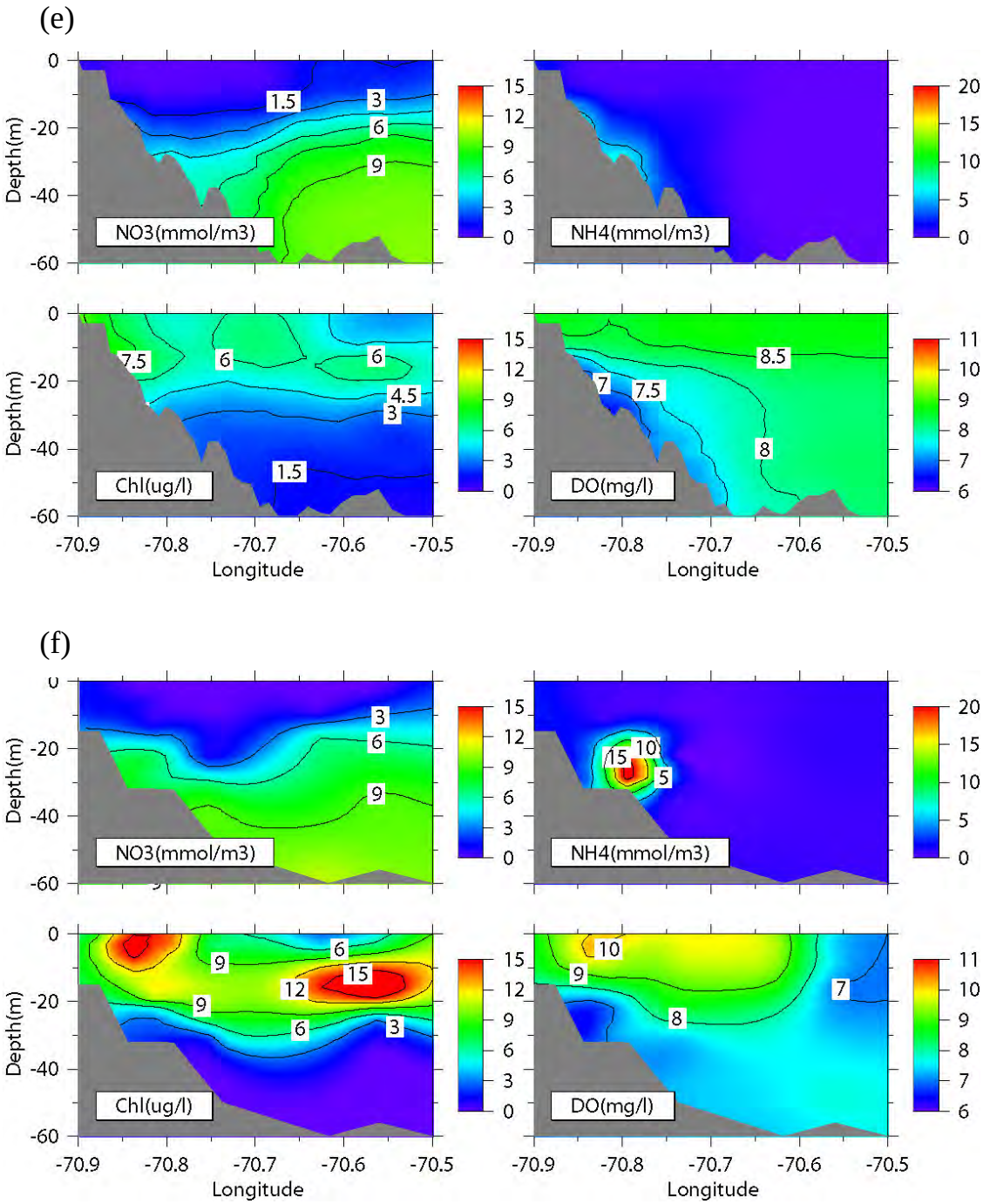

Figure 3.11. Continued.

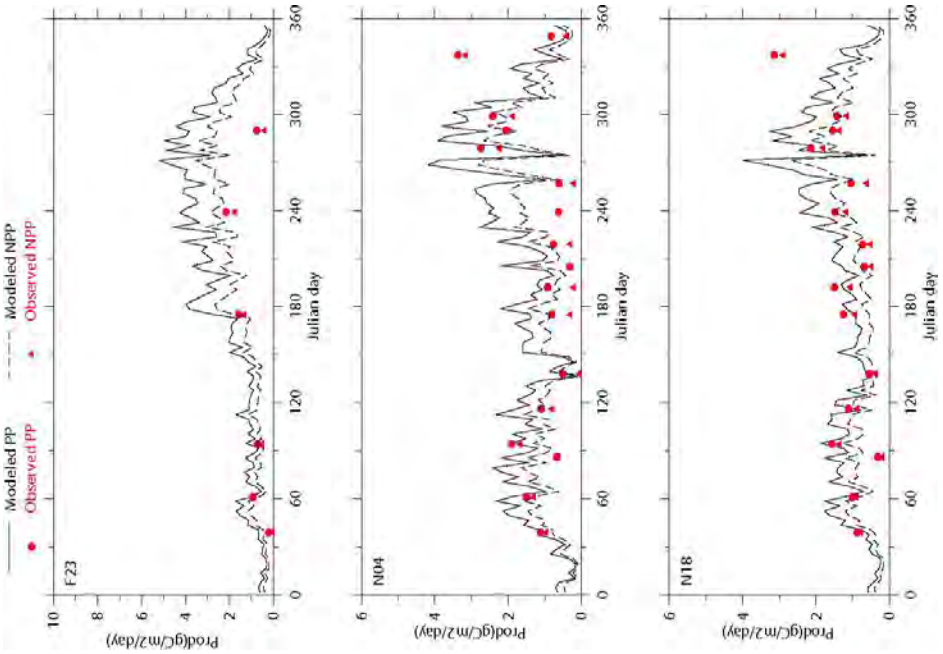

Figure 3.13. Modeled and observed primary production (PP) and net primary production (NPP) in 2001.

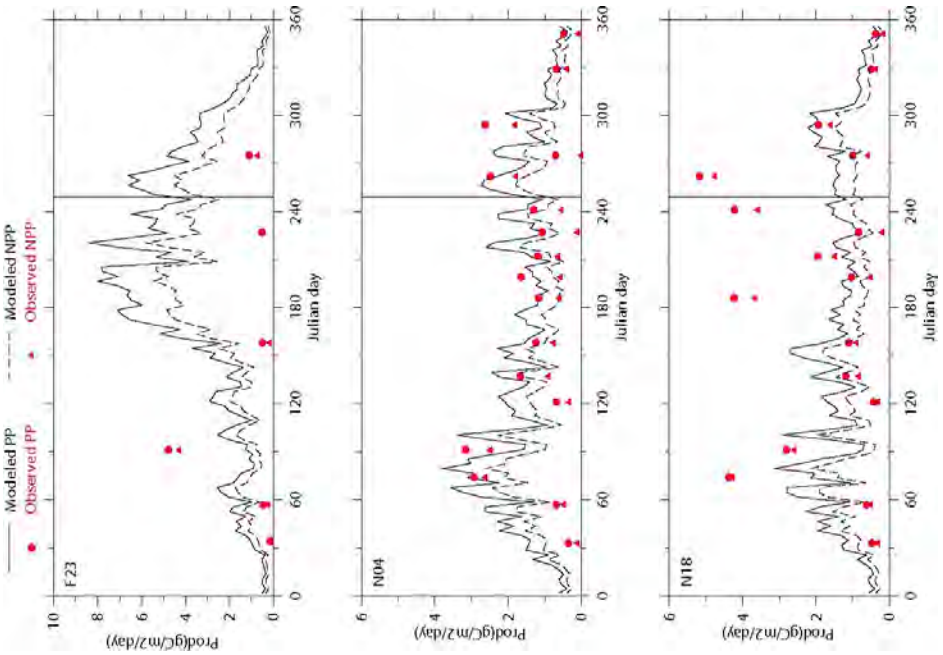

Figure 3.12. Modeled and observed primary production (PP) and net primary production (NPP) in 2000. The solid vertical line marks the startup of new outfall discharge (day 249).

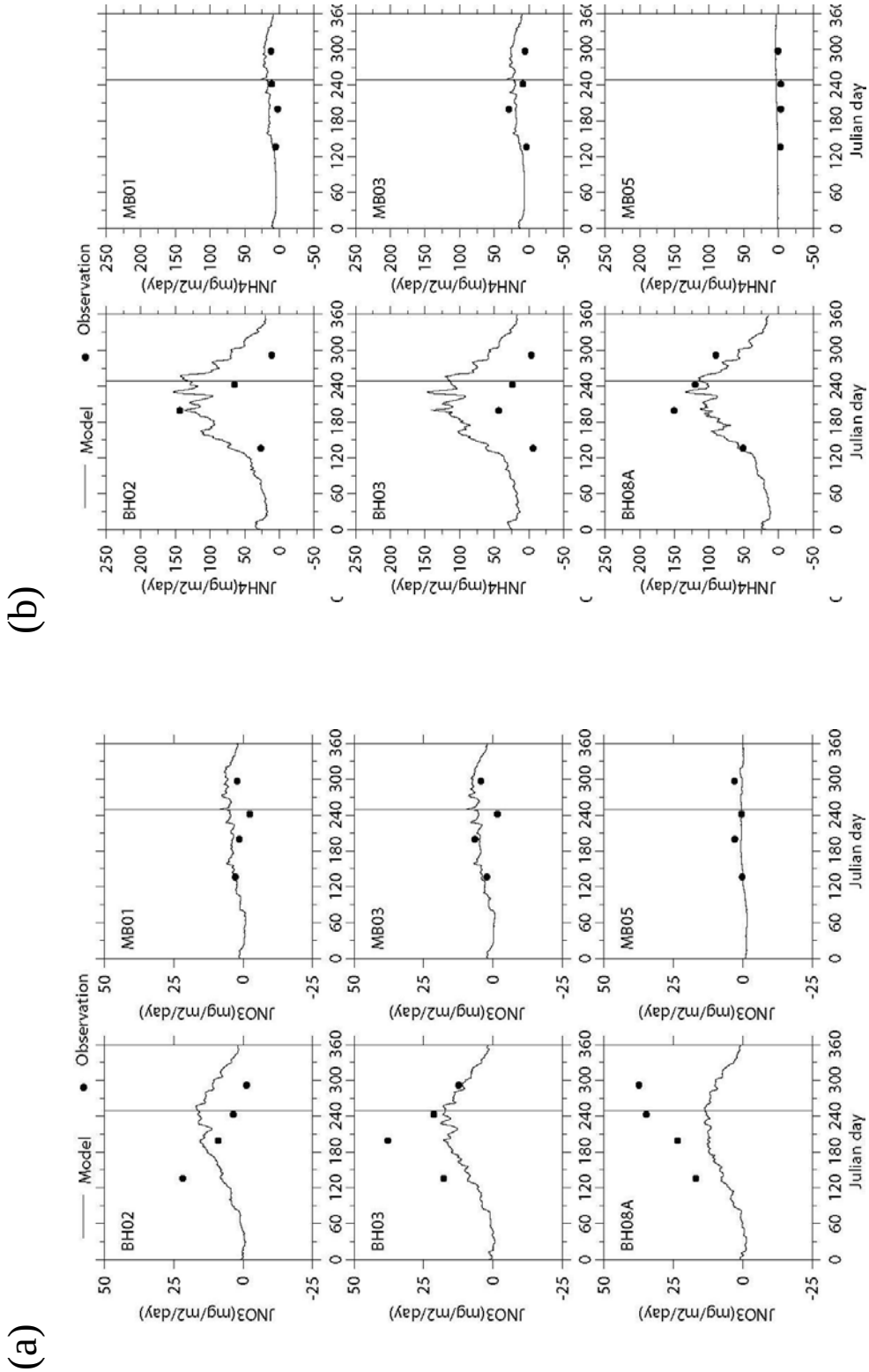

Figure 3.14. Nutrient fluxes and sediment oxygen demand in 2000: (a) JNO_3, (b) JNH_4, (c) JSi, (d) JPO_4, (e) SOD, and (f) JN_2. The solid vertical line marks the startup of new outfall discharge (day 249).

(to be continued on the next page)

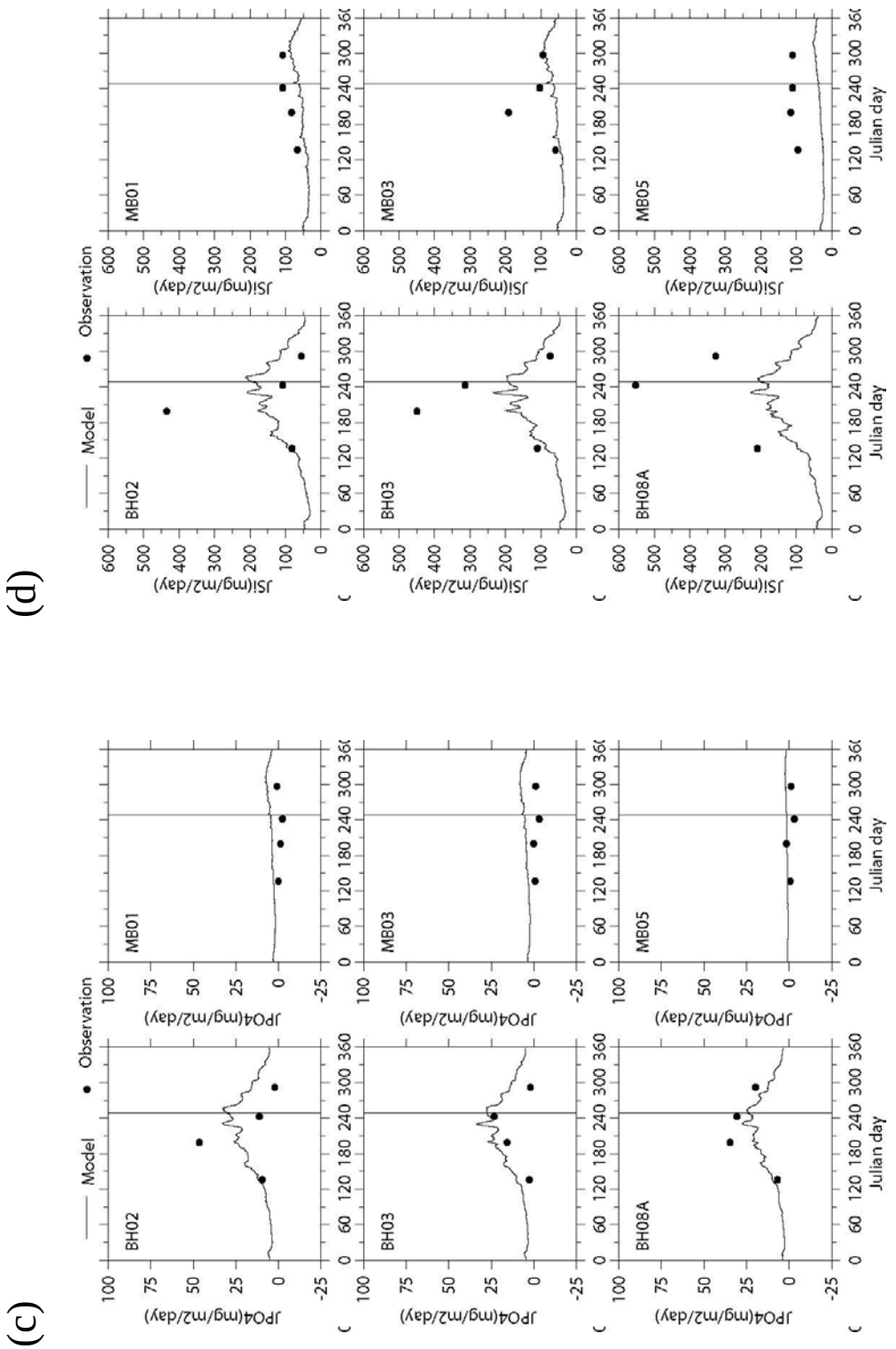

Figure 3.14. Continued

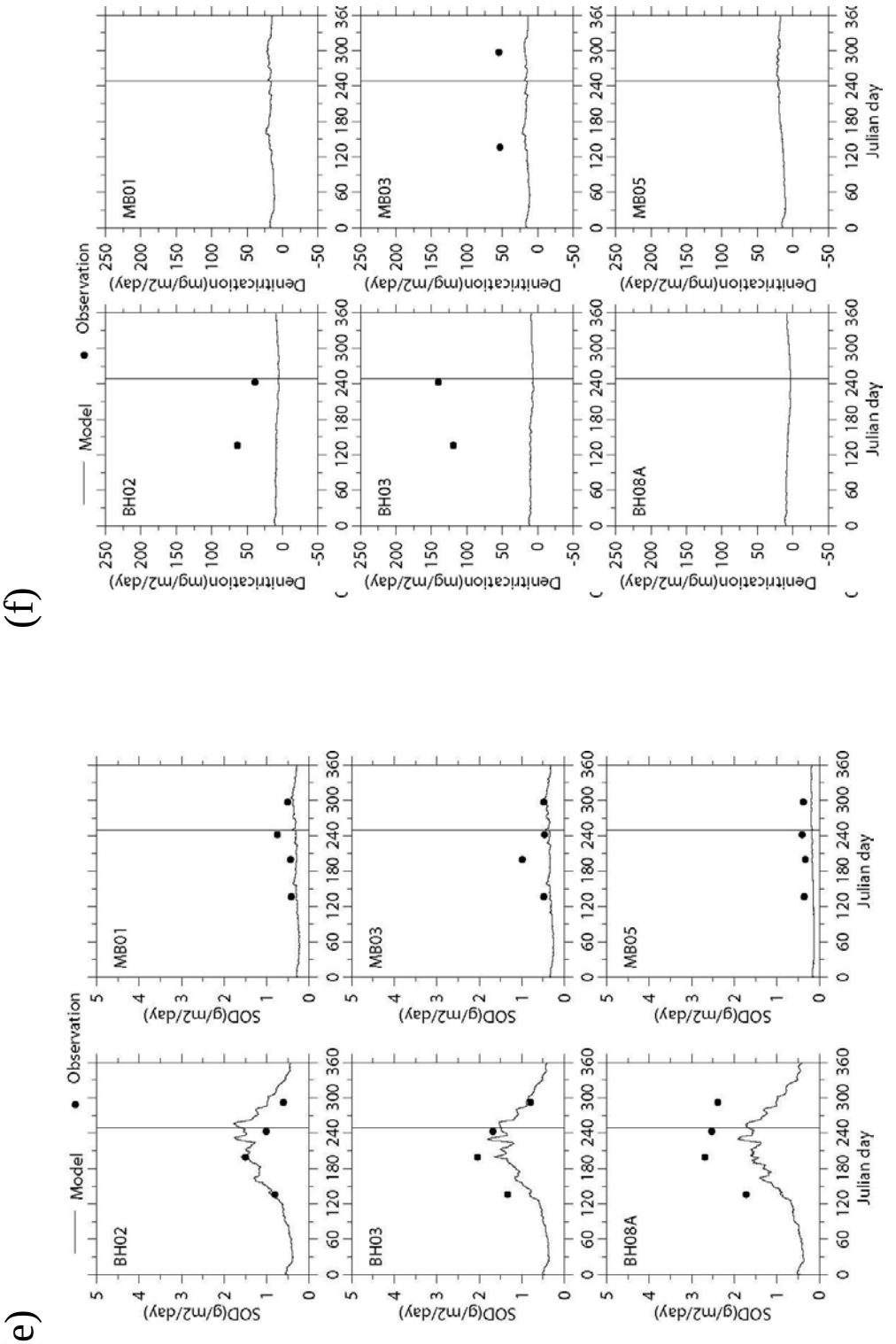

Figure 3.14. Continued

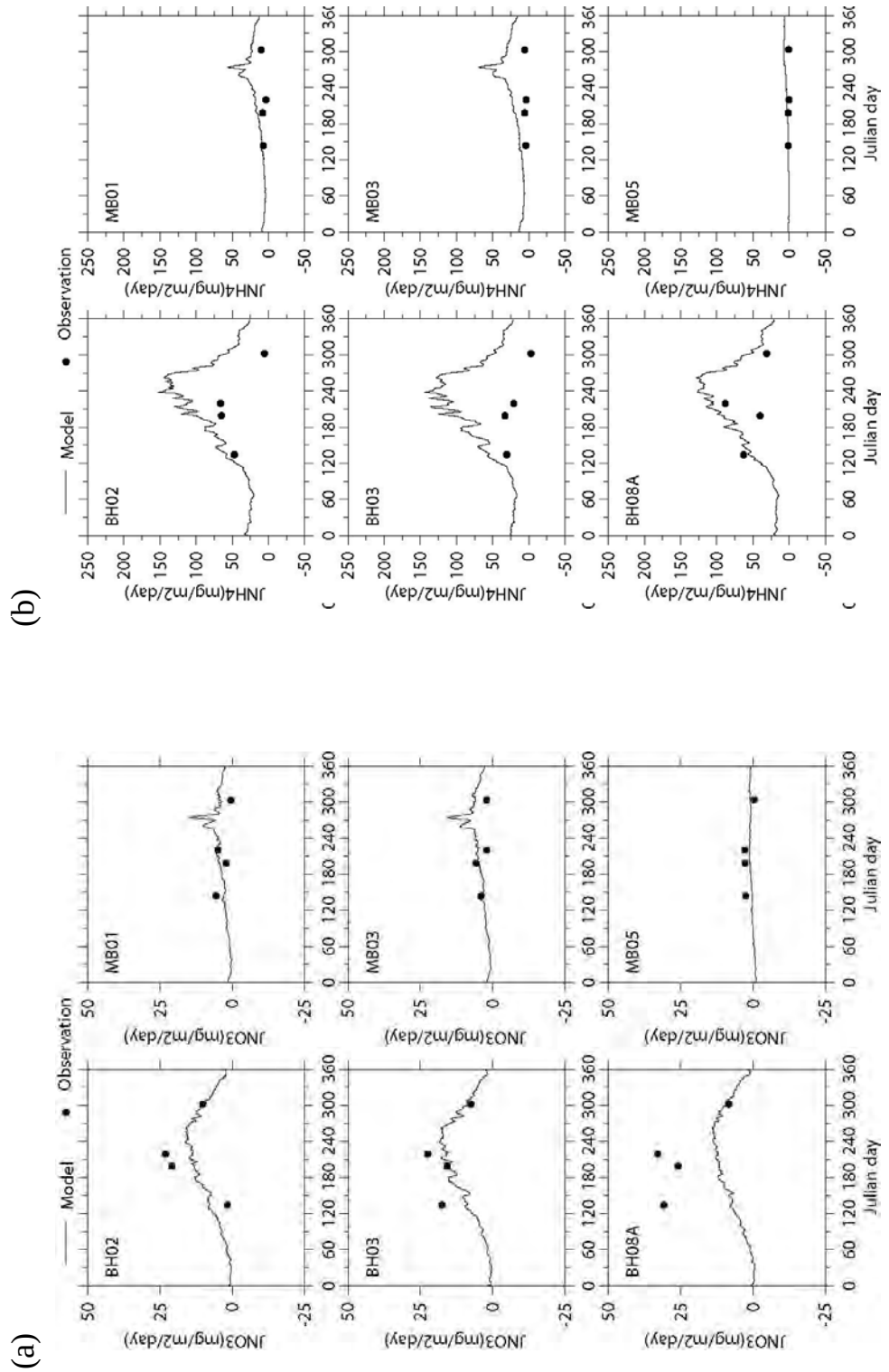

Figure 3.15. Nutrient fluxes and sediment oxygen demand in 2001: (a) JNO_3, (b) JNH_4, (c) JSi, (d) JPO_4, (e) SOD, and (f) JN_2. (to be continued on the next page)

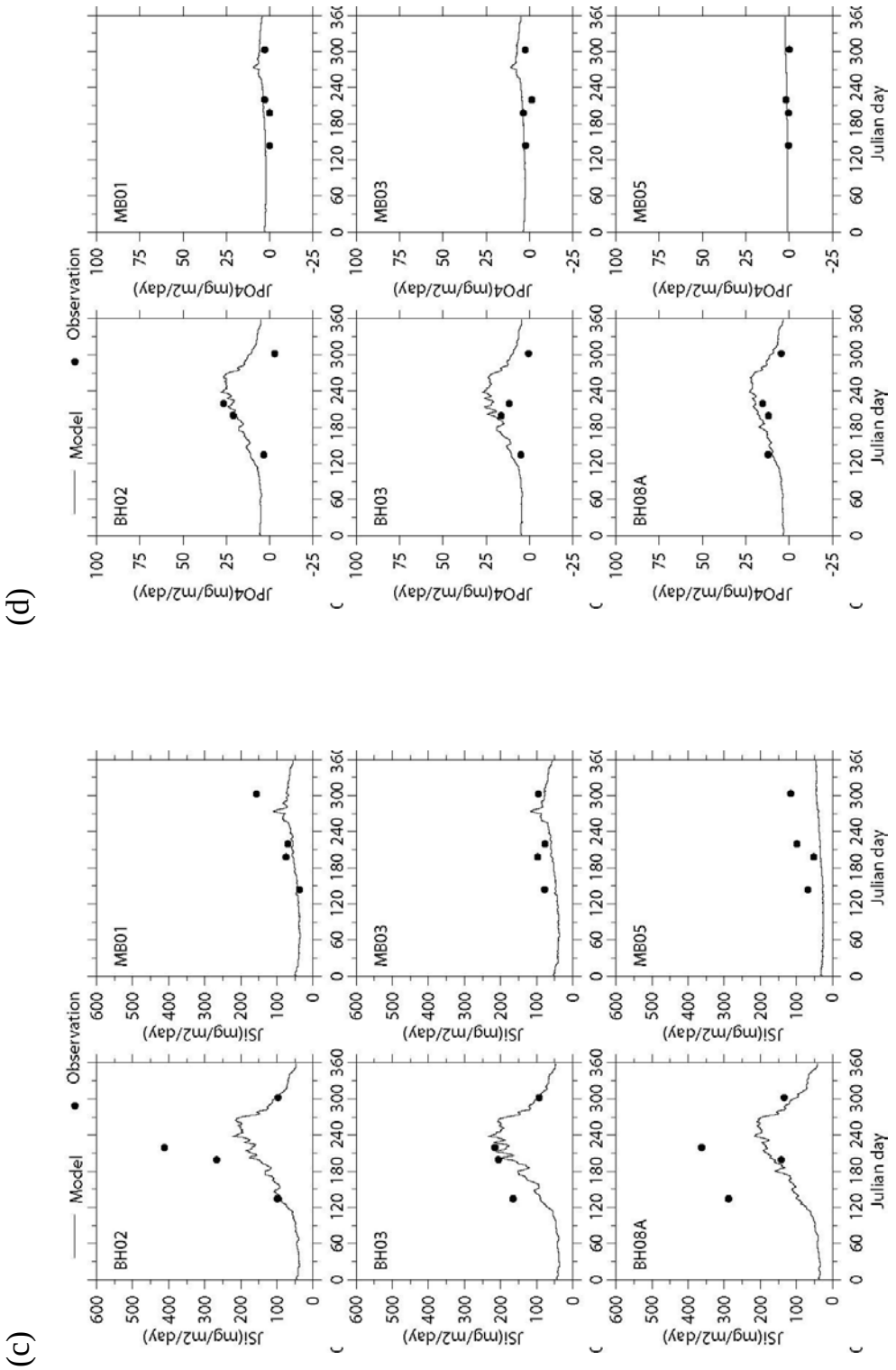

Figure 3.15. Continued.

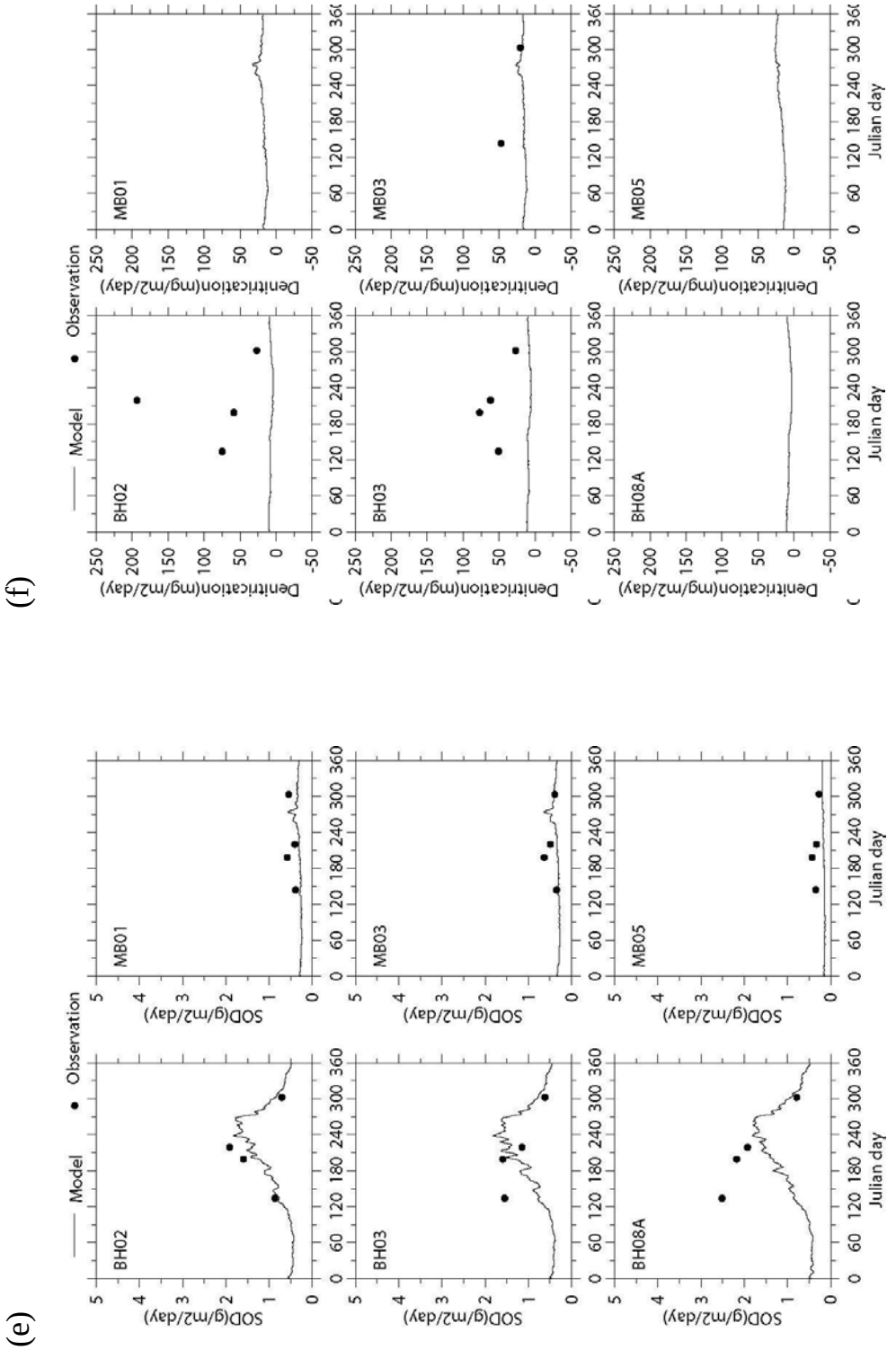

Figure 3.15. Continued.

4. SENSITIVITY EXPERIMENTS

In this section, the model sensitivities are analyzed against several key parameters and forcing conditions listed in Table 4.1.

4.1 Zooplankton grazing

One drawback of the current BEM is that zooplankton grazing is specified by a 10% instantaneous removal of phytoplankton standing stock though the development of zooplankton populations usually lags behind the phytoplankton by one to several weeks. In the MBS, the zooplankton abundance increases after a spring algal bloom, reaches the maximum in summer, and decreases in fall and winter (Libby et al., 2001). Because of the time lag between the phytoplankton and zooplankton populations, the zooplankton grazing rate should be lower in winter and spring, and higher in summer and fall. Thus a yearly averaged grazing rate will overestimate the grazing in winter and spring and underestimate the grazing in summer and fall.

It is a complicated question whether the zooplankton grazing formulation in the BEM leads to the discrepancy between model results and observations, which requires a detailed study. Nevertheless, the effect of zooplankton population dynamics on the zooplankton grazing is tested by simply introducing a time lag (τ) between phytoplankton and zooplankton populations, that is, zooplankton biomass $Z(t)$ at time t is equal to 10% of the phytoplankton biomass P at time t-τ, which can be expressed as

$$Z(t) = 0.1P(t-\tau) \tag{4.1}$$

Then the zooplankton grazing will be,

$$graz(t) = Z(t)\frac{P(t)}{k_p + P(t)} = 0.1\frac{P(t)}{k_p + P(t)}P(t-\tau) \tag{4.2}$$

where $graz(t)$ is the zooplankton grazing rate and k_p is the half food saturation constant for zooplankton grazing. When $P(t)$ is much higher than k_p, the grazing at time t equals to 10% removal of phytoplankton stock at time t-τ. Of course, this is a very simplified and conceptual model for elucidating the importance of zooplankton grazing. In the following experiment, k_p is chosen to be 0.01 mgC l^{-1}, and the time lag is 7 days. For convenience of discussion, we call the

original model results as the CONTROL and the results with the delayed zooplankton grazing as the GRAZ.

The results of both the CONTROL and GRAZ in year 2000 are shown in Figures 4.1 and 4.4. Clearly, the surface chlorophyll and phytoplankton biomass in GRAZ are higher than that of CONTROL throughout the year. A much stronger fall bloom in the surface chlorophyll is found in GRAZ, which is better compared with data than that of CONTROL. The differences between GRAZ and CONTROL are small during the first half of the year and dramatically increase in July when the summer algal group starts to dominate the population, and remain large in the summer and fall (Figure 4.3). The onsets of differences during mid-February and July coincide with significant increases in phytoplankton biomass. The higher chlorophyll in GRAZ is simply produced by using a smaller grazing rate parameterized by taking the phytoplankton biomass 7 days ago which is lower than the standing biomass. Since chlorophyll and phytoplankton biomass are accumulative, the differences between GRAZ and CONTROL remain through the later seasons though chlorophyll and phytoplankton biomass fluctuate.

The primary production shows a complicated response to the delayed grazing (Figure 4.4). During the spring, the differences in primary production between GRAZ and CONTROL are relatively small; during the summer, the primary production in GRAZ is lower because the surface nutrients are more severely depleted by higher phytoplankton biomass than that of CONTROL; and during the fall and winter, the primary production in GRAZ is in general higher than that of CONTROL.

The differences in phytoplankton biomass between GRAZ and CONTROL do not produce significant differences in surface dissolved oxygen (not shown), which is primarily controlled by air-sea gas exchanges. The differences of bottom DO are also small at most stations because phytoplankton is concentrated in the surface and subsurface layers. The bottom DO in Cape Cod Bay in GRAZ is however approximately 0.5 mg l^{-1} less than that of CONTROL during late summer, which is caused by higher biomass accumulation and higher oxygen demand of the regeneration processes predicted in GRAZ (Figure 4.5).

The comparison between the GRAZ, CONTROL and observed data cannot conclude that either the GRAZ or CONTROL is a better model because the simplicity of the time-delay model and the complexity of the water column ecosystem. However, the comparison demonstrates that the dynamic relationship between phytoplankton and zooplankton can lead to significantly different model results, such as the timing and magnitude of phytoplankton blooms.

4.2 Increasing chlorophyll inputs on the open boundary

The second experiment (experiment BCHL) was conducted to understand the influences of chlorophyll input from the GOM intrusion on the phytoplankton production in the MBS. Though sensitivity experiments have been conducted for the boundary nutrients and dissolved oxygen (HydroQual, 2001), the influences of biota inputs have not been studied. The boundary chlorophyll fluxes were increased by increasing the chlorophyll concentrations by 20% at the open boundary, approximately 1.5μg l^{-1} at the surface, starting from Julian day 75 (mid-March, set as Day 0 below) to Julian day 105 (mid-April). The differences of modeled surface chlorophyll, silicate and DO between BCHL and CONTROL are shown in Figures 4.6-4.8.

A plume is formed and penetrates into Massachusetts Bay along the north coast with a maximum difference of approximately 0.5 μg l^{-1} on day 3. High surface chlorophyll is also present on the eastern flank of Stellwagen Bank, but is blocked by the bank. On day 6, the plume turns southward and occupies most of Massachusetts Bay while being strengthened dramatically with maximum difference more than 1 μg l^{-1} in the North Passage. The 0.25 μg l^{-1} contour line of the plume clearly penetrates into Cape Cod Bay. On day 9, the plume retreats to the north and is pushed away from the coast though the difference of surface chlorophyll in the North Passage continues to increase. The retreat is likely produced by the burst of a strong southerly wind, which reverses the surface currents. On day 12, the core intrusion through the North Passage is stabilized. The difference of surface chlorophyll on the top of Stellwagen Bank remains small or negligible. Because higher chlorophyll leads to lower nutrients in surface layer, a plume of low silicate surface water can be seen in Figure 4.7. The plume of low silicate water

essentially develops and retreats following the plume of high chlorophyll water.

The elevated chlorophyll produces little change of the surface DO during the first 6 days (Figure 4.8). On day 9, the surface DO in BCHL is slightly lower than that of the CONTROL over the areas of the chlorophyll plume. On day 12, the surface DO in BCHL is significantly lower than that of CONTROL with the maximum difference up to 0.2 mg l^{-1}. This low DO in BCHL is produced by the increased regeneration of the organic matter within the plume. In the North Passage, the difference of surface DO is small, which is likely due to the compensation between regeneration and high photosynthesis before the drawdown of nutrients in the plume.

4.3 Spatially variable OBCs vs. uniform OBCs

The affected range and magnitude of different open boundary conditions (OBCs) can be elucidated and quantitatively analyzed from the comparisons in Section 4.2, that is, the disturbance on the open boundary can propagate deeply into the MBS. Under northerly wind conditions, the 50% contour (the chlorophyll difference is half of the boundary perturbation magnitude) reaches the upper Massachusetts Bay, the 25% contour reaches the south shore, and 10% reaches Cape Cod Bay. In the 2000 and 2001 water quality runs, we take a new approach in constructing the open boundary conditions by using objective interpolation and monthly field observations. The newly constructed variable open boundary conditions (VOBCs) are time-dependent and 3-dimensional which are very different from the uniform open boundary conditions (UOBCs) used by HydroQual in previous simulations for 1992-94 and 1998-99 (HydroQual, 2000; HydroQual, 2003). In order to evaluate the differences in modeled fields using different OBCs, the UOBCs are set by values at node 45 located at the entrance of the North Passage, and the VOBCs are set by the objective interpolations which is also the CONTROL case. The comparisons of surface chlorophyll, primary production and surface DO between UOBC and CONTROL are shown in Figures 4.9-4.12.

The difference of surface chlorophyll between UOBC and CONTROL is negligible during the winter and early spring whereas it is detectable throughout the summer (Figure 4.9-4.10). Within the large oscillations in 20-30 day periods, the maximum difference is

about 1 μg l^{-1}, approximately 10-15% of surface chlorophyll in CONTROL. The difference of surface chlorophyll in the fall is relatively small.

The impacts of different open boundary conditions can be further demonstrated in the primary production predictions (Figure 4.10). Although the differences are generally negligible, in the early summer the difference of primary production between the two experiments is largest, reaching a maximum of 1 gC m^{-2} day^{-1}, approximately 40% of the primary production of that time. During fall, a detectable difference of primary production can also be seen at some stations, for example, N04.

Similar to the experiment BCHL, the differences of phytoplankton biomass and primary production between UOBC and CONTROL do not affect the surface DO because of the dominance of surface gas exchange. The time scale of regeneration is much longer than the wind events and boundary variation in 20-30 day periods. The change of bottom DO is determined by the long-term accumulation of biomass. As a result, the bottom DO does not show considerable differences.

We note that the boundary condition used in the experiment UOBC is the mean of objectively interpolated values, which incorporate all neighbouring stations. Thus the difference between UOBC abd CONTROL is only the spatial anomaly. If the the OBCs are constructed only by stations F26, F27 and F29, the mean can be biased by averaging only values from these three stations. Thus, the manually-constructed OBCs based solely on measurements at station F26, F27 and F29 (HydroQual, 2000; HydroQual, 2003) could produce a systematic bias.

Table 4.1. Summary of the numerical experiments.

Experiment Name	Descriptions
CONTROL (VOBC)	Standard experiment
GRAZ	Delayed grazing, τ = 7 day, k_p = 0.01 mgC/l
BCHL	Increase chlorophyll at OBC in March and April by 20%
UOBC	Use open uniform open boundary conditions, node = 45

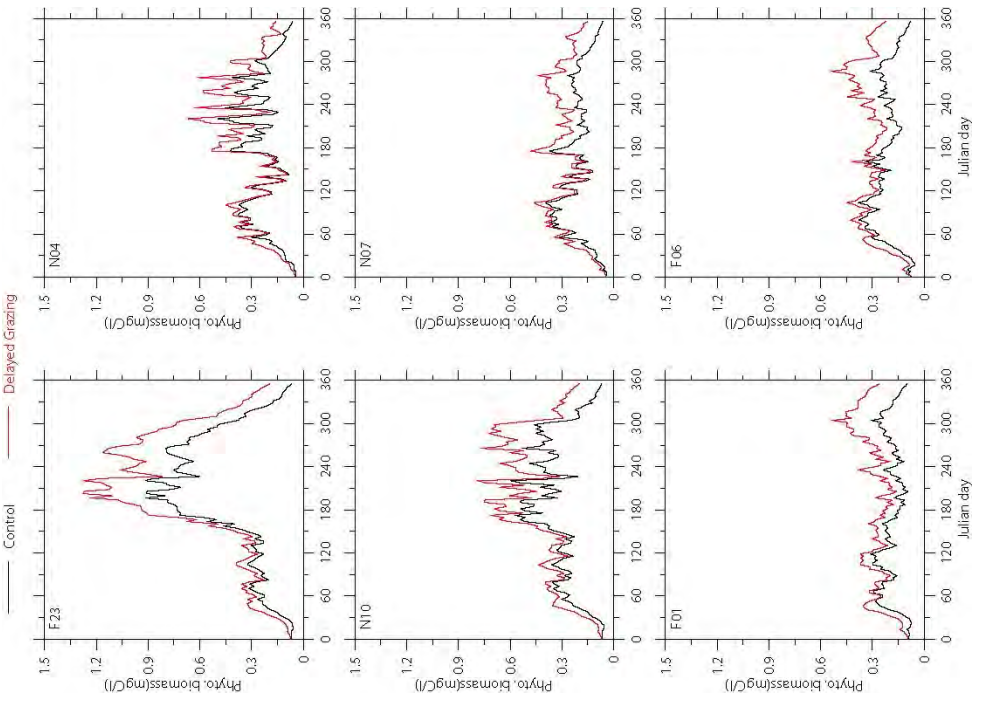

Figure 4.2. Surface phytoplankton biomass in CONTROL and GRAZ experiments.

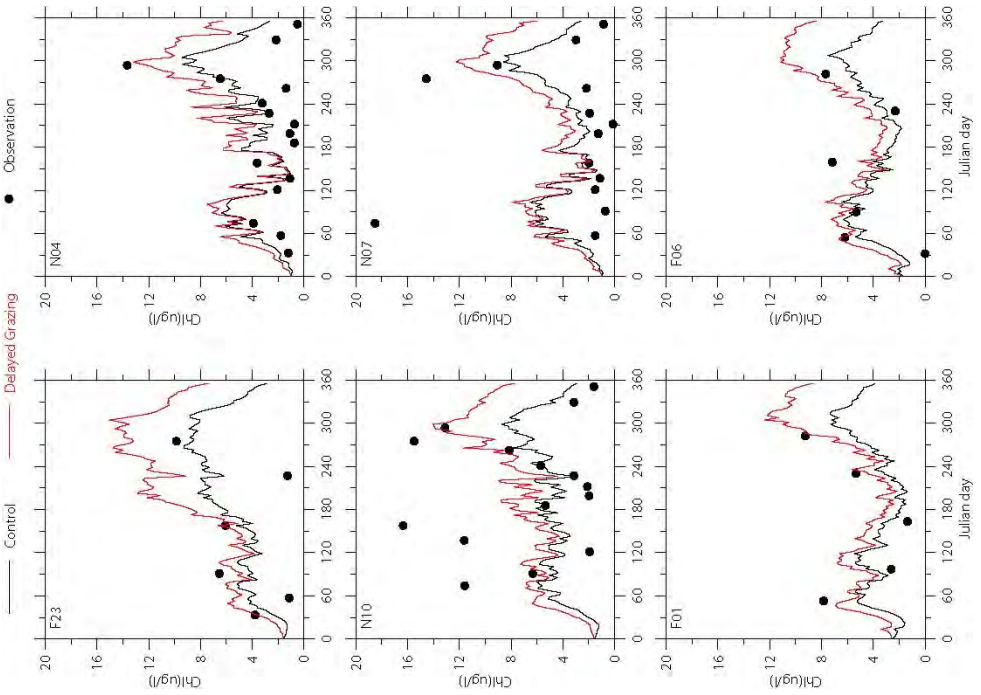

Figure 4.1. Surface chlorophyll in the CONTROL and GRAZ experiments.

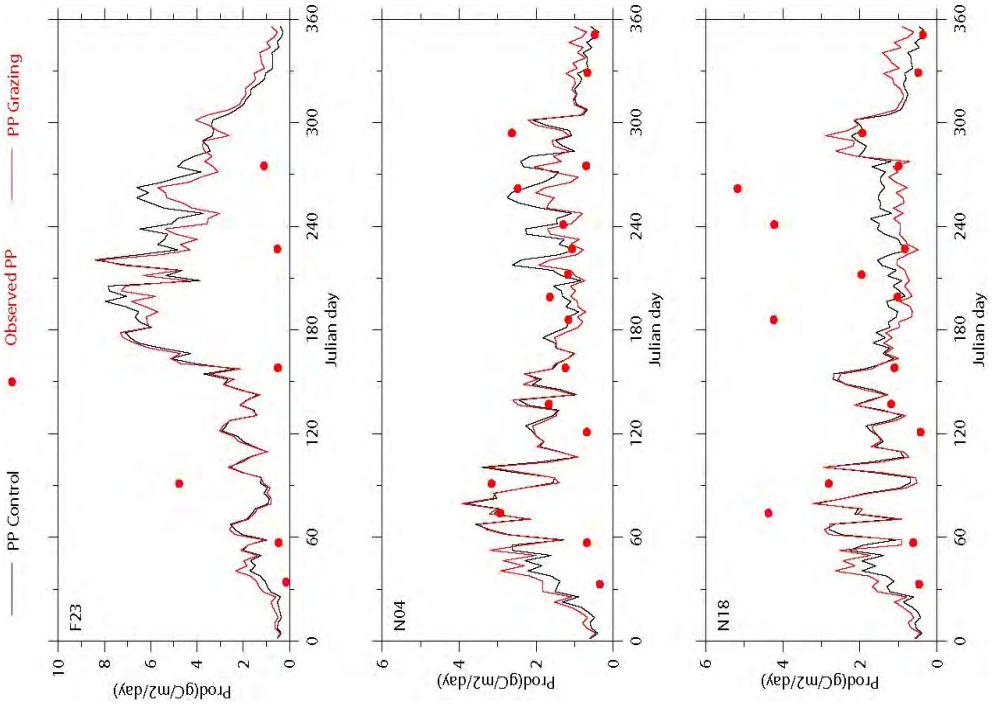

Figure 4.4. Primary production in the CONTROL and GRAZ experiments.

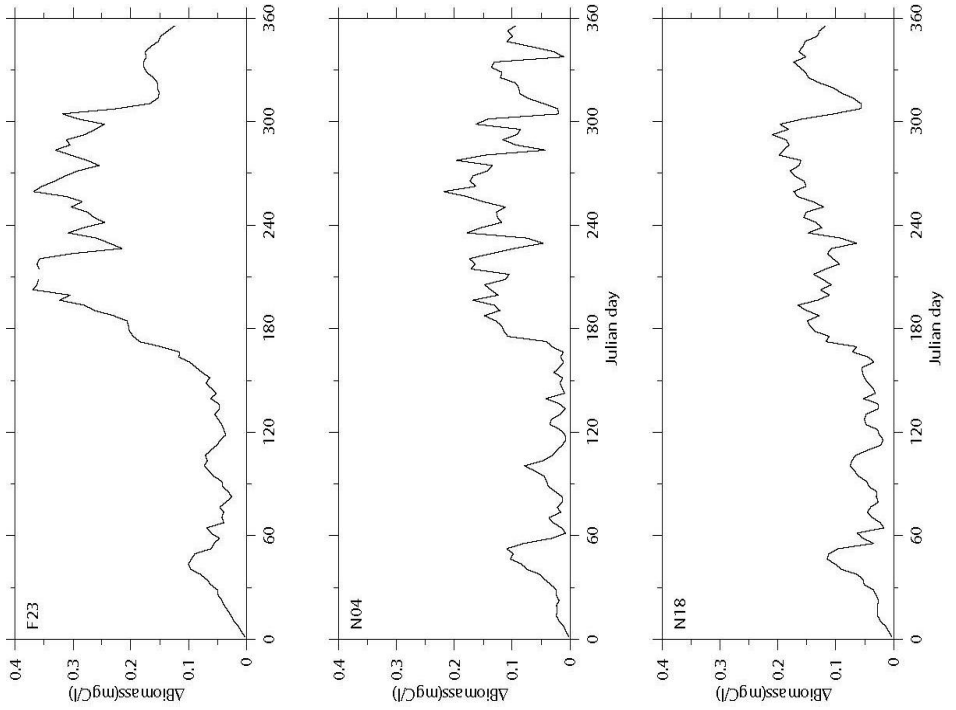

Figure 4.3. Difference of surface phytoplankton biomass between the CONTROL and GRAZ

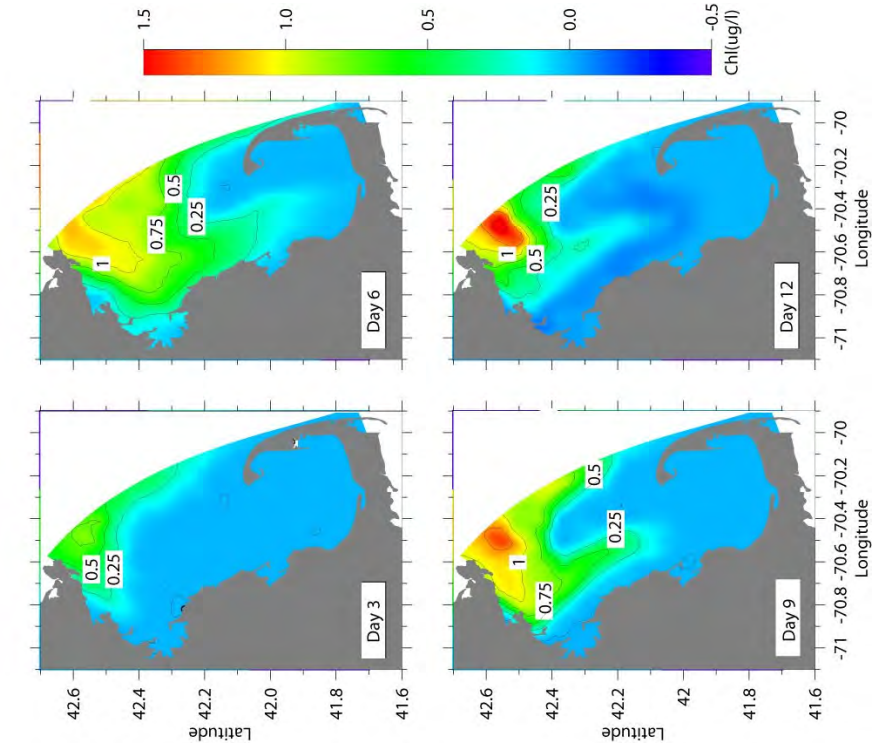

Figure 4.6. Difference of surface chlorophyll between the CONTROL and BCHL experiments.

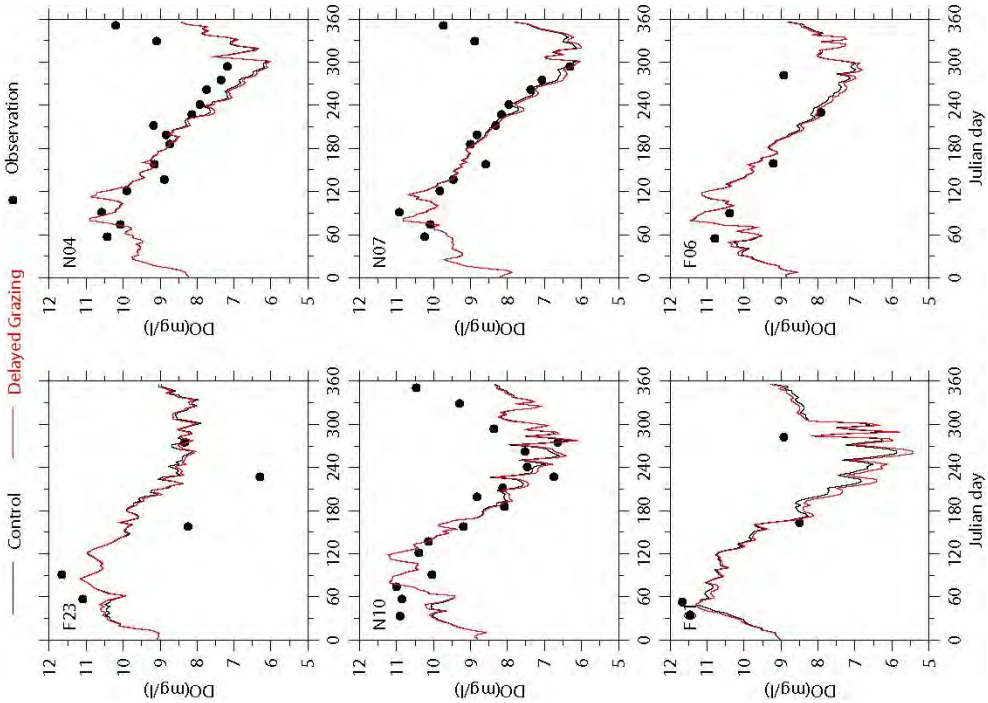

Figure 4.5. Bottom DO in the CONTROL and GRAZ experiments.

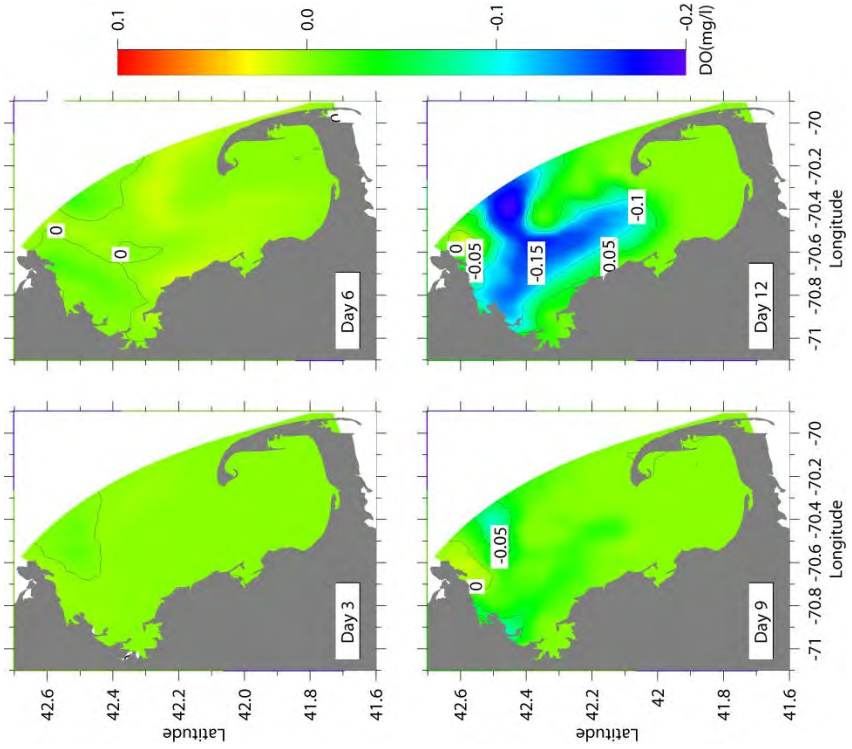

Figure 4.8. Differences of surface DO between the CONTROL and BCHL experiments.

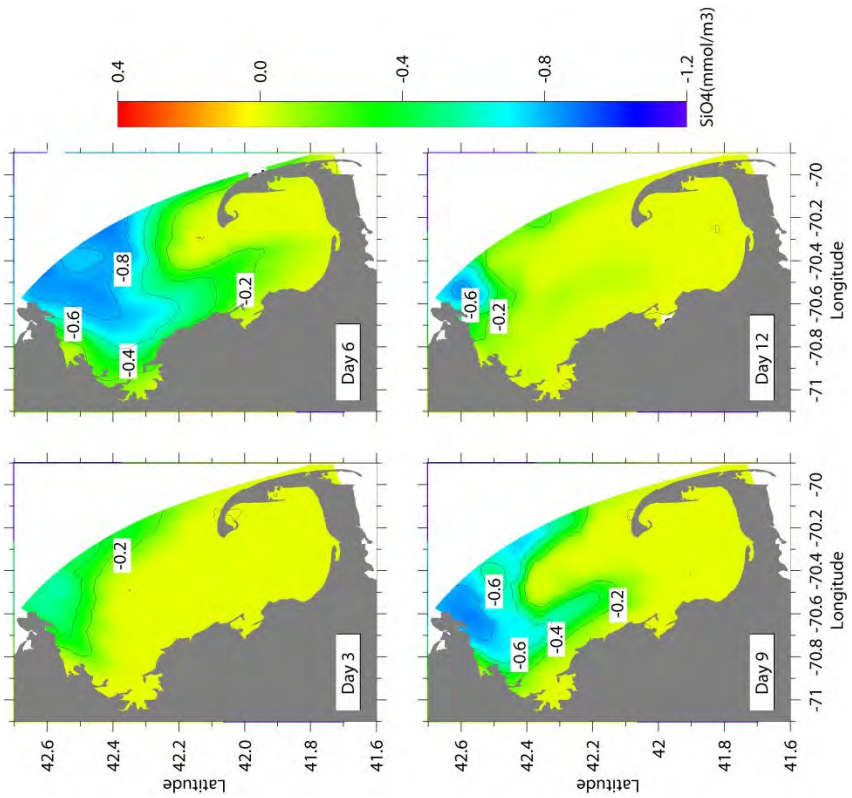

Figure 4.7. Difference of surface silicate (SiO_4) between the CONTROL and BCHL experiments.

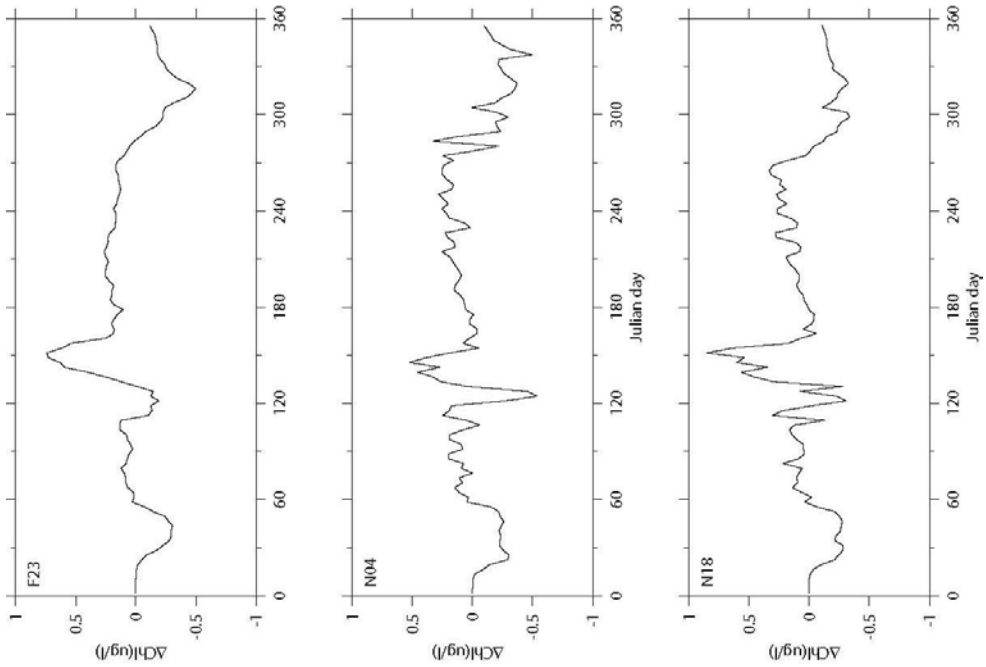

Figure 4.10. Difference of surface chlorophyll between the CONTROL and UOBC experiments.

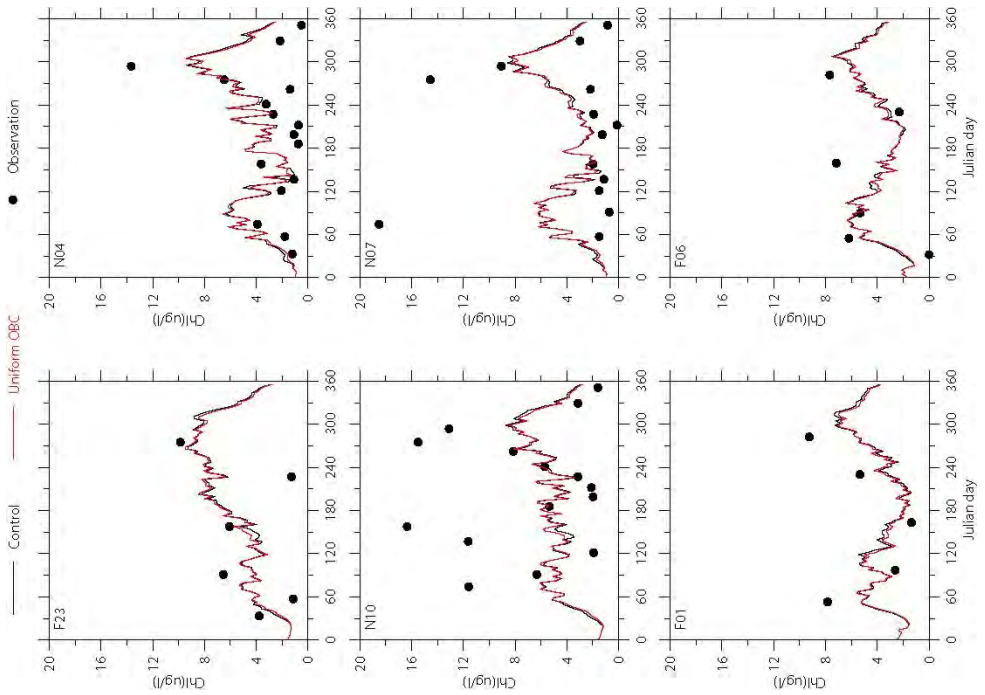

Figure 4.9. Surface chlorophyll in the CONTROL and UOBC experiments.

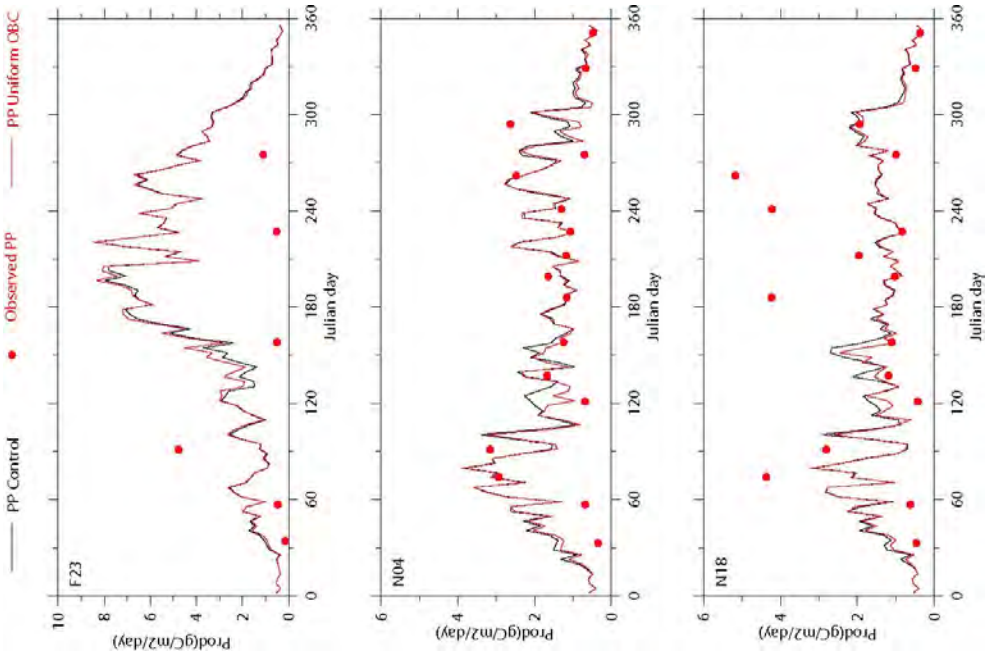

Figure 4.11. Primary production in the CONTROL and UOBC experiments.

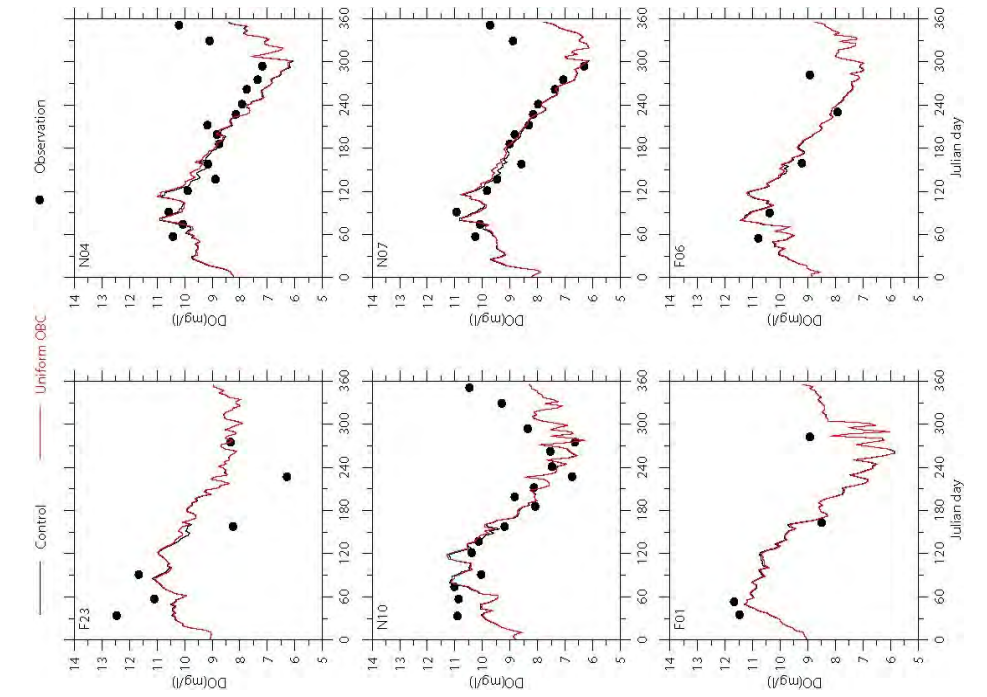

Figure 4.12. Bottom DO in the CONTROL and UOBC experiments.

5. DISCUSSION

5.1 Summer nutrient accumulation in central Cape Cod Bay

The MBS has a long stratification period from early May to October. During this period, the water is warm which leads to fast decomposition of organic matter. Because the stratification effectively limits vertical mixing, nutrients are depleted within the upper mixed layer while they accumulate below the seasonal thermocline. The distributions of nutrients, chlorophyll and DO along section 3 through mid-bay from Nahant to Barnstable (Figure 3.1) in early October, 2000 are shown in Figure 5.1. The water column is still strongly stratified at this time of the year. The nutrients within the mixed layer are nearly depleted except in nearshore areas. A high ammonia spot on the northern slope can be identified, which probably originates from the MWRA effluent. In CCB, a large pool of very high ammonia and silicate concentrations is found below the thermocline, where no external nutrient sources are present. The DO concentration within this pool is approximately 1 mg l^{-1} lower than that of surrounding areas, which suggests local intensive nutrient regeneration from organic matter. This high nutrient low DO pool (HNLO) occupies most of the area deeper than 25m in CCB. This HNLO persistently occurs during summer-fall season in all four year model runs (1998-2001).

Earlier field surveys indicated the existence of this HNLO in CCB. Measuring phosphate and silicate along a mid-bay transect from Nahant to Cape Cod, Becker (1992) observed high subsurface phosphate and silicate in Stellwagen Basin and Central Cape Cod Bay in July 25-27 and in October 16-18, 1990. Between these two surveys, nutrients were significantly reduced in Stellwagen Basin but increased in central CCB. A field survey conducted during September 28-29 1998 using an autonomous underwater vehicle indicated high concentrations of suspended sediments in central CCB (Yu et al., 2002). Furthermore, sediments in central CCB have been found to contain higher silver concentrations than those of coastal CCB and Stellwagen Basin (Bothner et al., 1993). All these results suggest that the regeneration of accumulated organic matter in central CCB leads to elevated nutrient concentrations during late summer as a recurring phenomenon.

The evolution of this HNLO can be clearly seen in the time series of bottom temperature, nutrients and DO along a west-east section in central CCB, which crosses the center of the HNLO (Figure 5.2). A strong spring bloom occurs between late March and early April, which is marked by a large increase of PON. PON decreases in early June but remains relatively high throughout the summer. During this period, the change in PON is characterized by episodic impulses due to horizontal transport. From the trends in PON, an abnormally fast accumulation of PON in CCB may indicate an influx or accumulation of PON in CCB during the winter-spring season, and a decrease in PON may suggest regeneration and a net efflux of PON from CCB during the summer-fall season. DON reaches a maximum in winter, and decreases throughout the spring and summer. The bottom ammonia field shows two cycles within a year. First, it increases in the late winter and spring from the remineralization of DON and decreases in spring during the spring phytoplankton bloom when the water is weakly stratified. Second, it increases and peaks in the mid summer from the decay of PON and remineralization of DON and then decreases again in the winter. The strengthening of the ammonia pool co-occurs with the decrease of DO in central CCB. The short-term events of offshore transport during the summer and fall erode this ammonia pool, probably in combination with mixing. This pool of PON and ammonia rapidly disappears after a northerly wind event that causes strong offshore transport in November.

Many pieces of evidence indicate that the formation and disappearance of this HNLO are driven by transport and mixing. In winter-spring, nutrients and biota are transported into CCB by the seasonal counter-clockwise circulation. The sluggish current in CCB allows the accumulation and deposition of organic matter. In summer, the fast heating of water in CCB produces a warm water pool in CCB and forms a closed clockwise circulation which effectively blocks the Massachusetts Bay coastal current intrusion, confirmed by drifter trajectories (Geyer et al., 1992) and our numerical experiments (not shown). The pool of high nutrients and low oxygen is produced by the decomposition of POM and DOM accumulated in central CCB, and is retained by the closed clockwise circulation. During summer and early fall wind events, strong coastal jets, deep intruding currents and eddies can be formed associated with upwelling or downwelling fronts. These meso-scale physical processes in MBS transport nutrients, POM and DOM in or

out of CCB (Jiang and Zhou, 2004a). Finally in late fall and winter, the prevailing northerly wind establishes a strong counter-clockwise coastal current in the MBS, which penetrates deeply into CCB and exits at the South Passage off Race Point. The HNLO is flushed quickly by this strong current.

Modeled seasonal and short-term circulation patterns suggest three mechanisms that may contribute to the formation of the HNLO in Central CCB: 1) the southward coastal current in Massachusetts Bay that transports organic matter into central CCB in spring and early summer, 2) the deep southward intruding current in Stellwagen Basin during summer and early fall that transports organic matter into central CCB (Jiang and Zhou, 2004a), and 3) high settlement rates in central CCB due to slow horizontal motion. These physical processes lead to the accumulation of sediments in central CCB, and biogeochemical regeneration processes produce the pool of high nutrients.

5.2 Ecosystem responses to wind events in summer

The wind forcing exhibits large low frequency events in the summer, representing synoptic atmospheric processes of 5-10 days. The predominant wind orientation is in the north-south direction. Winds parallel to the coastline are favorable for inducing offshore or onshore Ekman transport. From the modeling study in the MBS, Jiang and Zhou (2004a and b) indicate that during northerly wind events, warm water accumulates along the coast due to the onshore Ekman transport. A coastal downwelling front is produced. The surface slope and density front create a narrow southward coastal jet. The accumulation of water in the southern portion of the MBS produces a north-south pressure gradient blocking the bottom water intrusion from the GOM. During southerly wind events, an upwelling front is produced by the offshore Ekman transport. The slope and upwelling front produce a northward coastal current. While the deep water from Stellwagen Basin is transported to the shallow coastal regions by Ekman pumping, the loss of deep water in Stellwagen Basin is in turn compensated by the deep water intrusion from the GOM.

Adjustment of the circulation in response to a wind event leads to adjustment of the ecosystem in the MBS. The time series of modeled nutrients and phytoplankton biomass

at the USGS Scituate Buoy reflect the ecosystem responses to wind events during August, 2000 (Figure 5.3). The salinity variability indicates two upwelling and one downwelling events in this month: the first upwelling occurs from day 0 to day 10; it is followed by a downwelling identifiable from the deep penetration of the surface low salinity water between day 10 and day 20; and the second upwelling occurs from day 20 to day 30. NO_3 is much lower than SiO_4, and thus limits the phytoplankton growth in this period. The upwelling brings much needed NO_3 into the upper water column at this shallow station. On day 4, the phytoplankton biomass starts to increase rapidly. The phytoplankton biomass increases dramatically during the transition from upwelling to downwelling. During the transition period and the downwelling event, the phytoplankton biomass maximum remains beneath the upper mixed layer. Phytoplankton biomass increases again in the second upwelling event, and the maximum is elevated close to the surface.

Such downwelling and upwelling events occur along the entire western coast during the summer season as shown in Figures 5.4 and 5.5, respectively. A downwelling event is marked by a strong surface intruding current from the North Passage, flowing along the coast, intruding into CCB. The flow in the South Passage can be either in-coming or out-going, depending on the details of wind and timing. Warm water with low nutrients accumulates near the western coast (Figure 5.4). The unstable coastal jet forms a filament extending offshore from Plymouth to Race Point. On the contrary, an upwelling event is marked by northward coastal jets and cold upwelled deep water with rich nutrients and high chlorophyll (Figure 5.5). The GOM intrusion at the surface is reduced.

Along section 1 from Hull to the North Passage, the high salinity water is suppressed by the downwelling in the western slope of Massachusetts Bay and eastern flank of Stellwagen Bank on August 15 (Figure 5.6). The phytoplankton biomass maximum is located in the subsurface water 6-10 km offshore. On August 25, the upwelling uplifts the high salinity water to the surface on the western slope of Massachusetts Bay and eastern flank of Stellwagen Bank where excessive silicate and elevated phytoplankton biomass are found. However, the dilution of GOM water keeps the phytoplankton biomass low on top of Stellwagen Bank.

In summary, short-term wind events in summer could play an important role in changing the phytoplankton production, transporting nutrients and biota, and the renewal of bottom water.

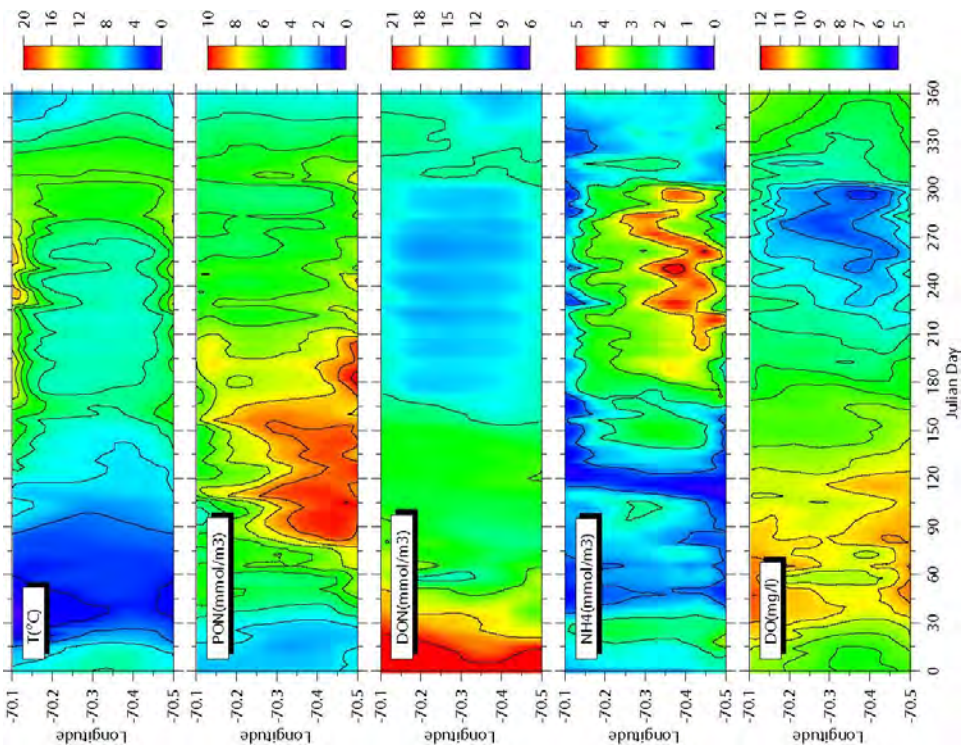

Figure 5.2. Time series of temperature, PON, DON, NH_4 and DO in the HNLO pool along a section from Plymouth Harbor to Race Point in 2000.

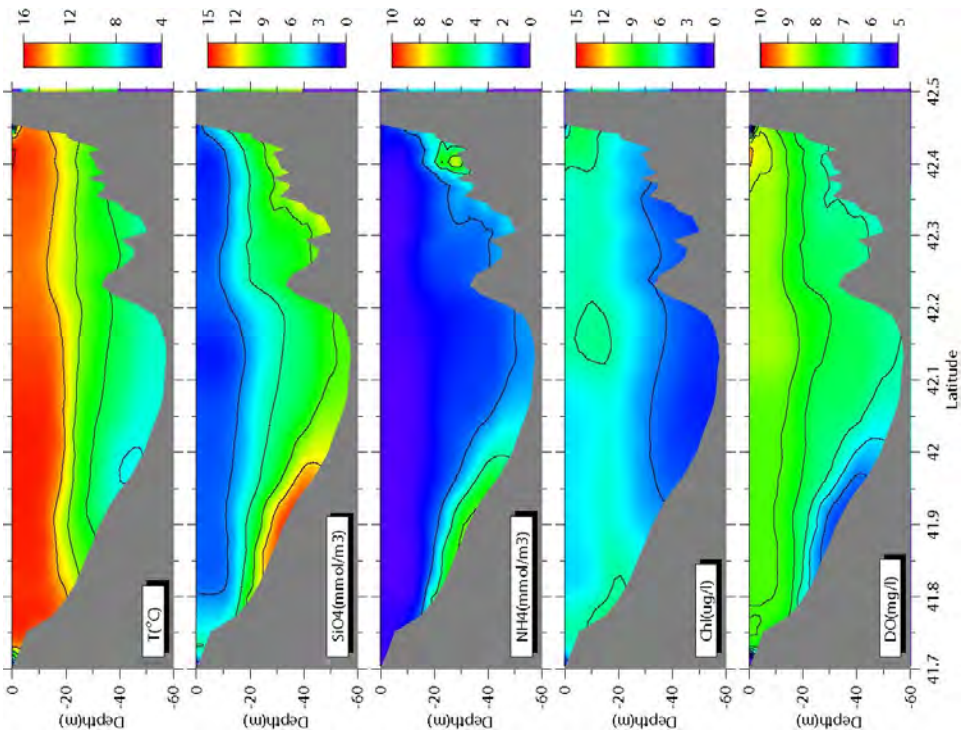

Figure 5.1. Vertical transects of temperature, SiO_4, NH_4, chlorophyll, and DO along section 3 (see Figure 3.1) in late summer 2000.

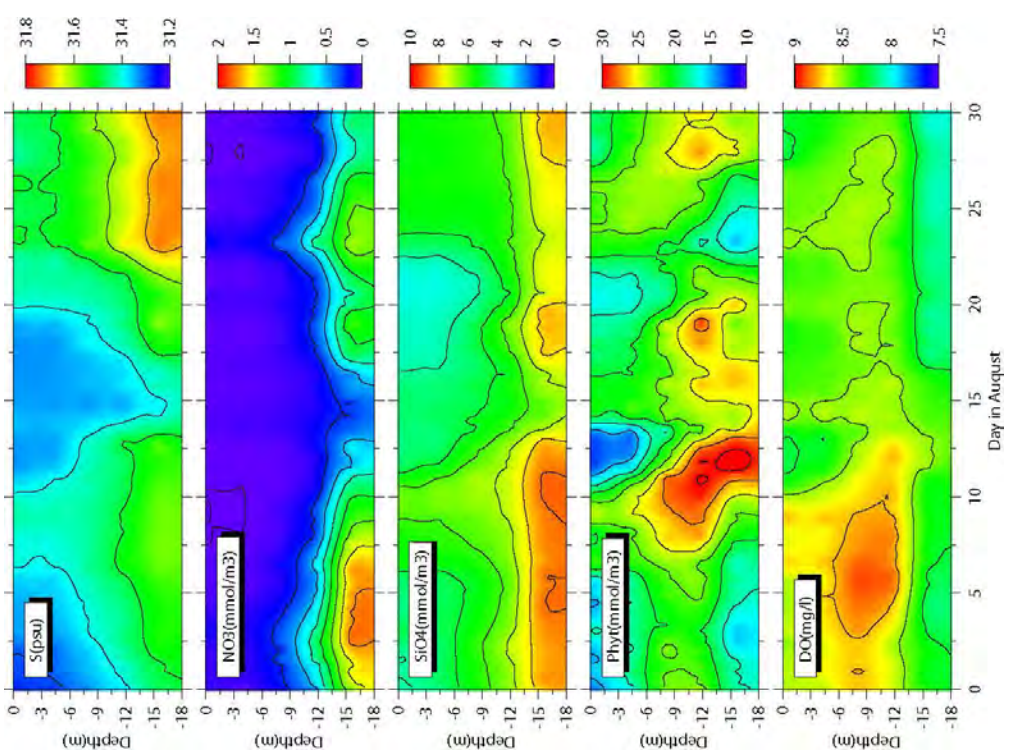

Figure 5.3. Temperature, NO_3, SiO_4, phytoplankton biomass, and DO off Scituate in August, 2000.

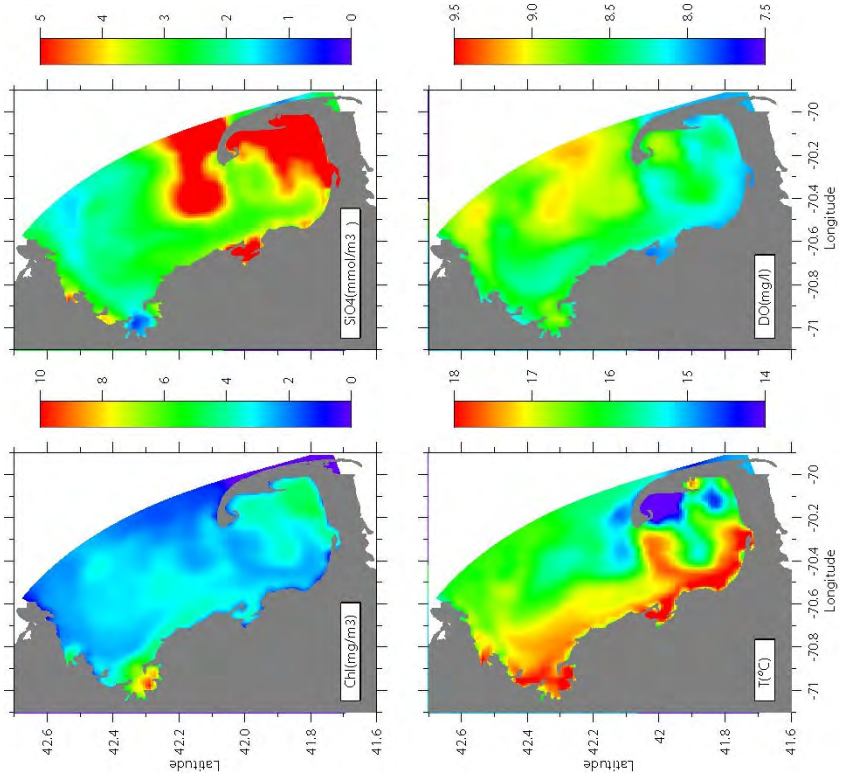

Figure 5.4. Surface distributions of chlorophyll, SiO_4, temperature and DO on August 15, 2000.

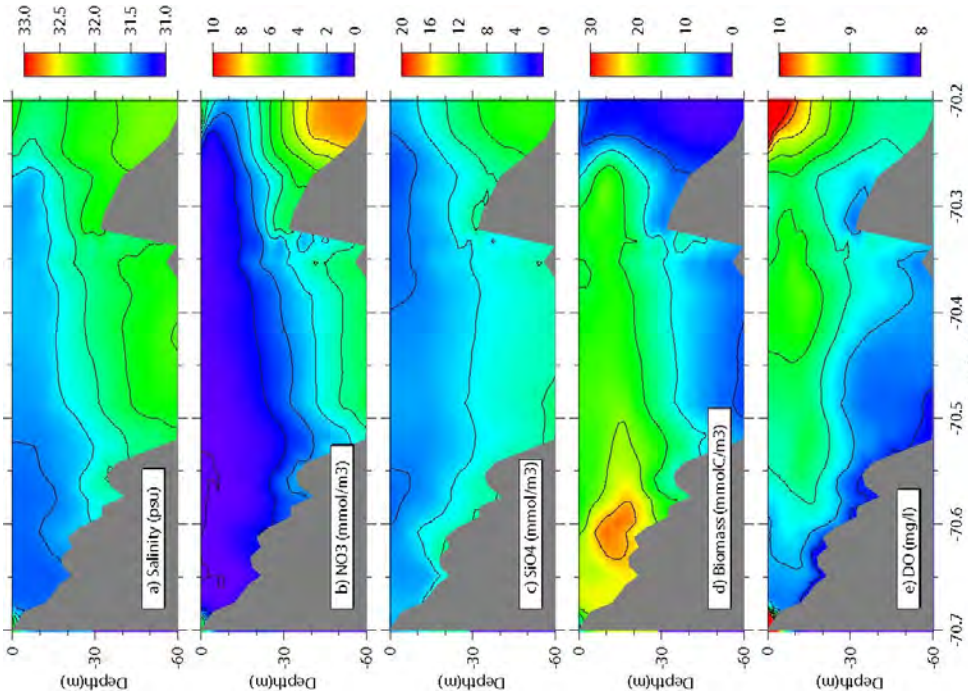

Figure 5.6 . Vertical distributions of salinity, NO_3, SiO_4, phytoplankton biomass, and DO along section 1 (see Figure 3.1) on August 15, 2000.

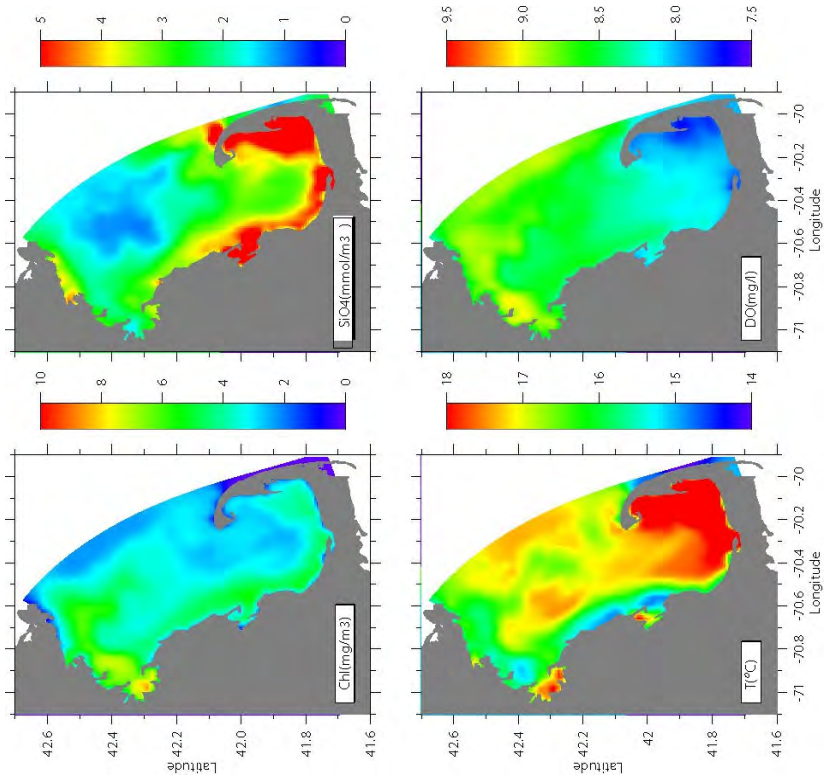

Figure 5.5. Surface distributions of chlorophyll, SiO_4, temperature and DO on August 25, 2000.

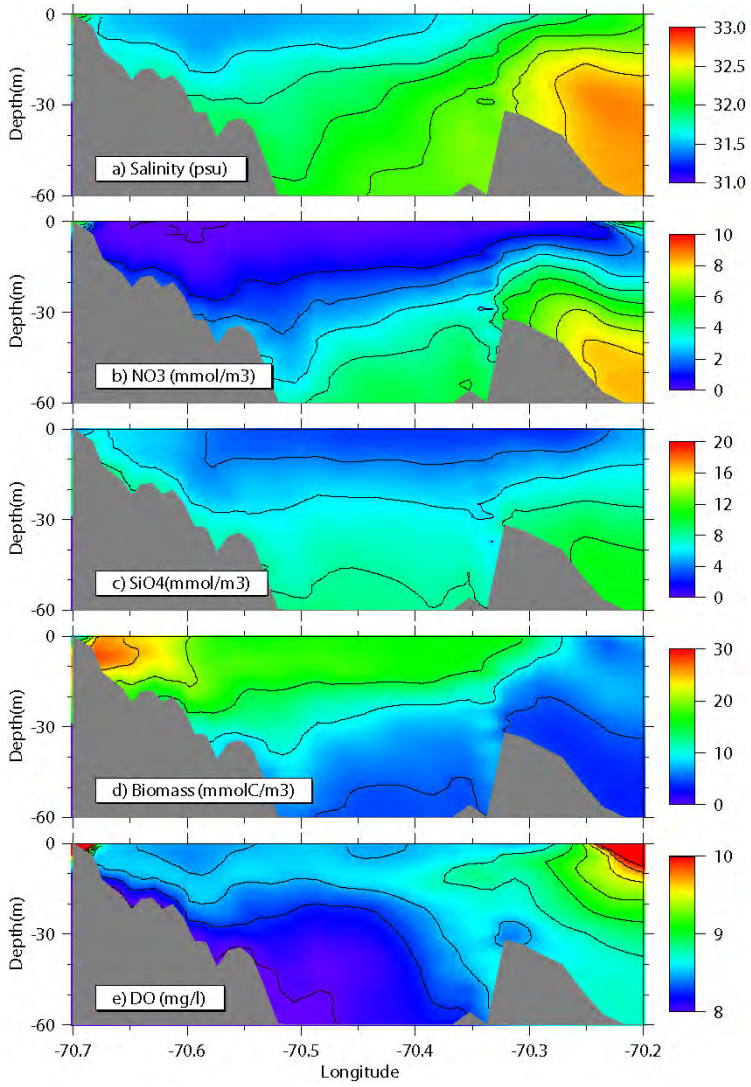

Figure 5.7. Vertical distributions of salinity, NO_3, SiO_4, phytoplankton biomass, and DO along section 1 (see Figure 3.1) on August 25, 2000.

6. SUMMARY AND RECOMMENDATIONS

6.1 Summary

The comparison study concludes that the modeled water quality variables and processes from the 2000-2001 water quality model run well represent physical, biological and chemical processes of water column and sediment in the MBS: 1) time series from model results well represent the seasonal cycles of phytoplankton abundance, nutrient concentrations and consumption-regeneration of DO, especially, the modeled DO series as the key water quality variable follows the observed values at monitoring stations; 2) the spatial patterns of modeled nutrients, phytoplankton biomasses and DO well represent the transport and accumulation of nutrients and organic matter, and local production and regeneration processes; and 3) the modeled primary production in the MBS agree with observed production very well, which is critical in constraining modeled phytoplankton growth rates.

The startup of the new outfall discharge is modeled and its effects on the surrounding area compare well with observations. High ammonia concentrations are produced by the model around the new outfall site as observed, though the detailed nature of the sewage plume between modeled and observed may differ. The responses of phytoplankton production and DO to the enhanced nutrients in the nearfield are more complicated because of transport and mixing processes associated with seasonal stratification, freshwater runoff and wind events. Though understanding these detailed processes requires more studies, it appears that the effluent has not produced any dramatic increase in primary production or decrease in DO at the new outfall site.

The key improvement in the model development for 2000-2001 simulation is use of the objective interpolation method for constructing the open boundary conditions based on observed values from monitoring cruises without any need of subjective modification of boundary values to achieve better fit between model and observed results.

The study also represents an effort to understand coupled physical-chemical-biological processes at seasonal and event scales and to study model sensitivities to different boundary condition settings and different formulations of water column

processes, which brought more insight into phenomena observed, and the causes of mismatch between modeled and observed results. Such efforts are essential for establishing the confidence of this model, minimizing the use of monitoring cruises and validating phenomena that are missed in monitoring data, and improving the MB Model in the future.

However, it remains unclear how the ecosystem responds to the effluent and the effects of an increase of nutrients on local water quality after outfall relocation. During short-term wind events, strong coastal jets may be formed, which rapidly transport high nutrient waters along the coast into embayments. Complex interactions between outflow from Boston Harbor, inflow from the Gulf of Maine, and local wind forcing make the nearfield an area of rapid changes in currents and hydrology, though the residual currents are small. We also do not know how the ecosystem responds to the effluent at the seasonal scale, i.e., where the biota are transported into or out of during different seasons and how the higher trophic levels in the ecosystem respond to the potential accumulation of biota due to excessive nutrient loads.

6.2 Recommendations

We echo the recommendations raised in the previous report (HydroQual, 2003).

Improving the boundary conditions. The monitoring stations near the open boundary should be prioritized and enhanced so that the construction of open boundary conditions can be automated, and errors can be reduced. A mooring station (GoMOOS A) as part of the Gulf of Maine Ocean Observing System (GoMOOS) has been deployed in the North Passage since August 2001, which monitors temperature, salinity and DO fields are invaluable information on the open boundary that need to be incorporated into future modeling. However, information at a single station alone is not sufficient to construct the open boundary conditions. We have to depend on empirical assumptions and approximations. While incorporating the mooring data into the open boundary conditions, we recommend increasing the boundary stations.

The effects of zooplankton grazing. As indicated in the sensitivity experiments,

zooplankton grazing can significantly affect the phytoplankton production based on a simple time-lag grazing model. A quantitative study based on zooplankton population models should be made to evaluate the effect of zooplankton grazing on the seasonal variation of phytoplankton groups.

Continuation of modeling efforts. The modeling effort should be continued for interpreting the monitoring results in terms of the long-term evolution of the MBS in response to outfall relocation, and for studying the MBS responses to short term events and seasonal variability.

7. REFERENCES

Becker, S., 1992, The seasonal distribution of nutrients in Massachusetts and Cape Cod Bays, MS thesis, University of New Hampshire, 127pp.

Bigelow, H.B. 1927, Physical oceanography of the Gulf of Maine (Part II). Bulletin of the Bureau of Fisheries, 40: 511-1027.

Bothner, M.H., Bucholtz T., Brink, M., Parmenter, C.M., d'Angelo, W.M., and Doughten, M.W., 1993, The distribution of silver and other metals in sediments from Massachusetts and Cape Cod Bays: U.S. Geological Survey Open-File Report 93-725. 31pp.

Butman, B., 1976. Hydrography and low frequency currents associated with the spring runoff in Massachusetts Bay Memoires. Societe Royale des Sciences de Liege, 6: 247-275.

Butman, B., Bothner, M.H. Lightsom, F.L. Gutierrez, B.T., Alexander, P.S., Martini, M.A., and Strahle, W.S., 2002, Long-term Oceanographic Observations in Western Massachusetts Bay offshore of Boston, Massachusetts: Data Repor for 1989-2000, U.S. Geological Survey Digital Data Series 74.

Geyer, W. R., Gardner, G. B., Brown, W. S., Irish, J., Butman, B., Loder, T., and Signell, R. P. 1992, Physical oceanographic investigation of Massachusetts and Cape Cod Bays. Massachusetts Bay Program. MBP-92-03, 497pp.

HydroQual, Inc. 2000, Bays Eutrophication Model (BEM): modeling analysis for the period 1992-1994. Boston, Massachusetts Water Resources Authority. ENQUAD 2000-02, 158pp.

HydroQual, Inc. 2001, Boundary sensitivity for the Bays Eutrophication Model (BEM). Boston: Massachusetts Water Resources Authority. Report ENQUAD 2001-14. 90pp.

HydroQual, Inc. 2003, Bays Eutrophication Model (BEM): modeling analysis for the period 1998-1999. Boston, Massachusetts Water Resources Authority. ENQUAD 2003-03, 318pp.

HydroQual, Inc. and Normandeau Associates, Inc. 1995, A water quality model for Massachusetts and Cape Cod Bays: Calibration of the Bay Eutrophication Model

(BEM). Boston, Massachusetts WAter Resource Authority. ENQUAD 1995-08, 402pp.

HydroQual, Inc. and Signell, R.P. 2001, Calibration of the Massachusetts and Cape Cod Bays Hydrodynamic Model: 1998-1999. Boston, Massachusetts Water Resources Authority. ENQUAD 2001-12, 170pp.

Jiang, M.S. and Zhou, M.2003, Massachusetts Bay Hydrodynamic Model and Water Quality Model results in 1998-99: Comparison Report between HydroQual and University of Massachusetts Boston Runs. Boston, Massachusetts Water Resources Authority. ENQUAD 2003-10, 42pp.

Jiang, M.S. and Zhou, M. 2004a, The summer Ekman pumping and its implications to the deep water renewal in Massachusetts and Cape Cod Bays. Proceedings of the 8th Estuarine Coatal Modelling. San Francisco. 11-3-0003. p929-948.

Jiang, M.S. and Zhou, M. 2004b. Calibration of the Massachusetts and Cape Cod Bays hydrodynamic model: 2000-2001. Boston, Massachusetts Water Resources Authority. Draft Report. ENQUAD 2004-08. 71pp.

Kropp, R. K., Diaz, R., Dahlen, D., Boyle, J. D., and Hunt, C. D. 2002, 2001 Harbor Benthic Monitoring Report. Boston, Massachusetts Water Resources Authority. ENQUAD 2002-19, 74pp.

Kropp, R. K., Diaz, R., Hecker, B., Dahlen, D., Boyle, J. D., Abramson, S. L., and Emsbo-Mattingly, S. 2001, 2000 Outfall Benthic Monitoring Report. Boston, Massachusetts Water Resources Authority. ENQUAD 2001-14, 148pp.

Libby, P. S., Hunt, C. D, Geyer, W. R., Keller, A. A., Oviatt, C. A., and Turner, J. T. 2000, 1999 Annual Water Column Monitoring Report. Boston, Massachusetts Water Resources Authority. ENQUAD 2000-09, 180pp.

Libby, P. S., Hunt, C. D, McLeod, L. A., Geyer, W. R., Keller, A. A., Borkman, D., Oviatt, C. A., and Turner, J. T. 2001, 2000 Annual Water Column Monitoring Report. Boston, Massachusetts Water Resources Authority. ENQUAD 2001-17, 196pp.

Libby P.S., Geyer W.R., Keller A.A., Turner J.T., Borkman D., Mickelson M.J., Hunt C.D., Oviatt C.A. 2002**.** 2001 Annual Water Column Monitoring Report. Boston: Massachusetts Water Resources Authority. Report ENQUAD 2002-22. 100pp.

Lynch, D.R., Naimie, C.E. and Werner, F.E., 1996. Comprehensive coastal circulation

model with appliction to the Gulf of Maine. Cont. Shelf Res., 12: 37-64.

Maciolek, N. J., Diaz, R. J., Dahlen, D., Hecker, B., Gallagher, E. D., Blake, J. A., Williams, I. P., Emsbo-Mattingly, S., Hunt, C., and Keay, K. E. 2003, 2002 Outfall Benthic Monitoring Report. Boston, Massachusetts Water Resources Authority. ENQUAD 2003-13, 166pp.

Signell, R.P., Jenter, H.L., and Blumberg, A.F., 1996. Circulation and effluent dilution modeling in Massachusetts Bay: model implementation, verification and results. USGS Open File Report 96-015, U.S. Geological Survey, Woods Hole.

Smolarkiewicz, P. K., 1984, A fully multidimensional positive definite advection transport algorithm with implicit diffusion. *J. Comput. Phys.*, **54**, 325-362.

Taylor D. 2001, Trends in water quality in Boston Harbor during the 8 years before offshore transfer of Deer Island flowsBoston, Massachusetts Water Resources Authority. ENQUAD 2001-05, 54pp.

Tucker, J., Giblin, A. E., Hopkinson, C. S., and Vasiliou, D. 2001, Benthic Nutrient Cycling in Boston Harbor and Massachusetts Bay: 2000 Annual Report. Boston, Massachusetts Water Resources Authority. ENQUAD 2001-07, 48pp. 2001.

Tucker, J., Kelsey, J., Giblin, A., and Hopkinson, C. S. 2002, Benthic Metabolism and Nutrient Cycling in Boston Harbor and Massachusetts Bay: Summary of Baseline Data and Observations after One Year of Harbor-to-Bay Diversion of Sewage Effluent. Boston, Massachusetts Water Resources Authority. ENQUAD 2002-13, 83pp.

Turner, J.T., 1994, Planktonic Copepods of Boston Harbor, Massachusetts Bay and Cape-Cod Bay, 1992. *Hydrobiologia*. 293: 405-413.

Werme, C and Hunt, C. D. 2002, 2001 outfall monitoring overview. Boston: Massachusetts Water Resources Authority. ENQUAD 2002-18, 84pp.

Werme, C. and Hunt, C. D. 2000, 1999 Outfall monitoring overview. Boston, Massachusetts Water Resources Authority. ENQUAD 2000-14, 72pp.

Werme, C. and Hunt, C. D. 2003, 2002 Outfall monitoring overview. Boston, Massachusetts Water Resources Authority. ENQUAD 2003-12, 80pp.

Yu, X., T. Dickey, J. Bellingham, D. Manov, and K.Streitlien, 2002, The application of autonomous underwater vehicles for interdisciplinary measurements in Massachusetts and Cape Cod Bays, *Continental Shelf Research*, **22**, 2225-2245.

Massachusetts Water Resources Authority
Charlestown Navy Yard
100 First Avenue
Boston, MA 02129
(617) 242-6000
http://www.mwra.state.ma.us